Design and Optimization of Renewable Energy-Based Electrification and Water Pumping Systems

by

Misagh IRANDOOSTSHAHRESTANI

THESIS PRESENTED TO ÉCOLE DE TECHNOLOGIE SUPÉRIEURE IN PARTIAL FULFILLMENT OF THE REQUIREMENTS FOR THE DEGREE OF DOCTOR OF PHILOSOPHY
Ph.D.

MONTREAL, AUGUST 22, 2025

ÉCOLE DE TECHNOLOGIE SUPÉRIEURE
UNIVERSITÉ DU QUÉBEC

BOARD OF EXAMINERS

THIS THESIS HAS BEEN EVALUATED

BY THE FOLLOWING BOARD OF EXAMINERS

Mr. Daniel R. Rousse, Thesis Supervisor
Department of Mechanical Engineering at École de technologie supérieure

Mr. Ricardo Izquierdo, President of the Board of Examiners
Department of Electrical Engineering at École de technologie supérieure

Mr. Didier Haillot, Member of the Jury
Department of Mechanical Engineering at École de technologie supérieure

Mr. Christophe Ménézo, External Evaluator
Professor at Université Savoie Mont Blanc,
Director of the Fédération de Recherche sur l'Energie Solaire

THIS THESIS WAS PRESENTED AND DEFENDED

IN THE PRESENCE OF A BOARD OF EXAMINERS AND PUBLIC

JULY 11, 2025

AT ÉCOLE DE TECHNOLOGIE SUPÉRIEURE

ACKNOWLEDGMENT

I would like to sincerely thank my parents, my partner, and my friends for their support throughout my studies. I am deeply grateful for their encouragement. I also thank the director of the t3e group, Dr. Daniel R. Rousse, for his support and valuable advice. In addition, the support provided for this research by the Fonds de recherche du Québec– Nature et technologies (FRQ-NT) through the Programme de bourses d'excellence pour étudiants étrangers (PBEEE) is acknowledged.

CONCEPTION ET OPTIMISATION DE SYSTÈMES D'ÉLECTRIFICATION ET DE POMPAGE D'EAU BASÉS SUR LES ÉNERGIES RENOUVELABLES

Misagh IRANDOOSTSHAHRESTANI

RÉSUMÉ

Dans cette recherche, la conception et l'optimisation d'un système basé sur les énergies renouvelables pour une double application, à savoir l'électrification et le pompage de l'eau, sont étudiées. L'énergie produite par le système renouvelable est d'abord utilisée pour l'électrification, tandis que l'excédent d'énergie est utilisé pour le pompage d'eau à diverses fins, comme l'approvisionnement en eau d'une petite communauté ou l'irrigation. Deux concepts, la probabilité de perte d'alimentation électrique (LPSP) et la probabilité de pénurie d'eau (WSP), sont utilisés pour évaluer la fiabilité du système. Par ailleurs, pour évaluer la faisabilité de l'étude, divers paramètres économiques, tels que la période de retour sur investissement, les dépenses en capital (CAPEX) et le coût actualisé de l'énergie, sont pris en compte. Deux types de systèmes énergétiques sont considérés dans cette recherche : un système photovoltaïque (PV) avec stockage par batterie (BESS) et un système combinant PV, éolienne (WT) et BESS. Le premier système énergétique (PV-BESS) est supposé être utilisé pour une petite maison avec une consommation énergétique constante tout au long de l'année, où l'excédent d'énergie est affecté à l'irrigation d'une ferme située dans le sud de l'Iran, une région dotée d'un fort potentiel solaire. Le second système énergétique (PV-WT-BESS) est évalué pour une petite communauté au Québec, où la consommation d'électricité varie au cours de l'année (nettement plus élevée en hiver). Dans ce cas, l'excédent d'énergie des éoliennes et des panneaux photovoltaïques est utilisé pour approvisionner la communauté en eau. Un algorithme personnalisé pour les calculs numériques et une stratégie de répartition énergétique sont employés. En résumé, dans cette stratégie, la priorité est donnée à la production d'électricité, suivie de la charge des batteries. Une fois ces conditions remplies, l'excédent d'énergie est employé pour le pompage de l'eau. L'objectif principal de cette étude est de démontrer la faisabilité d'un système basé sur les énergies renouvelables pour l'électrification et l'utilisation de l'excédent d'énergie pour le pompage de l'eau. De plus, cette recherche vise à montrer dans quelle mesure la tolérance de l'utilisateur, en termes de LPSP ou de WSP, peut réduire la taille du système et, par conséquent, son CAPEX. Une optimisation multi-objectifs est réalisée en utilisant la méthode NSGA-II afin de trouver un front de Pareto qui satisfait les utilisateurs ayant diverses tolérances ainsi que des objectifs économiques. Il convient de noter que cette étude prend en compte le fait que, dans des projets réels, un système conventionnel tel qu'un générateur diesel doit être intégré à la conception pour pallier l'intermittence des énergies renouvelables ou les problèmes de maintenance. Cependant, cette étude vise à augmenter la pénétration des énergies renouvelables dans les communautés éloignées ayant un accès limité ou inexistant à l'électricité du réseau.

Mots-clés: système photovoltaïque ; énergies renouvelables ; électrification ; pompage d’eau ; la probabilité de pénurie d'eau; la probabilité de perte d'alimentation électrique

DESIGN AND OPTIMIZATION OF RENEWABLE ENERGY-BASED ELECTRIFICATION AND WATER PUMPING SYSTEMS

Misagh IRANDOOSTSHAHRESTANI

ABSTRACT

In this research, the design and optimization of a renewable energy-based system for the dual application of electrification and water pumping is investigated. The power generated by the renewable system is initially used for electrification purposes, and the excess power is used for water pumping for different purposes, like providing water for a small community or supplying water for irrigation purposes. Two concepts, loss of power supply probability (LPSP) and water shortage probability (WSP) are used for assessing the reliability of the system. In addition, for evaluating the feasibility of the study, various economic parameters, including payback period, CAPEX, and levelized cost of energy, are considered. Two types of energy systems are used in the study: solar photovoltaic (PV)- battery energy storage system (BESS) and PV-wind turbine (WT)- BESS. The first energy system (i.e., PV- BESS) is assumed to be used for a small house with constant energy consumption throughout the year, where the excess power is used for irrigating a farm in southern Iran, a region with abundant solar potential. The second energy system (i.e., PV- WT- BESS) is evaluated for a small community in Quebec with variable electricity consumption throughout the year (considerably higher in cold seasons), where the excess power from the wind turbines and PV panels is used for providing water for the community. A custom algorithm for numerical calculations and a dispatch strategy are employed. In brief, in this dispatch strategy, the priority is to generate electricity and then to charge the bank of batteries. If these conditions are met, the excess power is used for water pumping. The main goal of the study is to show the feasibility of a renewable energy-based system for electrifying and using the excess power for water pumping. Furthermore, this research is aimed at showing how much the user`s tolerance in terms of LPSP or WSP can lower system size and consequently its CAPEX. A multi-objective optimization is conducted by using NSGA-II method to find a Pareto front that satisfies users with various tolerances, and economic objectives. It is worth noting that this study does not disregard the fact that in real-world projects, a conventional system like a diesel generator should be included in the design to account for renewable energy's intermittent nature or maintenance issues. However, this study aims to increase renewable energy penetration for remote communities with limited access to grid electricity.

Keywords: PV-powered system; renewable energy, electrification; water pumping; water shortage probability; loss of power supply probability

TABLE OF CONTENTS

LIST OF TABLES

Page

LIST OF FIGURES

Page

LIST OF ABREVIATIONS AND ACRONYMS

AC	alternating current
ADOPT	adoption and diffusion outcome prediction tool
BLDC	brushless direct current
CAD	canadian dollars
CAPEX	capital expenditure
CFD	computational fluid dynamics
CWR	crop water requirement
DC	direct current
DNI	direct normal irradiation
EES	engineering equation solver
EOT	equation of time
FOB	free on board
ha	hectare
hp	horsepower
IBC	installed battery capacity
IODC	indian ocean data coverage
IWR	irrigation water requirement
LCOE	levelized cost of energy
LL	local longitude
LT	local time
LSTM	local standard time meridian
LPSP	loss of power supply probability

LPS	loss of power supply
MPPT	maximum power point tracker
NASA	national aeronautics and space administration
NREL	national renewable energy laboratory
NSRDB	national solar radiation database
OPEX	operational expenditure
PSM-v3	physical solar model version 3
PVWPS	photovoltaic water pumping system
PPA	power purchase agreement
PV	photovoltaic
PCM	phase change materials
SDG	sustainable development goals
STC	standard test condition
ST	solar time
WBG	world bank group
WSP	water shortage probability
WS	water shortage

LIST OF SYMBOLS AND UNITS OF MEASUREMENT

d	number of the day [-]
EP_t	electricity production in year t [kWh]
F_t	fuel cost [IRR]
G	incident solar irradiation [W/m^2]
G_{STC}	incident solar irradiation on STC [W/m^2]
g	gravitational acceleration [m/s^2]
H	total dynamic head [m]
I_β	global solar radiation on an inclined surface [W/m^2]
I_b	direct beam radiation [W/m^2]
I_d	diffusive radiation [W/m^2]
$I_{0\text{-}pv}$	investment cost of PV panel [IRR/W]
$I_{0\text{-}pump}$	investment cost of pump [IRR/W]
I_{PV}	current of the panel [A]
I	global horizontal irradiance [W/m^2]
$I_{PV,r}$	rated current of the panel [A]
M_t	scheduled maintenance cost [IRR]
n	number of the day [-]
N_{PV}	number of PV panels [-]
$N_{PV,\,max}$	maximum number of PV panels [-]
O_t	unscheduled operational cost [IRR]
PPV	output power of the PV panel [W]
Pl	load power [W]

r	real discount rate [%]
R_t	replacement cost [IRR]
$R_{inverter}$	replacement cost of inverter [IRR]
$R_{battery}$	replacement cost of battery [IRR]
T_{amb}	ambient temperature [°C]
R_b	geometric factor [-]
T_C	temperature of panel [°C]
STC	temperature of the cell at STC [°C]
t	time [hour]
V_{PV}	voltage of the panels [V]
θ	angle of incidence [°]
V	volumetric flow rate [m^3/s]
β	tilt angle [°]
σ	hourly self-discharge rate [-]
ρ	density [kg/m^3]
α	temperature coefficient [%/°C]
π	pumping power [W]
η_{bc}	efficiency of battery at charge mode [%]
η_{bd}	efficiency of battery at discharge mode [%]
η_{inv}	efficiency of inverter [%]
θ_z	zenith angle [°]
μ	albedo coefficient [-]

δ	declination angle [°]
ω_{ss}	sunset hour angle [°]
ω_{sr}	sunrise hour angle [°]
φ	latitude [°]
ω	hour angle [°]
Γ	argument of EOT [-]
λ	longitude [°]
γ	azimuth angle [°]

INTRODUCTION

Context

The energy demand is expected to become at least doubled and tripled by 2050 and 2100, respectively (Lewis et al., 2005). In developing countries, solar water pumping is one of the main uses of photovoltaic systems, and it can be considered as a criterion of economic and social developments (Abdolzadeh & Ameri, 2009). Utilization of solar water pumping for agricultural purposes is of reasonable reliability since the highest water demand is in accordance with maximum solar availability in summer (Chahartaghi & Nikzad, 2021). Production in the agriculture sector in developing countries is highly dependent on the supply of water, and it can be affected if enough water is not supplied (Chandel, Naik, & Chandel, 2017). In fact, social, economic, and ecological problems can happen due to water stress and it can affect sustainable development (Guo et al., 2022). Furthermore, solar water pumping systems can considerably reduce GHG emissions with low O&M costs; however, the main drawback of this system is its high initial capital cost (Chandel, Nagaraju Naik, & Chandel, 2015; Sontake & Kalamkar, 2016). Gualteros and Rousse (Gualteros & Rousse, 2021) created accessible software designed to aid in various stages of prefeasibility assessment, system dimensioning, optimization, ongoing maintenance, and economic assessments. The main objective of this research was to provide support to individuals with limited knowledge regarding PVWPS in remote and rural regions. Their findings indicated that the community's tolerance for water shortages significantly influenced the system's size and cost. In another study, Bhayo et al. (Bhayo, Al-Kayiem, & Gilani, 2019) studied a PV electrification system for a home in a rural area. They showed that there is extra energy production, and this excess power can be used for water pumping purposes. They also evaluated LCOE of this system. However, their study lacked optimization of the system. Furthermore, some assumptions were used that could considerably affect the sizing of the system and the reliability of the results. For example, the simple correlation for head vs. volumetric flow rate of the pumping system is used which assumes constant efficiency at different solar irradiations and hence different input powers and their investigation did not consider addition of water reservoir to the system. In addition, this system was using PV as the only energy production source with battery banks

and using one source of electricity generation could lead to reliability issues. The addition of another energy generating source could make the system more stable which will be evaluated in this research.

Aims and motivations

In this study, the main goal is to design and optimize an autonomous standalone renewable energy-based system with a dual-function of providing the required electricity for residential load as well as to run a motor-pump for water pumping by using the excess power while considering techno-economic parameters like LPSP, LWSP, capital expenditure, payback period, etc. The multi-objective optimization process leads to a Pareto front that satisfies users with various tolerances, and economic objectives. To the best knowledge of the author, there is no research evaluating technical and economic parameters of an integral dual-purpose renewable energy system for providing electricity and water needs.

Content of the thesis

In the first chapter, a thorough review of the status of solar water pumping systems is investigated for Iran. Various studies of SWPS in Iran are reviewed chronologically. In the second chapter, the case study of (Bhayo et al., 2019) is selected for validation purposes. Then, a city in the south of Iran is selected for our research where a small house with constant daily consumption is considered for electrification by a PV-BESS system, and the excess power is used for irrigation of a 1-ha citrus farm. In the third chapter, a more comprehensive study will be done. A PV+WT+BESS is designed and optimized for electrifying a small community of 100 people on a remote island in Quebec which is equipped with large water tankers to be used for reserving water for the community.

Expected benefits and social, environmental, and industrial impact of the research can be summarized as:

- Scientific impact: To deepen the knowledge of renewable energy-based electrification and water pumping.

- Technological impact: To improve the performance of the available water pumping systems in terms of electricity production and to minimize water shortage.
- Social impact: To facilitate access to electricity and water in remote areas
- Financial impact: To lower levelized cost of electricity by using renewable sources
- Environmental impact: To reduce emissions and carbon footprint.

The study can shed light on the effect of parameters of LPSP and WSP for a standalone system that relies on a renewable energy system. This renewable system can be used for remote areas where limited access to power lines exists. Furthermore, this system can be used to increase the reliability of the power supply in case of a power shortage due to natural disasters. Despite the technological aspects of this project, it can help deepen research in this field, as there are limited studies evaluating both effects of WSP and LPSP on the size and capital expenditure of such systems. The developed code can be used for any location with known solar irradiations, wind speed, and geographical features like latitude, longitude, etc.; therefore, it can be easily applied to any location.

CHAPTER 1

STATUS OF SOLAR PHOTOVOLTAIC WATER PUMPING SYSTEMS IN IRAN: A COMPREHENSIVE REVIEW

M. Irandoostshahrestani[a], and D. R. Rousse[a]

[a] Industrial Research Group in Technologies of Energy and Energy Efficiency (t3e), École de technologie supérieure (ÉTS), University of Quebec, Montreal, Canada

Paper published in *Water Science and Technology,* June 2024

NOTE: This paper is originally published under the following information: Misagh Irandoostshahrestani, Daniel R. Rousse; Status of photovoltaic water pumping systems in Iran: A comprehensive review. Water Sci Technol 15 June 2024; 89 (12): 3270–3308. doi: https://doi.org/10.2166/wst.2024.149. The content of this section is adjusted slightly to make sure it is consistent, and it respects regulations and formatting standards.

ABSTARCT

This study investigates the current status of solar photovoltaic water pumping technology in Iran, a country with considerable solar irradiation potential, especially in southern and central regions. Despite this potential, there are limited comprehensive studies on SWPS in Iran. This research conducts a thorough review of existing studies to evaluate the state of solar water pumping in the country. While not all provinces have adopted this technology, most regions have been subject to investigations into solar water pumping. Iran's widespread utilization of photovoltaic water pumping can be attributed to its ample solar irradiation, even in the north of the country, which has relatively limited solar irradiation levels. Remarkably, there are limited comprehensive studies evaluating different aspects of solar photovoltaic water pumping systems like technical, economic, environmental, and social. Most of the research has been done during the last few years, which shows an increased acknowledgment of the potential benefits of this technology. Finally, this review provides understanding for

researchers and shows the benefits of SWPS. It also provides ideas for innovation and solar water pumping use in the country, and shows the requirements for assessments of this system.

Keywords: Iran, Irrigation, Photovoltaic systems, Review, Solar energy, Water pumping

HIGHLIGHTS

- It promotes knowledge and provides understanding for policymakers, researchers, and farmers
- It showed that there is limited research in spite of Iran's considerable solar potential
- There is an increasing interest in using solar energy for agricultural purposes
- The adaptability of SWPS in different provinces of Iran is shown.
- The benefits of PV water pumping are elaborated, and the necessity for more innovation in agriculture is discussed.

1.1 Introduction

The requirement for water is critical in industrial and urban development. Lack of water access adversely affects the quality of life globally. The effects of water stress are across social, economic, and ecological dimensions, thereby posing significant challenges to sustainable development (Guo et al., 2022). Estimates indicate a double increase in energy demand by 2050 and a triple increase by 2100 (Lewis et al., 2005). Consequently, many studies tried to address water supply concerns for both residential and industrial applications. This increasing need for energy has led to the development of renewable energy systems for both residential and industrial use. Solar energy is one of the most used energy sources in recent years.

In recent times, photovoltaic solar energy has garnered growing interest, fueled by the declining costs of PV panels, even as their efficiency continues to improve (International Renewable Energy Agency, 2022; Ray & Douglas, 2020). Figure 1.1 depicts the evolution of the levelized cost of energy over the decade 2010-2020 for various sources. Notably, in 2020,

solar PV emerged as the most cost-effective technology when compared to other alternatives. Moreover, PV Magazine ('Solar Module Prices Continue to Fall', 2023) reported an overall average reduction of 25% across all module technologies since the start of the year 2023. The same magazine reported in October 2023 ('Solar Module Prices Dive to Record Low', 2023) record low prices of \$0.14/W_p for Mono PERC modules from China. However, recently it was shown that the quality of PV panels has decreased considerably (Libra et al., 2023), and this decline is more in harsh conditions like deserts (Desai, Rathore, & Singh, 2022). The authors concluded that this could have a negative impact on the lifetime of PV power plant projects. Solar water pumping, a widespread application of photovoltaic systems in developing countries, is used for evaluating both social and economic development (Abdolzadeh & Ameri, 2009). The utilization of solar water pumping in the agricultural industry shows reliability, since the peak water demand is aligned with the highest solar energy availability during summer (Chahartaghi & Nikzad, 2021). In developing countries, agricultural production is dependent on water supply, and consequently, its productivity is influenced if water supply is not sufficient (Chandel et al., 2017). While most systems are fossil fuel-based, a solar water pumping system can significantly mitigate greenhouse gas emissions while maintaining low operation and maintenance costs. Nonetheless, the primary drawback of such a system resides in its substantial initial capital investment (Aliyu et al., 2018) and especially in developing countries (Sontake & Kalamkar, 2016).

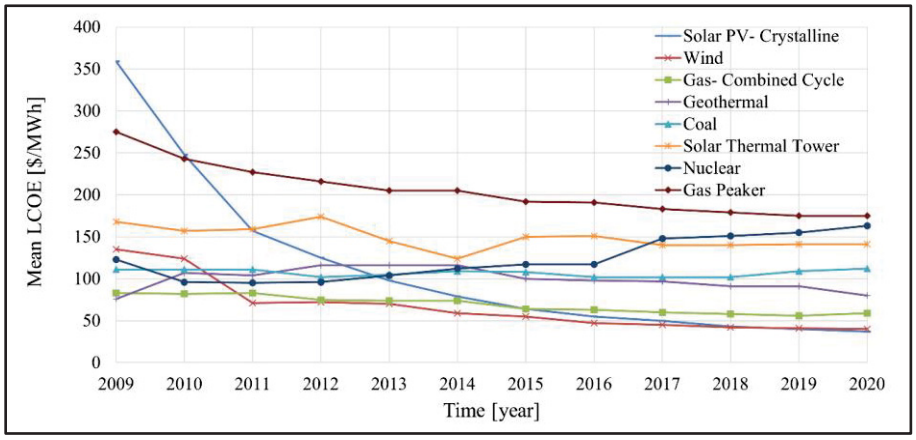

Figure 1.1 LCOE comparison for various energy generation technologies, reproduced and adapted with the permission of (Ray & Douglas, 2020)

1.2 Improvements in efficiency of PV systems

As previously mentioned, the global demand for energy is increasing, which encourages scholars and industries to find ways to improve the efficiency of solar energy systems. Since the primary focus of this research is on solar PV renewable energy, this section provides a brief overview of techniques implemented to enhance the efficiency of PV panels. Considerable research has been dedicated to exploring both active and passive cooling techniques. Shalaby et al. (Shalaby, Elfakharany, Moharram, & Abosheiasha, 2022) conducted an experimental study investigating the impact of water cooling on the rear side of photovoltaic panels in order to run a reverse osmosis system and preheat its feed water. PVC tubes were attached to the back of a 250 W module, providing direct contact between water and the panel. Coolant circulates with a constant mass flow rate of 0.15 kg/s. The location of the experiments is not explicitly mentioned in the article. However, maximum ambient temperature and solar irradiance at around noon on September 1st were shown to be 43.5˚C and 1013 W/m^2, respectively. Their research revealed a notable maximum of 14.1% increase in power generation for the panel with cooling (from 173 W to 197 W). The temperature decrement was in the range of 5-10˚C and 4-13˚C for the front and back sides of the panel, respectively. In addition, the efficiency improved from 17.4% to 19.8% through the implementation of this cooling technology. In another investigation, Gomaa et al. (Gomaa, Ahmed, & Rezk, 2022) studied the impact of the coolant's mass flow rate on both the temperature distribution of the panel and the outlet temperature of the coolant for a PV thermal system. Their research also examined the influence of solar irradiation intensity on these parameters. To conduct their investigations, three-dimensional CFD model simulations of ANSYS 19.2 software were used. They considered two distinct cooling cross-finned channel box configurations, one thin (3mm) and the other thick (15mm), and scrutinized the thermal behavior of the entire system. Ambient air and inlet coolant temperature were set to 25˚C, and five water cooling flow rates of 0.5, 1, 1.5, 2, 3, and 4 L/min were considered at solar irradiances of 200, 400, 600, 800, and 1000 W/m^2. By evaluation of the module temperature contours, they showed that the optimal coolant

mass flow rate was 3 L/min for both channel box configurations at the maximum solar irradiance. Although the criteria for selecting the optimal mass flow rate were not explicitly mentioned in the paper, however, reaching a cool PV surface while keeping the mass flow rate as low as possible to avoid extra pressure drop penalties seems to be considered for selecting the optimum coolant mass flow rates. In another study (Maleki, Ngo, & Shahrestani, 2020), researchers examined the influence of ambient temperature (25, 35, and 45˚C), solar irradiance (600, 800, and 1000 W/m^2), and coolant inlet velocity (0.5, 0.7, 0.9 m/s) on both the temperature distribution and efficiency of PV cells. A serpentine channel of the rectangular cross-section with a width of 5 mm and height of 3 mm was used at the rear side of the panel. The pitch of the serpentine channel was 100 mm while the length and width of the panel were 850 and 541 mm, respectively. Therefore, nine cooling lines were incorporated on the back of the panel. ANSYS CFX for modeling and ANSYS Mesh for grid generation were used. The findings demonstrated that the cooling channels employed at the rear of the PV cell naturally exhibited greater effectiveness under conditions of high solar irradiation and elevated ambient temperatures. However, they observed that increasing the mass flow rate of the coolant had a lesser impact at higher fluid flow rates. Hence, instead of conventional water coolants, nanofluids which are mixtures of base fluids with nanoparticles like silver (Masoud Parsa et al., 2022), silica (Cao, Kamrani, Mirzaei, Khandakar, & Vaferi, 2022), titanium or aluminum oxide (Ebaid, Ghrair, & Al-Busoul, 2018), graphene nanoplatelets (Venkatesh, Manikandan, Selvam, & Harish, 2022), magnesium oxide (Fakruddin Babavali et al., 2023) have been explored as an alternative to enhance the efficiency of cooling in PV or PV thermal systems. In addition to the active cooling methods discussed earlier, passive cooling techniques have also been the subject of numerous studies. Zhou et al. (Zhou et al., 2022) conducted research in which they employed rectangular wing vortex generators installed on the rear of the panels to augment the heat transfer rate from the cell under natural convection conditions (no wind flow over the panel). They conducted their study both numerically, using computational fluid dynamics, and experimentally, employing particle image velocimetry. They showed that the use of these vortex generators can decrease the panel temperature by 2-3˚C and that the aerodynamic geometry of these vortex generators can considerably alter the form of the vortices and consequently affect a uniform cooling pattern. The utilization of phase change

materials (PCMs) is one of the passive methods that has gained attention in recent years. They act as thermal storage and can absorb considerable amounts of heat from PV panels during the daytime and undergo a phase change. PCMs can be the only cooling technique used like the utilization of paraffin wax RT-42 with three different thicknesses of 1, 2, and 3 cm attached to the back sheet of a PV panel (Maghrabie, Mohamed, Fahmy, & Abdel Samee, 2023). In this study, four different tilt angles of 15, 20, 25, and 30 degrees were considered for two similar PV panels with nominal power generation of 40 W, one reference (PV_r) and the other one equipped with PCM (PV-PCM). The tests were done in the hot climate of Gena City in Egypt. It was concluded that the upper side of the panel had higher temperatures due to PCM melting and the formation of a vacuum area with no cooling. Specifically, 17.1%, 15.7%, and 13.2% higher temperatures at the upper side of the PV-PCM at PCM thicknesses of 1, 2, and 3 cm, respectively, for a tilt angle of 15 degrees. In addition, it was shown that the electrical efficiency of PV-PCM with maximum PCM thickness (i.e., 3 cm) was improved by 14.4%, leading to 15.8% more output power production at an optimal tilt angle of 30-degree compared to PV_r. PCMs were also simultaneously employed with other cooling techniques like the utilization of PV panels with plates equipped with ribs or dimples as another passive method to enhance heat transfer rates (Abo-Elnour, Zeidan, Sultan, El-Negiry, & Soliman, 2023). In this study, ANSYS 2020 Fluent was used to evaluate cell temperature and electrical efficiency of bifacial PV panels at three different configurations: first, a PV panel with a single PCM (RT-35), second, a ribbed unit with two PCMs (RT-27 and RT-35), and third, a bifacial panel with no cooling system. L-shaped mirrors were used to reflect the irradiation to the bottom cells. Three different solar irradiances of 800, 1000, and 1200 W/m^2 were considered. The novel multiple PCM model showed around 13˚C reduction in its cell temperature compared to PV without cooling, while its efficiency increased to 16.68% compared to the efficiency of PV with no cooling system (15.5%).

In addition to cooling techniques, optimizing the position of the panels can impact system power generation considerably. The tilt angle has been a subject of investigation in numerous studies. Mamun et al. (Mamun, Islam, Hasanuzzaman, & Selvaraj, 2022) conducted experimental research assessing the impact of tilt angle on PV module performance under two

conditions: constant solar irradiation with varying tilt angles and constant tilt angles with varying solar irradiation intensity, conducted in both outdoor conditions in Kuala Lumpur with latitude of 3.117°N and longitude of 101.667°E and indoor settings at Solar Thermal Research Lab of University of Malay. Their evaluation covered parameters such as temperature of cell, short-circuit current, open-circuit voltage, output power, efficiency, etc. It was shown that cell temperature increases by 7.5°C and 5.7°C for 100 W/m^2 irradiance improvement at indoor and outdoor conditions, respectively. Furthermore, the optimal tilt angle for Malaysia was about 15 degrees, based on the outdoor experiments. In a study by Liu et al. in China (Liu et al., 2022), satellite data from 133 stations were utilized to evaluate traditional latitude-based models in regions characterized by significant climate variations. These data were used to estimate the diffuse fraction through the Boland–Ridley–Lauret model (Ridley, Boland, & Lauret, 2010). This is a generic model for diffuse solar fraction estimation through global radiation. This model was shown to perform better, especially at northern and southern hemisphere locations although it can be utilized as a universal model. The research of Liu et al. (Liu et al., 2022) highlighted that the optimized tilt angle of panels is highly associated with diffuse fraction and latitude with correlation coefficients (R) of 0.8 and 0.86, respectively. They also mentioned that on average, PV panels with optimal tilt angle can produce 13.7% higher power compared to panels with no tilting.

In addition to the previous methods, enhancing power generation and efficiency also involves cleaning and dust removal processes for panels. Recently, Zarei et al. (Zarei, Abdolzadeh, & Yaghoubi, 2022) studied the impact of key factors, like relative humidity, rainfall, and gravity on PV dust accumulation. They compared decrease in power production capacity of PV panels in several locations worldwide due to dust deposition. Furthermore, they reviewed studies that utilized artificial particles generated from sources of pollution including industrial pollutants and the smoke of vehicles. In another study, Salamah et al. (Salamah et al., 2022) reviewed the effect of various climates on dust accumulation and PV performance in different regions of the world. It was concluded that shading or dust accumulation on PV modules decreases received irradiance and simultaneously elevates the PV cell temperature resulting in a reduction in the module’s open circuit voltage. In addition, the presence of dust on the surface causes a decrease

in both module's short circuit current and transmittance. The degree of this decrease is influenced by factors such as the concentration of particles with a maximum size of 10 μm (PM_{10} concentration), dust loading, tilt angle, and particle concentration. In another study, Fan et al. (Fan et al., 2022) evaluated the correlation between duct accumulation on PV modules and their efficiency for energy conversion by using CFD. ANSYS Fluent 15.0 was used as the modeler, and ICEM was applied for domain grid generation. They employed the realizable k-ϵ model and discrete phase model (DPM) for the turbulent flow and dust deposition estimation, respectively. Three different wind speeds of 1.3, 2.6, and 3.9 m/s and four tilt angles of 5°, 15°, 30°, and 45° were considered. In addition, the dust particle diameter ranged from 1 to 300 μm. The findings reveal that the spiral vortex, which is formed by dust particles, becomes more prominent and gradually disperses with an increase in tilt angle. The vortex's length and angle at the rear side of the panel peak at a wind velocity of 3.9 m/s and tilt of 45°. For the dust particle diameter less than 120 μm, wind speed exerts the maximum effect on the PV panels' conversion efficiency, demonstrating a linear relationship with deposition time. The increment of the diameter of the dust particle and wind velocity results in an increase in the conversion efficiency loss, reaching a maximum of 72.9% loss for the PV panels. In another study (Panidhara & Ramamurthy, 2021), an experimental laser in-situ thickness measurement technique was developed to evaluate the correlation of PV panel efficiency with dust accumulation. It was revealed that a dust layer with a thickness of 500 μm can increase the temperature of the PV panel by 2°C, leading to a reduction in photocurrent and a 50% reduction in the panel's conversion efficiency. They concluded that as the dust thickness rises, the infrared radiation transmittance increases which consequently leads to the degradation of the panel. In another study, Ekinci et al. (Ekinci et al., 2022) used three different chemical solutions to evaluate the performance improvements of PV panels cleaned by a robot manufactured by means of 3-D printing technology. The robot is equipped with in-line pressurized water-spraying fogging nozzles. The experiments were done in Adana City, Turkey. The impact of dust accumulation on short circuit current and open circuit voltage of five 50 W panels with different cleaning conditions of dust, solution 1 (2-propanol), solution 2 (ethanol), solution 3 (acetone), and water was evaluated. The three solutions were all 5% v/v. It is worth mentioning that the contact angle values were 53.3°, 57.4°, and 60.2° for Solutions 1, 2, and 3, respectively.

These values were less than 90°, showing the usefulness of the solutions. It was shown that the output power has increased by 15%, 14%, and 11% when cleaned with Solutions 1, 2, and 3, respectively.

Furthermore, improving the efficiency of entire PV systems, including inverter, battery, etc., was also the subject of many studies. For example, Ketjoy et al. (Ketjoy, Chamsa-ard, & Mensin, 2021) studied three parameters affecting the efficiency of PV inverters. The first parameter was the duration of operation and the investigation of an inverter that worked for four years showed that its efficiency decreased negligibly from 91% of the manufacturer`s specification of 90%. This was due to the cool temperatures of the storage room where the inverter was operating. The second factor was the type of PV panel that was connected to the inverter, and it was shown that the type of panel has the least effect. In fact, the power input from the PV affects the efficiency of the inverter and it was revealed that inverters connected to a p-Si PV panel had a maximum efficiency of 91%. Finally, the last factor was the irradiance level and it was shown that inverters work at their maximum efficiency of 90% for irradiances higher than 350 W/m^2. It is important to note that the efficiency of the PV panel or the entire system is not the only objective of the studies and some researchers explored the economic parameters like minimizing the LCOE (Osmani, Ramadan, Lemenand, Castanier, & Haddad, 2021). We stop here reviewing the methods of increasing the efficiency of solar PV systems, and we focus on solar water pumping systems in the next sections.

1.3 Solar photovoltaic water pumping systems

One of the main applications of solar energy is in solar water pumping systems. With regards to the importance of energy supply and water stress, solar water pumping has gained attention, even from organizations like the World Bank Group (WBG). In a report by the WBG (Kristoffer Welsien, Christopher Purcell, Reuben Kogi, 2018), an extensive investigation into the fundamentals of solar water pumping is conducted, encompassing aspects such as design, sizing, key components, installation, operation, maintenance, and life cycle cost assessment. Another notable report forming basic information, conducted by Argaw et al. (Argaw, Foster,

& Ellis, 2003), presents a comprehensive study for selecting the best energy system for water pumping purposes in rural areas. This study introduces a methodology for economic and efficient selection of the pump and energy source while considering both renewable and conventional energy resources. This research is affiliated with the National Renewable Energy Laboratory (NREL) and evaluated all technical parameters of water pumping, including solar and diesel systems. This report tries to compare power sources for rural water pumping and focuses on water supply, irrigation, and livestock watering applications. The goal is to assess the effect of collaboration between governments, NGOs, and institutions on the sustainable utilization of renewable energy systems. In another study, Chandel et al. (Chandel et al., 2015) performed an in-depth literature review on solar pumping technology, and they studied research gaps and considered economic and environmental parameters. Their research also evaluated the performance assessment of PV systems, like sizing, degradation of power in pumping systems, characteristics of PV panels, and efficiency improvements. They expressed that most photovoltaic pumping systems use two-axis manual tracking, that enhances the efficiency of the system by up to 20%. The payback period for photovoltaic water pumping systems typically ranges from 4 to 6 years, and some systems have reported even shorter payback periods. PV panel manufacturers provide a 20 to 25-year power warranty due to the reliability of the panels, with real lifespans of more than 30 years. They concluded that as PV module costs decrease and incentives for PV system installations, particularly in India, become available, the payback period is anticipated to further decrease.

In another study by Bhayo et al. (Bhayo et al., 2019), a solar PV system is explored for generating the required electricity for a rural household, with a focus on utilizing excess power for water pumping. This study is conducted in the region of Malaysia, considering specific electricity consumption patterns that account for a daily load demand of 3.2 kWh per day. To ensure system reliability during cloudy or rainy conditions or at night, a bank of batteries is integrated and charged during surplus electricity production. A MATLAB code is developed, and the study is conducted over a 30-day period, using real-time weather data. The system includes PV panels, battery banks, a motor-pump unit, and inverters. The study evaluates the levelized cost of energy, conducts technical assessments of the system, and explores sizing

considerations. The cost of energy for varying numbers of PV panels and battery capacities was evaluated. Furthermore, the research studies the volume of water that can be pumped through the excess power. The research shows that low irradiation at some hours of day can impact system size. It was shown that for an LPSP of 0, the number of PV panels depends on the day with the worst radiation condition. A system consisting of 8 PV panels with a total power capacity of 2.44 kW and an installed battery capacity of 3.533 kWh was suggested to meet the daily load demand. The proposed system requires about 16 m^2 of installation space and can pump 363 m^3 of water per day to an elevation of 6.0 m by using the excess power. The levelized cost of electricity for this system was 0.3750 $/kWh.

Hadj Arab et al. (Hadj Arab, Chenlo, & Benghanem, 2004) studied the estimation of loss of load probability (LLP) of a PV water pumping system. They considered a constant profile (i.e., total 6 m^3 of water consumption per day) with a two-day autonomy tank and used a centrifugal pump and presented a technique for LLP calculation as well as a tool for system sizing. The method allows the creation of LLP maps using meteorological data. They validated the models developed for photovoltaic arrays and motor-pump units experimentally. They selected four sites in Algeria as case studies: Algiers, Bechar, Oran, and Tamanrasset. Bechar and Tamanrasset are located in the Sahara region of the country, and these regions represent 80% of Algeria with arid or semi-arid climates. The approach uses a computer program employing mathematical models from actual measurements of a motor-pump and photovoltaic system. The PV array model considers the non-linear characteristics of the irradiation. Results revealed that southern locations need smaller PV arrays due to higher solar radiation, while northern locations are less sensitive to sizing errors. They showed that the size and techniques for calculating power loss can be used for any location. In another study conducted by Gualteros and Rousse (Gualteros & Rousse, 2021), a program was developed by Python. The goal was to help people in rural areas with limited knowledge of solar energy and pumping technology. This software helps users in analyzing the PV panel size and reservoir volumes, and finally improves their access to water resources. The study introduced the water shortage probability concept as a tool for assessing the size of the system. The research showed that the most important criterion in sizing a water pumping system is the willingness of water users to

tolerate periods of limited access to water. It was shown that water shortages occur in November, December, and mid-January, with a maximum of 0.5 percent in early December. The study concluded that even a slight improvement in the reliability of water access could potentially lead to a doubling in the required size of PV panels or water reservoirs.

In a study conducted by Santra (Santra, 2021), solar water pumping for a farm in a hot arid area of India, western Rajasthan, was examined through pressurized irrigation systems. This region benefits from 5.75 $kWh.m^{-2}.day^{-1}$ solar irradiation, which is higher than the yearly average for India (i.e., 5.4 $kWh.m^{-2}.day^{-1}$). In addition to the technical considerations, the study also evaluated different parameters of PV water pumping systems by micro-irrigation techniques of drippers, mini, and micro sprinklers. It was concluded that using 3-hp or 5-hp high-capacity water pump systems, which are common for irrigation of India`s farms, leads to water stress. However, in this research, a 1-horsepower solar water pumping system was used. This indicated a feasibility study for low-power water pumping systems for small farms. The results revealed that solar systems show more favorable environmental effects compared to conventional systems. Specifically, when considering carbon footprint (measured in kg CO_2-equivalent per hectare-millimeter), the solar system yielded emissions of 0.009 kg, whereas grid-connected electric pumps and diesel pumps produced 1.214 kg and 0.382 kg of emissions, respectively, for 1 HP pump capacity and 20 m of total head. In terms of kg CO_2-equivalent per kWh, these values would be 0.011, 1.439, and 0.743 for these three types of irrigation systems, respectively. In general, this study showed the feasibility of using a low-power irrigation system for small-scale farms in western Rajasthan in the water scarcity situation of the region. In another study by Vishnupriyan et al. (Vishnupriyan, Partheeban, Dhanasekaran, & Shiva, 2022), the impact of varying tilt angles on the performance of a solar water pumping system was investigated for irrigation as well as drinking water supply. The researchers used PVsyst software for their numerical study, and they considered four different tilt angles (8, 15, 30, and 45 degrees). They evaluated the performance of the system with regard to solar production and performance ratio. The findings showed that the system reached its optimal performance at a 30-degree tilt angle. The optimization of tilt angles has been a subject of investigation by many researchers, with the choice of the most suitable angle depending on the

users' objectives to get maximum gain from solar and the intended application. In research in Australia by Powell et al. (Powell, Welsh, Pannell, & Kingwell, 2021), the adoption of SWPS by sugarcane farmers was studied. The survey used the Adoption and Diffusion Outcome Prediction Tool (ADOPT). This is a numerical tool that was designed for practical purposes. This tool considered over 1000 users in 43 countries (CSIRO, 2022). The survey includes different questions and evaluates common opinions and the underlying reasons. In addition, the study evaluated constraints that influence the adoption of solar PV systems by farmers. It was shown that the adoption of a solar system by the farmers is under influence of various factors, like risk factors, financial status, relative advantages, and environmental benefits, etc. The findings from this study provide valuable understanding for governments and policymakers about trends in farmers' adoption of solar systems.

In a study by Ashraf and Iqbal (Ashraf & Iqbal, 2020), two solar water pumping systems were compared in weather conditions of Rahim Yar Khan, Pakistan, with global horizontal irradiance ranging from 3.6 to 7.26 kWh/m^2/day. The goal of the study was to provide water for the irrigation of a Rhodes Grass farm of around 97 hectares. One system incorporated a battery bank, while the other featured a cylindrical water tank. HOMER software was employed for system design, sizing, and steady-state analysis, while MATLAB/Simulink was used for dynamic simulations of a solar water pumping project of 25 years lifetime. The sizing of both systems revealed that for the first configuration (i.e., system with battery), 73.8 kW of PV panel, and 450 Trojan SAGM 12V 105 Ah battery are required to run a motor of 11 kW. On the other hand, for the other configuration, a 72.3 kW PV panel is needed to power a 55-kW motor. The capacity of the water tank was about 4900 m^3. The economic evaluation showed that the SWPS designed with a water tank resulted in a cost-effective solution in comparison to a battery bank counterpart. More specifically, the system with a battery storage system had a net present cost of $273,570, while the system with a water tank resulted in a net present cost of $158,399. In another study, Ghoneim (Ghoneim, 2006) conducted an optimization study on a direct-coupled PV water pumping system in 2006. The performance of this system was evaluated from both technical and financial perspectives for a residential complex in remote areas of Kuwait, accommodating 300 individuals. The region has high

radiation of about 6 sun-hours per day. The analysis considered a water consumption rate of 40 liters per day per person, resulting in a daily water pumping commitment of 12 m^3. A computer program was developed to model the PV panel, MPPT, DC motor, centrifugal pump, and storage reservoir. The evaluation encompassed the sizing and orientation of the PV system, as well as system performance. They used a motor-pump model developed by (Eckstein, 1990) and (Al-Ibrahim, 1996). In their model, the pump's performance can be estimated by applying the affinity laws, which establish a correlation between the pump speed, flow rate of fluid, head, and power. Finally, the life cycle cost method was used to assess the financial feasibility of the system. The financial assessment indicated that the capital cost of the PVWPS was lower than that of a conventional diesel-based pumping system, while considering the high prices of PV panels at the time of the study. It was concluded that it was expected that the price of water pumps and PV panels would decrease each year, making the PV pumping systems more feasible. In 2020, on-farm applications of solar PV systems were evaluated by Gorjian et al. (Gorjian, Singh, Shukla, & Mazhar, 2020). They concluded that more technical and socio-economic research is needed to increase PV system adoption in the farming industry. They summarized the benefits and drawbacks of PV systems in the agriculture sector in Table 1.1.

Table 1.1 Advantages and disadvantages of PVWPS adoption in agriculture sector (Gorjian et al., 2020)

Advantages	**Disadvantages**
Being environmentally friendly	The reduction of efficiency due to the temperature increase of the panels
Easy to use in a hybrid model with conventional technologies	Being unpredictable and requiring storage options
Being noise-free	High investment costs
No inconformity between solar generation and consumption	High payback periods with a low benefit-to-cost ratio
Suitable for remote regions with limited access to fuel or grid electricity	PV cleaning requires water, which is scarce in arid areas
Adaptable in versatile combinations	Low energy and output power
Continuously reduced unit prices through mass production	Operation control, and optimization as major research areas.

In addition to the previously mentioned techniques, controlling strategies in solar systems are of high importance to maximize power generation. In this regard, Ammar et al. (Ammar,

Hamraoui, Belguellaoui, & Kheldoun, 2022) employed a DC-DC converter accomplished as maximum power point tracking in a battery-less PV water pumping system. They utilized a Brushless Direct Current (BLDC) motor to maximize the utilization of power generated by the array and to increase the reliability of the system. To improve control performance when there is partial shading, the authors suggested an MPPT strategy based on Cuckoo Swarm Optimization (CSO) and Perturb and Observe (P&O) techniques by using MATLAB/Simulink. P&O is one of the most common schemes used for maximum power point tracking (Zaheeruddin, Mishra, & Haque, 2016). The investigation of Ammar et al. revealed that the P&O method was not successful in searching for the global maximum power point. In contrast, the CS approach successfully identified the global peak while evading local maxima at partial shading conditions. Furthermore, the CS technique showed faster convergence and reduced oscillation around the maximum power point.

It is worth mentioning that there are numerous studies investigating different solar water pumping systems all over the world. For instance, in a study by Shahverdi et al. (Shahverdi, Bellos, Loni, Najafi, & Said, 2021), an organic Rankine cycle was employed to generate the necessary electricity for operating a pump responsible for water supply to a 3-hectare farm located in the southeastern part of Zanjan province. To provide the required heat for the Rankine cycle, a parabolic trough concentrator was utilized. The study explored eight different organic fluids, and the mathematical model was solved using EES Software. The results obtained from the numerical study were validated by experimental tests (Kasaeian, Daviran, Azarian, & Rashidi, 2015). The findings revealed that using Methyl Diethanolamine as the working fluid resulted in the best performance, leading to an efficiency of 12.19% for the system. However, it was shown that the payback period for the system was relatively high, calculated at 18 years. Since the main focus of this study is reviewing solar photovoltaic water pumping systems in Iran, we stop here and continue a literature review of PV water pumping systems in Iran in the following sections.

1.4 Aim of the study

As reviewed, numerous studies have been conducted on solar water pumping systems in various countries, including India (Rathore, Das, & Chauhan, 2018), China (Yu, Liu, Wang, Xiang, & Zhou, 2017), Saudi Arabia (Benghanem, Daffallah, & Almohammedi, 2018), Thailand (Imjai et al., 2020), and various regions around the world. For Iran, in spite of its significant solar potentials, there are limited research on SWPS. To the best of the authors' knowledge, there is no literature review on the subject of SWPS in Iran. The goal of this paper is to assess the status of research and application of solar water pumping technology in Iran. It aims to summarize the findings and compare the results of these investigations in accordance with the United Nations' Sustainable Development Goals (SDGs), particularly SDG 7 (affordable and clean energy), SDG 9 (industry, innovation, and infrastructure), SDG 11 (sustainable cities and communities), and SDG 13 (climate action), among the 17 established goals (United Nations, 2022). Initially, the paper discusses geographical location of Iran and its solar energy potentials. Then, it reviews solar water pumping research and technologies used in the country.

1.5 Geographical location of Iran and its solar energy potential

Iran, situated in the southwestern part of Asia, is a vast country with a latitude ranging from 25 to 40 degrees North and a longitude spanning from 44 to 65 degrees East (Moshir Panahi, Kalantari, Ghajarnia, Seifollahi-Aghmiuni, & Destouni, 2020). The total land area of Iran encompasses approximately 1.648×10^6 square kilometers (Rahimi, Ebrahimpour, & Khalili, 2013). The climate of major areas of this country is characterized as arid and semi-arid, and precipitation is limited to the winter months and is generally minimal, except on the northern flanks of the Alborz mountains, where it varies from 40 to 80 inches per year (Dewan & Famouri, 1968). On the other hand, Iran is ranked as the second-largest extractor of groundwater, with 56% of this water being used in the agricultural sector for food production as well as trade (Dalin, Wada, Kastner, & Puma, 2017). Eventually, Iran will be on the brink of a severe water crisis in the years ahead, mainly due to the rise in evapotranspiration rates that are attributed to climate change and global warming (Barati, Pour, & Sardooei, 2023). For

instance, the water reserves in the southwestern part of Iran have an annual evaporation rate of approximately 5 x 10^3 mm/year (Bazzi, Ebrahimi, & Aminnejad, 2021).

Table 1.2 and Figure 1.2 (Saatsaz & Rezaei, 2023) provide an overview of Iran's 31 provinces and its geographical map, respectively. The adoption of PV systems in Iran commenced in 1982 in Fars province, where they were initially used to supply the necessary electricity for a telecommunications site (Zabihi, Asl Soleimani, & Farhangi, 1998). Subsequently, the utilization of solar energy has gained momentum throughout the country. For example, in 1993, Iran's Ministry of Post, Telegraph, and Telephone initiated a production line for solar cells in Tehran (Zabihi et al., 1998).

Table 1.2 Provinces of Iran

Tehran	Kermanshah	Yazd
Alborz	Ilam	Esfahan
Markazi	Lorestan	Semnan
Ghazvin	Khuzestan	Mazandaran
Gilan	Chahar Mahaal and Bakhtiari	Golestan
Ardabil	Kuhgiluya and Buyer Ahmad	North Khorasan
Zanjan	Buschehr	Razavi Khorasan
East Azarbaijan	Fars	South Khorasan
West Azarbaijan	Hormozgan	Ghom
Kordestan	Sistan and Baluchestan	
Hamedan	Kerman	

It is noteworthy that the agriculture industry in Iran consumed a substantial amount of fossil fuels in 2016, including at least 2.7 billion liters of diesel fuel, 16.25 million liters of kerosene, 5.4 million liters of fuel oil, and 237 thousand liters of gasoline. This extensive fuel consumption resulted in the emission of approximately 12.5 million tons of CO_2 (Chahartaghi & Nikzad, 2021). Iran is blessed with abundant solar irradiation, experiencing more than 300 sunny days annually (SATBA Iran, 2022). Alamdari et al. (Alamdari, Nematollahi, & Alemrajabi, 2013) concluded that the central and southern regions of Iran exhibit a more favorable potential for the utilization of solar energy.

Figure 1.2 Map of Iran with its 31 provinces,
taken from (Saatsaz & Rezaei, 2023); reused under
('CC BY 4.0; Attribution 4.0 International', 2022)

In addition to the high solar energy potential of the country, Gorjian et al. (Gorjian, Zadeh, Eltrop, Shamshiri, & Amanlou, 2019) summarized the obstacles to the PV industry in Iran into four categories. The first one is technical gaps leading to the production of low-efficiency PV panels. The second one is Iran's dust and dry weather conditions, which both lead to a decrease in output power generation. The third one is the existence of weak governance laws like a rapid decline in government-guaranteed purchase rates. They finally declared the lack of a sustainable roadmap like not financing research and development in this sector, as the last barrier.

1.6 Solar photovoltaic water pumping systems in Iran

In the following first section, available research done in the country will be reviewed, and then in the second part, the results will be summarized to get a better insight.

1.6.1 Literature review of current status of PVWPS in Iran

As previously mentioned, there is a scarcity of studies on solar water pumping applications in Iran (Parvaresh Rizi, Ashrafzadeh, & Ramezani, 2019). This section aims to provide a chronological overview of all relevant studies pertaining to PVWPSs in Iran.

In 2006, Abdolzadeh et al. (Abdolzadeh, Ameri, & Mehrabian, 2011) evaluated the effect of water spray on the panel's front side on its performance. The experimental setup, located in Kerman, consisted of three and two photovoltaic modules, each with a nominal power of 45 W, one positive displacement water pump, a controller, a pyranometer, temperature sensors, and flow meters. Three different cases were considered. In case A, two PV panels were connected with a water spray flow rate of 25 liters/hour per module. In case B_1, three modules were connected with a water spray flow rate of 5 liters/hour per module. Finally, in case B_2, three panels were connected with a water flow rate of 25 liters/hour per module. In all cases, a total head of 16 m was applied for water pumping. The results of improvements in the performance of the panels and the system are shown in Table 1.3. It can be seen that in case A, the water pumping of the system increases by approximately 34.4% (from 479 to 644 L/h), while around 40% increment is seen in case B_2, where 25 L/h of cooling water is used per module (i.e., from 600 to 840 L/h). Furthermore, the module efficiency increases from 9.26 % to 12.35 % in Case A, and from 8 % to 10.16 % and 12.35 % in Cases B_1 and B_2, respectively, which are considerable improvements due to the hot weather conditions of Kerman City. The same authors (Abdolzadeh, Ameri, & Mehrabian, 2009) in the same year, evaluated the impact of operating head on PVWPS performance with the same setup in Kerman. The research investigated two different configurations (two and three panels, each 45 W connected in parallel) and four different operating heads (6, 10, 16, and 20 m) in order to increase the

efficiency of the system. Their investigation focused on the importance of selecting the maximum power for the chosen head to meet the needs of the user to decrease costs relevant to installation. Different parameters that affect the efficiency of PVWPS, like the arrangement of panels and pump flow rates, were evaluated. It was shown that the maximum efficiency happens at a head of 20m for a three-panel configuration, leading to an efficiency of about 10%. However, the efficiency decreases at lower heads due to a mismatch between PV and motor-pump power. The results show the significance of considering both the power of the pump at maximum speed and consumer needs in PVWPS design to minimize the capital costs of the project.

Table 1.3 Details of cooling effect on performance of the system (Abdolzadeh et al., 2011)

Parameters	**Two PV modules**		**Three PV modules**		
Case	No cooling	Water spray (A)	No cooling	Water spray (B1, B2)	
PV output power (W)	55.4	66.9	71.39	84.8	97
Pumping flow rate (L/h)	479	644	600	744	840
PV module efficiency (%)	9.26	12.35	8	10.16	12.35
Global irradiation (W/m^2)	800	800	800	800	800
Total Efficiency (%)	3.75	5.1	3.69	4.4	5.11
Water spray (L/h)	-	50	-	15	75

In 2010, Kordzadeh (Kordzadeh, 2010) studied the efficiency of PV panels in water pumping applications. The main goal of the research was to find techniques for increasing the efficiency of the system and hence the water pumping system. The location of the study was Kerman. This city has high solar potential. As the operating temperature of PV cells increases, their open-circuit voltage decreases, subsequently affecting their efficiency and output power. Therefore, the study aimed to explore the impact of system head and nominal power on the efficiency of SWPS. To lower the temperature increase of the panels, a thin layer of water was used for cooling. The experimental system had three panels, one controller, a motor-pump (PS150 Boost Lorentz), and a filter. The maximum head for pumping was 45 meters and the maximum flow rate was 1 x 10^3 liters per hour. The pump was responsible for supplying a thin film of water for the panels. Irradiance levels were monitored using a pyranometer. Two sets

of PV panels with nominal powers of 90 and 135 Watts were used (i.e., two or three panels each with 45 Watts nominal power). Three different system heads of 10, 12.5, and 16 meters were considered. The study showed that using a thin layer of water as a cooling system on the panels could enhance their optical characteristics and consequently their short-circuit current increases. Therefore, this improvement resulted in an enhancement of the overall output power. The study concluded that a reduction in nominal power of PV panels and an increase in the system head could lead to improvements in power generation and overall system efficiency. The panel efficiency is in the range of 7 to 14 percent for different conditions. In 2012, Tabaei and Ameri (Tabaei & Ameri, 2012) conducted a study to evaluate the impact of booster reflectors on the efficiency of a solar water pumping system at Shahid Bahonar University of Kerman in the city of Kerman during the summer season. The study evaluated two different materials for these reflectors: stainless steel 304 and aluminum foil. The goal was to evaluate their effects on power generation and water pumping flow rates. The PV panels had a tilt angle equal to the latitude of Kerman city (i.e., approximately 30 degrees). To improve energy extraction, an MPPT system was used. The study showed that aluminum foil reflectors had better performance compared to stainless steel in terms of both power generation and water pumping flow rates. This was attributed to the higher reflectivity characteristics of aluminum. It was found that the use of reflector boosters has two opposing effects on the performance of the system. On one hand, it improves irradiation values, which increases the output current of the panels. On the contrary, it resulted to an enhancement in panel temperature, which is not favorable since it decreases the voltage of the panel. However, the study showed that the positive effect outweighed the negative impact of voltage reduction. Therefore, the use of a reflector booster was deemed beneficial for the system. The study did not employ any cooling technique to keep the panel temperature low but suggested using passive or active cooling methods to improve the performance of PV panels with concentrators. The study indicated that the daily average power generation saw an increase of 14% with aluminum foil reflectors and 8.4% with stainless steel foil reflectors. Furthermore, an 18% increase in pump flow rates with the aluminum foil reflector and a 9% increase for the stainless-steel reflector were reported. In 2013, Rezae and Gholamian (Rezae & Gholamian, 2013) conducted a study relevant to solar water pumping in northern Iran. They employed RETScreen software to analyze the technical

and financial aspects of solar water pumping systems. The study focused on water pumping for a farm field located in Gorgan city, the administrative center of Golestan province, with a latitude of 36.8 degrees North and a longitude of 54.5 degrees West. The study reported the average solar irradiation in this city as 4.35 kWh/m^2-day, with a maximum of 6.42 kWh/m^2-day in June and a minimum of 2.2 kWh/m^2-day in December. Their investigation involved a PV panel (SANYO HIT Power 195 BA20) with two diodes. The model comprised a PV array, a power conditioner, a battery bank (ATLAS BX; 12 V-100 Ah), and a pumping system (MOTOGEN- CR90L2A electromotor) designed to meet the water demands of the farm during the irrigation time, which spans from April to September. The battery storage is used to provide energy at night for water pumping. Regarding financial analysis, the study compared the income generated by the renewable energy system with that of a conventional diesel pumping system. The project's expected lifetime was set at 25 years, with an inflation rate of 10 percent. Initially, the study considered the price of government-subsidized gasoil. The research demonstrated that the payback period for the renewable project was 14 years under these conditions. However, when considering the price of gasoil at the FOB Persian Gulf market, the payback period is reduced to six years, Figure 1.3. The study concluded that the adoption of solar energy could be further incentivized by government-provided loans for renewable energy projects. Furthermore, fixed efficiency for motor-pump systems is used, which can lead to substantial errors in numerical simulations.

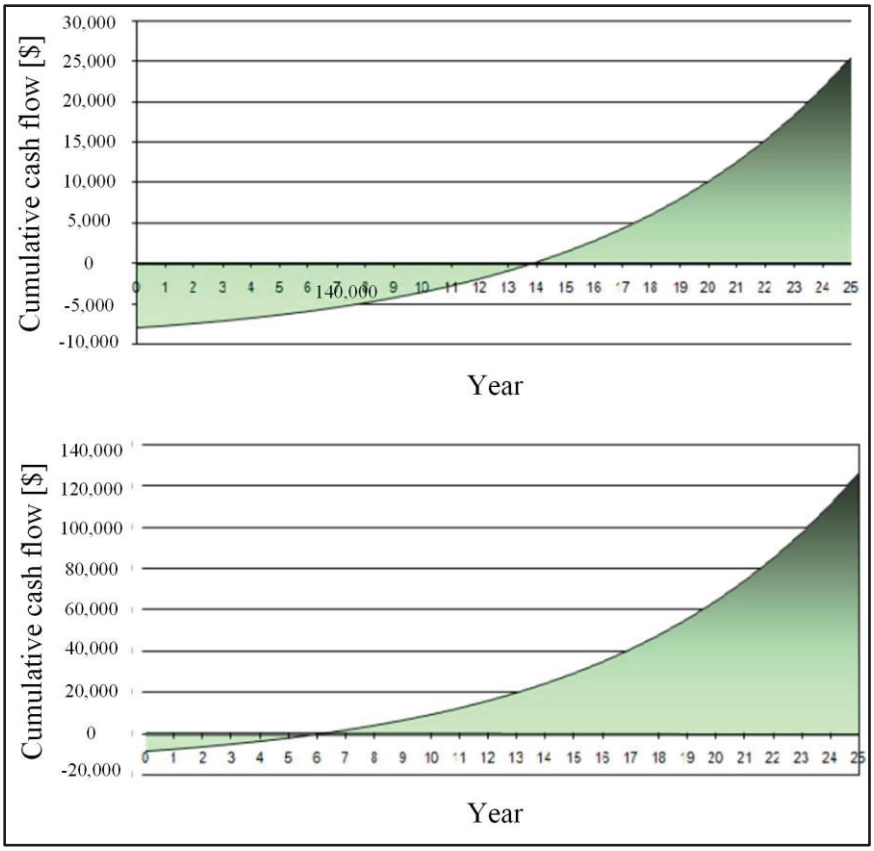

Figure 1.3 Cumulative cash flow for subsidized gasoil price (top) and Persian Gulf market gasoil price (bottom), taken from (Rezae & Gholamian, 2013)

In 2015, Habiballahi et al. conducted a study aimed at improving the efficiency of PV panels through water cooling (Habiballahi, Ameri, & Mansouri, 2015). The primary objective of the study was to enhance the efficiency of PV panels and consequently the water flow rate by implementing thermal collectors positioned beneath the PV surface. The pumping mechanism directs water through these collectors, where it serves to cool the system before being redirected into the primary water pumping path. The experimental setup, located in Kerman, consisted of three 45 W photovoltaic modules connected in series, one positive displacement water pump featuring a DC motor (PS150 Boost with 45 m maximum head and maximum flow rate of 850 L/hour), a controller, a pyranometer for measuring solar irradiance, three temperature sensors, and two flow meters. The PV panels were tilted at an angle of 30 degrees, matching the latitude of Kerman city. The study considered two different heads of 10 and 16 meters, along with three distinct collector mass flow rates. The results of the study revealed

that at a head of 16 meters and a collector mass flow rate of 310 L/hour, the photovoltaic cell efficiency and the overall efficiency of the PV water pumping system increased by 2.04% and 1.08%, respectively. This led to about a 20% improvement in mean power and a 29% increase in mean water flow rate. In another study conducted in 2015 by Tabaei and Ameri (Tabaei & Ameri, 2015), the detrimental impact of increasing cell temperature on the efficiency of PV panels within a solar water pumping system that incorporated booster reflectors was investigated. In this study, the panels were cooled by the circulation of water and by providing a continuous film of water on the front surface of the panels. The water was redirected into the main water pumping stream. The measurements were done within a three-week period in June and July. The optimized angle of the reflectors relative to the horizon was obtained to be 45 degrees, as shown in Figure 1.4. The study examined four different conditions for the PV panels: 1) without a reflector, 2) with a reflector, 3) without a reflector and with a water film, and 4) with a reflector and with a water film. The findings of the study indicated that panels equipped with booster reflectors and cooled with a water film demonstrated the best performance among the tested configurations. Specifically, panels with reflectors and a water film improved the panel's output power by up to 50.4%. For comparison, details are given in Table 1.4.

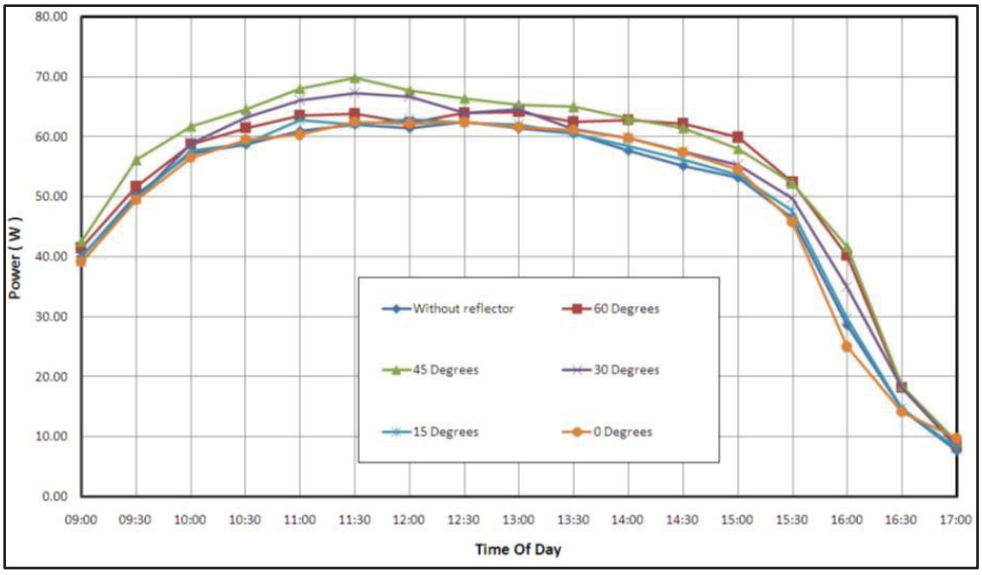

Figure 1.4 Variations of output power at different reflector positions, taken from (Tabaei & Ameri, 2015)

Table 1.4 Improvements in output power by using reflector and water cooling (Tabaei & Ameri, 2015)

	Conventional panels	**Panels with reflector**	**Panels with cooling**	**Panels with reflector and cooling**
Mean daily power (W)	51.6	58.8	60.8	77.6
Improvement (%)	Not Applicable	14.0	17.8	50.4

In 2015, Mohammadi (Mohammadi, 2015) conducted a numerical investigation to optimize the technical and economic aspects of an SWPS. While the exact location of the study was not specified, it was mentioned that the study focused on the southern part of Iran with the goal of providing 56 m^3 of water for irrigation and drinking each day. The analogy between a battery bank and water tank was applied in the simulation. Two key parameters, i.e., loss of load probability and life cycle cost, were considered to evaluate the performance of the water pumping system. The loss of load probability was defined as the ratio of water deficit to water demand. These two parameters showed a conflicting relationship: increasing the number of panels improved technical reliability but reduced economic viability. To address this complex problem, the non-dominated sorting genetic algorithm (NSGA) method was employed that

resulted in various decision variables for the obtained solutions. The number of PV panels was changed between 2 to 5 each panel with 55 W of nominal power and the autonomy days for the water tank varied between 3 to 9 days. In the same year, Karami Rad et al. (Karami Rad, Omid, Alimardani, & Mousazadeh, 2015) conducted a feasibility study in which they designed a standalone solar-based Microner sprayer, creating a prototype for technical evaluations. A small battery was employed to serve as a stabilizer in the system. The system consisted of a sprayer, a 10-W solar power supply, and a control system. Meteorological data from NASA for Karaj in the Alborz province were used in the study, with LabVIEW software employed for data acquisition. The system was capable of operating for 7 to 9 hours per day which makes it an applicable system for use in agriculture spraying. The study demonstrated that this designed system could be deployed in remote areas to address environmental challenges and the lack of access to traditional fossil fuel systems.

In 2017, Niajalili et al. (Niajalili, Mayeli, Naghashzadegan, & Poshtiri, 2017) investigated a solar water pumping system in the north of Iran, in Gilan province. This region experiences significant precipitation. It is worth noting that the cuisine in Iran is diverse, but rice-based dishes are common for most of people (Karizaki, 2016). Rice is a primary agricultural product in the northern part of the country. Given this, the use of a solar water pumping system for rice cultivation in the northern regions becomes particularly interesting. The study of Niajalili et al. (Niajalili et al., 2017) encompassed both technical and economic aspects of employing solar water pumping for rice fields. The technical analysis involved finding the sizing of the photovoltaic panels, while the economic study evaluated the lifecycle costs of the system and compared them to conventional pumping systems. One of the main challenges shown in the paper was the high CAPEX of solar systems. However, the decreasing price of PV panels and the instability of fuel prices were cited as compelling reasons for the growing interest in PV systems. Due to the relatively lower solar irradiation levels in Gilan province compared to other regions, the study considered only the sunny months of the year. During the summer, the average daily temperature in the region is around 25°C. Minimum relative humidity was 74 percent. On average, there are 5.81 hours of sunshine per day in summer, which makes it suitable for irrigation applications. The study focused on a rice field with an area of 5×10^3

square meters, using irrigation water requirements (IWR) as the basis for determining the water demand for the rice paddies. While there are many cloudy days, the average clearness index during the irrigation period justified the use of PV pumping systems in Gilan province. To account for cloudy days, the model included batteries to ensure continuous operation. To compare the PV system with conventional non-renewable water pumping systems, the study examined a gasoline-driven pump for supplying water to the rice paddy. The economic analysis showed that the initial cost of the PVWPS was seven times higher than that of the conventional gasoline motor-pumping system. However, it took about nine years for the total cost of both systems to become equal. After this payback period, the renewable system becomes more cost-effective than the gasoline system. Over a 25-year period of irrigation, the final expenses of the gasoline system were about 1.56 times that of the PV pumping system, demonstrating the cost-efficiency of the renewable system in the long term. Figure 1.5 illustrates the life cycle cost of the system.

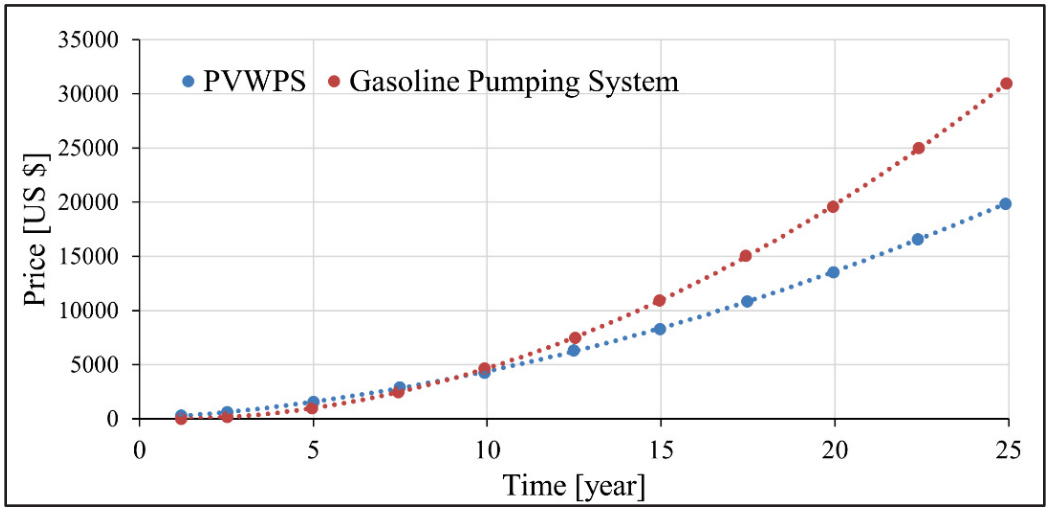

Figure 1.5 Lifecycle cost estimation over 25 years,
data from (Niajalili et al., 2017)

In 2018, Shirinabadi et al. (Shirinabadi, Samadi Saray, & Maanifar, 2018) evaluated the feasibility of solar PV systems for a water pumping station in Tabriz, northwest of Iran, aiming to reduce national grid use and to decrease the environmental impacts. They studied an 800 kW PV power plant equipped with a two-axis sun tracker. They used PVSYST software to simulate the performance of the system while taking into account parameters including losses

and geographic location. The annual global horizontal irradiation of the location was 1886.4 kWh/m^2 and the global panels' incident irradiation of 2169.1 kWh/m^2. They used 2670 PV panels each with nominal power of 300 W to produce the required electricity for running four AC horizontal centrifugal electro-pumps each with a capacity of 250 kW. The system consisted of 92 inverters of 8.6 kW nominal power with 96.5% efficiency. The goal of the study was to examine the feasibility of replacing a conventional grid-based water pumping system with PVWPS. They concluded that the proposed system can avoid the emission of approximately 509 tons of $CO_{2\text{-eq}}$ per year. In a 2019 study by Parvaresh Rizi et al. (Parvaresh Rizi et al., 2019), two case studies were analyzed, focusing on a citrus orchard in the southern city of Jahrom and a vineyard in the eastern city of Kashmar, both located in Iran. The research aimed to evaluate the financial aspects of SWPS in comparison to conventional pumps that use grid electricity or fossil fuels. Three types of pumps are considered: solar, diesel, and electricity-driven. The study showed some critical results. For pumps with power ratings more than 3 kW, it was more economical to obtain the required electricity from a private power line compared to electricity generation locally by a solar PV system. Especially if the transmission line was located within 2 kilometers of the site. However, for pumps with power ratings less than 4.5 kW, a PVWPS was found to be competitive with conventional fossil fuel-based systems. The study showed that Iran's subsidies for fossil fuels result in low fuel and electricity costs. Therefore, investment in solar pumping systems has financial challenges and may become feasible with incentives. In addition, the research showed that the high interest rates make renewable energy systems less attractive. The dependency on imported components for SWPS is another factor that affects the adoption of solar systems in the country. This is due to the fact that the prices of these components are dependent on the exchange rate. This exchange rate is subject to significant fluctuations and it is often linked to Iran's foreign policy decisions. This can negatively affect the affordability and feasibility of solar systems. In brief, SWPS have benefits for irrigation in the country, however, some economic and challenges that are relevant to the policy of the country, like fuel subsidies, interest rates, etc., affect their adaptation in the country.

In 2019, a research study was conducted at the Gharakhil Weather Station in Mazandaran province, located at a latitude of 36 degrees North and a longitude of 52 degrees East (Chahartaghi, Mehdi, & Jaloodar, 2019). This study focused on solar water pumping and involved mathematical modeling. The goal was to understand how tilt angle affected the water pump's discharge rate. In addition, the study evaluated effect of ambient temperature on the efficiency of the water pump. The novelty of the research was in the implementation of a SWPS for a drip irrigation network. The solar water pumping system in this investigation was designed for direct coupling with drip irrigation, and notably, it did not incorporate a battery bank. The findings indicated that the system achieved its maximum annual water discharge when the solar panels were tilted at angles close to the latitude (i.e., at a tilt angle of 41 degrees). Moreover, it was shown that an increase in the panel temperature could lower power generation capacity, mainly in the hot season, leading to an 11% reduction in PV panel efficiency.

In another 2019 study, Zamanlou and Iqbal (Mohammad Zamanlou;Tariq Iqbal, 2019) conducted a feasibility analysis of a solar water pumping system in Urmia City, West Azarbaijan, located in northwest Iran. Their study focused on a grape garden spanning an area of 2.36 hectares and 9638 cubic meters of water requirement for irrigation per year. This amount of water should be pumped to an elevation of around 25 meters with a friction loss of 2.15 meters. Based on the average sunshine hours of the region, which equals 8.8 hours per day, they selected a volumetric flow rate of 6 cubic meters per hour for the garden irrigation. The system was equipped with battery banks and MPPT in order to maximize irradiation harvest. To determine the irrigation water requirements, they employed the CropWat model. The selection and sizing of electrical components for the system were carried out using HOMER Pro software. The researchers used the Lorentz Compass program to choose an appropriate water pump, and MATLAB Simulink was utilized for assessing the dynamic performance of the system in terms of electricity generation and load requirements. Despite the feasibility study and from an economic perspective, they estimated the total cost of the irrigation system to be approximately C$24 thousand. They also showed that the MPPT system was successfully operating and its voltage at maximum point tracking was very close to the PV voltage at laboratory conditions of 25°C and 800 W/m^2 irradiance.

In 2019, a case study on solar water pumping was conducted in the city of Sari, located in Mazandaran province in northern Iran, with coordinates at approximately 36.57 degrees North latitude and 53.06 degrees East longitude (Nikzad, Chahartaghi, & Ahmadi, 2019). This study included a notable comparison of solar irradiation levels in Mazandaran province with those in Germany. The average solar irradiation in the region was in the range of 3.8 to 4.2 kWh/m^2-day, and it was higher than the average of 3.3 kWh/m^2-day for Germany. It's worth mentioning that other regions in Iran have higher solar irradiation potentials compared to the northern parts. The study encompassed a comprehensive analysis of economic, environmental, and technical aspects related to a 1-hectare (1 x 10^4 square meters) rice paddy. One novelty of the research was the consideration of electricity generation during non-irrigation months and selling the excess electricity to the government under a power purchase agreement (PPA). This PPA ensured the procurement of the generated electricity by the government. However, the land should be situated in proximity to a power grid. The study also showed reductions in CO_2 emissions, noise pollution, and savings in fossil fuels. The researchers also studied parameters like optimal tilt angle for the panels, their sizing and arrangement, and the design of a battery storage system. A VICTRON Energy MPPT charge controller is used to increase power generation. A growing period of 145 days was considered for the cultivation of rice, from April 15 to September 6. In addition, the research considered 15 cloudy days, with the possibility of a maximum of three consecutive cloudy days for each month. Two scenarios were evaluated: an off-grid and an on-grid model. In the on-grid model, excess power could be sold to the government under an agreement. It was indicated that the CAPEX of the on-grid model was 2.41 times that of the conventional system, as illustrated in Figure 1.6. However, the life cycle cost of the conventional system would be 2.89 times that of the on-grid model over the life cycle of the system. The payback period for the on-grid model was estimated to be about 4.7 years. On the other hand, the CAPEX of the off-grid model was 2.14 times that of the conventional system. Nevertheless, after 20 years of operation, the life cycle cost of the conventional diesel system would be only 1.30 times that of the off-grid renewable model. The payback period for the off-grid model was 5.6 years. In addition, the results showed that using the off-grid solar system could avoid the production of about 5 tons of CO_2. In addition, this

would result in less diesel fuel and engine oil consumption by about 1750 and 85 liters, respectively. In terms of noise pollution, the on-grid solar water pumping system emitted 71 percent less noise compared to the conventional diesel motor-pump system. The noise produced by the diesel engine was experimentally measured by the Sound Meter Smart Tools software installed on a Samsung cellphone. It's important to note that the off-grid model did not contribute to noise pollution.

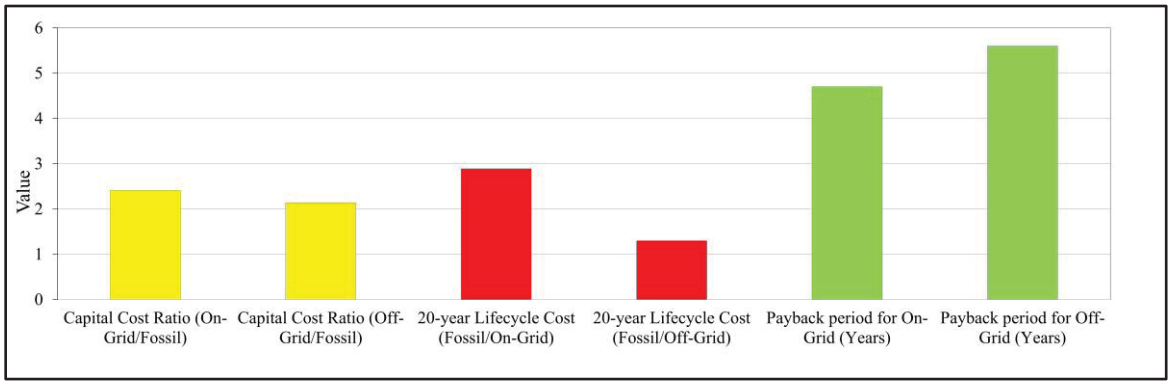

Figure 1.6 Financial comparison of different models for reference (Nikzad et al., 2019)

In a study conducted by Shayeteh and Kardehi Moghaddam (Shayeteh, Reihaneh, & Moghaddam, 2020) in 2020, a multi-objective firefly algorithm based on crowding distance (CD-MOFA) was employed to optimize a PV water pumping station located in Bojnurd, North-East of Iran. This battery-less system comprised PV arrays, inverters, an AC motor-pump system, and a storage reservoir. The system is designed to pump water to a hydraulic head of 84 m. The climate data specific to the station were obtained from Metronome software, and MATLAB was employed for numerical simulations. The non-optimized system was introduced as an existing system with 25 PV arrays with a total power capacity of 3.96 kW tilted at 39 degrees with an azimuth angle of -5 that could produce 76 m^3 of water per day. The optimization process focused on two key variables: the solar azimuth angle and the tilt angle. By optimizing these variables, the researchers aimed to increase the water pumping capacity of the system while simultaneously minimizing its overall cost. In fact, they considered two conflicting objective functions. Annual revenue and life cycle cost of the system. The algorithm optimizes the income by making a balance between annual revenue, CAPEX, O&M

and replacement costs. This leads to an improvement in water output and hence maximizes profits from water sales. In addition, it decreases system size, and lowers overall costs. It was concluded that the utilization of this method results in a considerable reduction in the system's cost and payback period, and a reduction of 19 percent is obtained compared to a system with no optimization.

In another study conducted by Ghasemi-Mobtaker et al. in 2020 (Ghasemi-Mobtaker, Mostashari-Rad, Saber, Chau, & Nabavi-Pelesaraei, 2020), a 100-hectare barley farm located in Hamedan was subjected to numerical analysis for two distinct irrigation scenarios: surface irrigation (SFI) and sprinkler irrigation (SPI) by using grid electricity and fossil fuel. The study aimed to evaluate the potential of using a PV system for irrigation named SFI-PV and SPI-PV. TRNSYS was used, and the climate data were extracted from Metronome database. The energy consumption and environmental impact of each irrigation scenario were evaluated. For energy inputs, for SFI, electricity has the main contribution (around 50%) while diesel fuel has the main share for the SPI method (around 40%). To evaluate energy indices of barley production and based on the definition of energy use efficiency (EUE), which is total output energy (TOE) divided by total input energy (TIE), they showed that EUE for SPI and SFI techniques are 2.8 and 2.85, respectively. Energy equivalent values for the diesel fuel used in both irrigation techniques are calculated and added to the electricity energy used and the total amount that should be replaced by solar PV panels is obtained as 1959 and 2285 kWh for SFI and SPI, respectively. The TRNSYS simulations for irrigation for the production period of barley cultivation showed that the maximum photovoltaic power for SFI-PV and SPI-PV systems are 4.55 and 5.20 kW, respectively. Furthermore, the results of the study revealed that, given that pumping stations typically rely on diesel fuel for pumping operations, the sprinkler irrigation method resulted in substantial CO_2 emissions equal to 1184 kg/ha compared to 425 kg/ha for SFI. On the other hand, it was concluded that, the surface irrigation method with PV panels (SFI-PV) was the most favorable option from an environmental aspect since it has the least damage.

In a study by Chahartaghi and Nikzad (Chahartaghi & Nikzad, 2021) in 2021, different technical parameters related to SWPS for irrigation of a 1-hectare potato farm located in Isfahan were studied. These parameters involved PV panel temperature and its arrangements, PV efficiency, output power, pump speed, and the pump's discharge rate. In addition, the study evaluated the exergy efficiency of the PVWPS. Different water requirements during the crop growth period from February 3rd to June 14th (130 days) were considered. An ideal tilt angle of 25 degrees was obtained based on the maximum total global irradiation during this period. It was shown that using two parallel strings, each with 16 panels of 300 W nominal power, would be sufficient. They concluded that when irradiation values are higher than 900 W/m^2, the influence of ambient temperature on pump outlet discharge is negligible. They also studied exergy efficiency as the ratio of total output to total input exergy of the system. For sensitivity analysis, solar irradiations of 600, 700, 800, 900, 1000, and 1100 W/m^2 were considered at different ambient temperatures of 10, 14, 18, 22, 26, and 30 ˚C. It was shown that the maximum and minimum exergy efficiencies are 3.56 and 0.27 %, much lower than the conventional values for PV electrical efficiency. In fact, the exergy efficiency for irradiations between 600 to 800 W/m^2 did not consistently exhibit upward or downward trends. This is because while an irradiation improvement at a constant ambient temperature consistently leads to a great rise in input exergy, the corresponding increment in output exergy, however, is not as pronounced in that radiation range. Furthermore, it was shown that using a solar system could avoid the annual emission of 4.8 tons of CO_2, equal to 11.1 barrels of crude oil. The study also studied the use of a sun tracker system along with its economic effects. Ultimately, due to higher capital and operational costs, as well as increased system complexity and space requirements, the use of a sun tracker system was not deemed suitable for their model. In another investigation conducted in the same year by Heydari et al. (Heydari, Maleki, Jabari Moghadam, & Haghighat, 2021) , the feasibility of solar water pumping was assessed in three provinces: North Khorasan, Khorasan Razavi, and South Khorasan. This assessment was carried out using a multi-criteria decision-making method. The researchers considered a total of 93 sites across these three provinces and applied 15 significant criteria, including factors like solar irradiation, wind speed, precipitation, distance from the river, and proximity to the grid. Each criterion was weighted using the Shannon entropy method. This technique uses a criterion–option matrix, as

introduced by Shannon (Mark A. Shannon; Paul W. Bohn; Menachem Elimelech; John G. Georgiadis; Benito J. Mariñas; Anne M. Mayes, 2008), to measure the uncertainty level of a continuous probability distribution. The main concept of this method is that a criterion with high dispersion is supposed to have significant importance. 30 different sensitivity analyses were done to ensure the reliability of the results. The study revealed that Sarayan was identified as the most suitable site for establishing a stand-alone water pumping station in 28 out of 30 analyses. The second-best site was found to be the Isk station. They concluded that these results provide a practical framework for selecting the most suitable site within a region for implementing a solar water pumping project.

In 2022, Jahanfar and Tariq Iqbal presented the main findings of their research at two conferences. In the first article (Jahanfar & Iqbal, 2022a), optimization of the size of the hybrid (Battery+ Water tank) system was done by using HOMER Pro. The design of a reliable system with adequate storage and minimum life cycle cost. A 2-hectare cherry and apple garden near Mashhad city, north-east of Iran was selected where a conventional diesel generator was the energy source for providing about 180 m^3 of water per day. The Imperialist Competitive Algorithm (ICA) was used as the optimization tool for replacing the current conventional system with PVWPS. This algorithm was first developed by Atashpaz Gargari (Atashpaz-Gargari & Lucas, 2007) and it works by selecting an initial point at random, named a "country." These countries are then divided into two sets: imperialists and colonies, with each colony being affiliated with an imperialist. Then, imperialists participate in a competition among themselves to acquire control over more colonies. Finally, the most dominant imperialists take control of all countries, guiding them toward an optimal state. The results of the optimization analysis led to a system with 40 batteries (each 100Ah) and 140 cubic meters of water tank with approximately C$20 thousand total cost. In the second article (Jahanfar & Iqbal, 2022b), they evaluated the reliability of a PVWPS in the hybrid storage mode of the battery bank system and water tank. The hybrid storage system proposed in the previous study was shown to be a cost-effective solution to ensure the system's operation even in zero or low irradiations. They used MATLAB Simulink to study the dynamic response of the system in different conditions of load changes and temperature variations and showed that the proposed system is

stable in variable weather conditions. It was shown that temperature variations do not considerably affect the system's performance.

In 2023, Irandoostshahrestani and Rousse (Irandoostshahrestani & R. Rousse, 2023) developed a MATLAB code for the evaluation of PVWPS in the south of Iran, in Bandar Abbas city. The algorithm was designed in order to provide power for a rural house with typical load demand and to charge the batteries when the residential load demand is met and finally, to run a water pumping system in case the batteries are full with the excess electricity produced by the PV panels. Details about the algorithm can be seen in Figure 1.7. The pumped water was aimed at irrigating a citrus farm with an area of 1 hectare and a bell-shaped irrigation water requirement profile in different months of the year. The total dynamic head was set to 8m and monocrystalline panels with a nominal power of 305 W were used. They used water shortage probability (WSP) and loss of power supply probability (LPSP) concepts in their design. Different configurations with various installed battery capacities and PV panels were suggested. They concluded that the selection of the best configuration depends on the WSP and LPSP tolerance of the users. In fact, a slight increment of power loss tolerance can considerably decrease the system's size, capital cost, and LCOE, with minimal effect on WSP. This implies that users with constrained financial resources have to explore additional plans to prevent irrigation water shortage. It was also concluded that there exists a minimum point on the CAPEX versus PV panels number diagram. Limited changes in WSP and LCOE occur with additional increments in the panel number. This is attributed to the rapid increase in battery bank requirements lower than the minimal panel numbers, Figure 1.8.

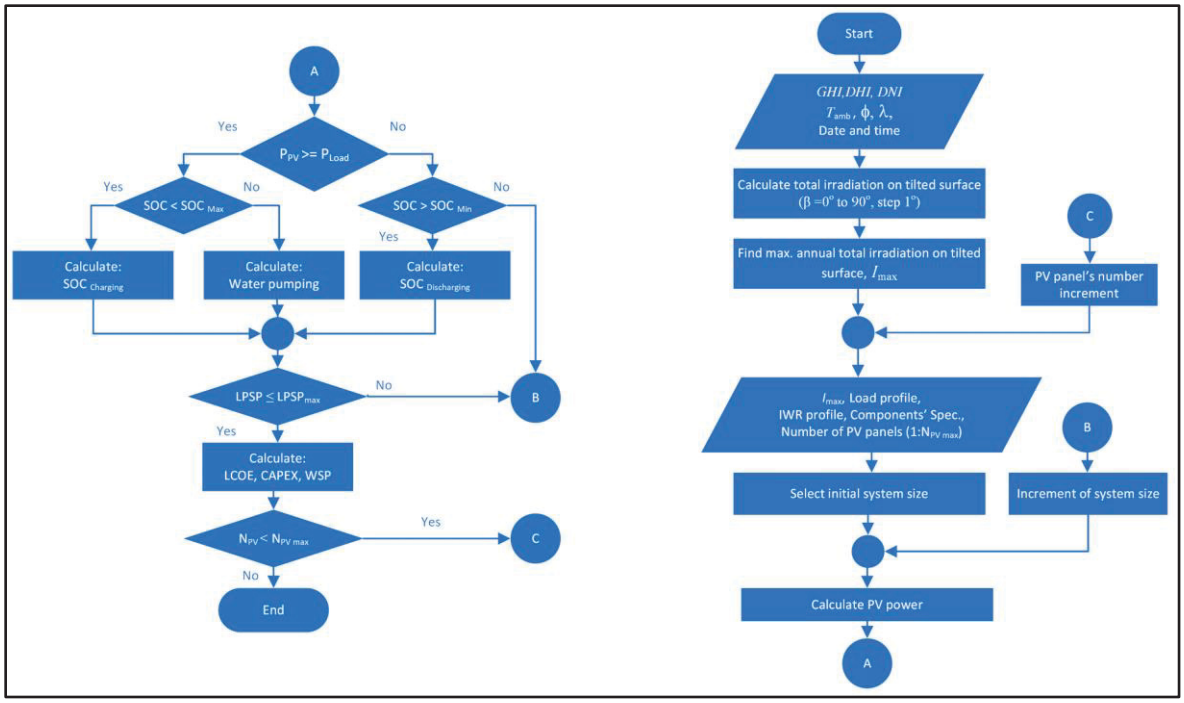

Figure 1.7 The PVWPS algorithm used in reference,
Taken from (Irandoostshahrestani & R. Rousse, 2023)

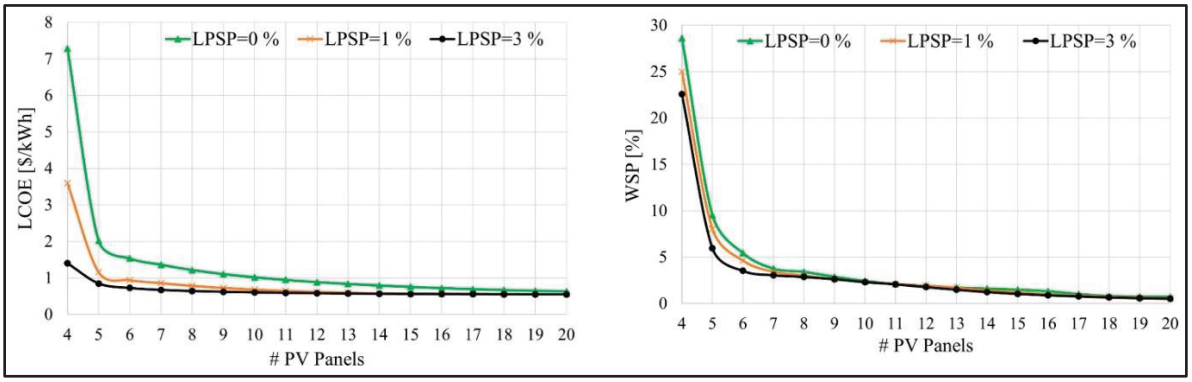

Figure 1.8 Variations of LCOE and WSP with PV panel numbers at different LPSPs,
taken from (Irandoostshahrestani & R. Rousse, 2023)

1.6.2 Summary of the PVWPS in Iran

For comparison purposes, we have summarized the results of the study in Table 1.5. It can be seen that only a few investigations have comprehensively explored solar water pumping from technical, economic, and environmental aspects. In addition, no study has evaluated the social

implications of adopting SWPS. Many of these researches have been done in recent years, as shown in Figure 1.9. The number of studies shows a considerable increase in the utilization of solar water pumping in the country in the past few years. Almost all of these studies have experimental setups or numerical simulations, and they are primarily focused on the feasibility study for agricultural irrigation. Not all regions of Iran have been evaluated for SWPS. However, the available research has covered a wide range of locations. This diverse implementation is a result of the country's good potential for solar energy. Even in the northern regions with lower solar irradiation intensity compared to the southern and central areas, renewable energy solutions for water pumping remain a viable and attractive option.

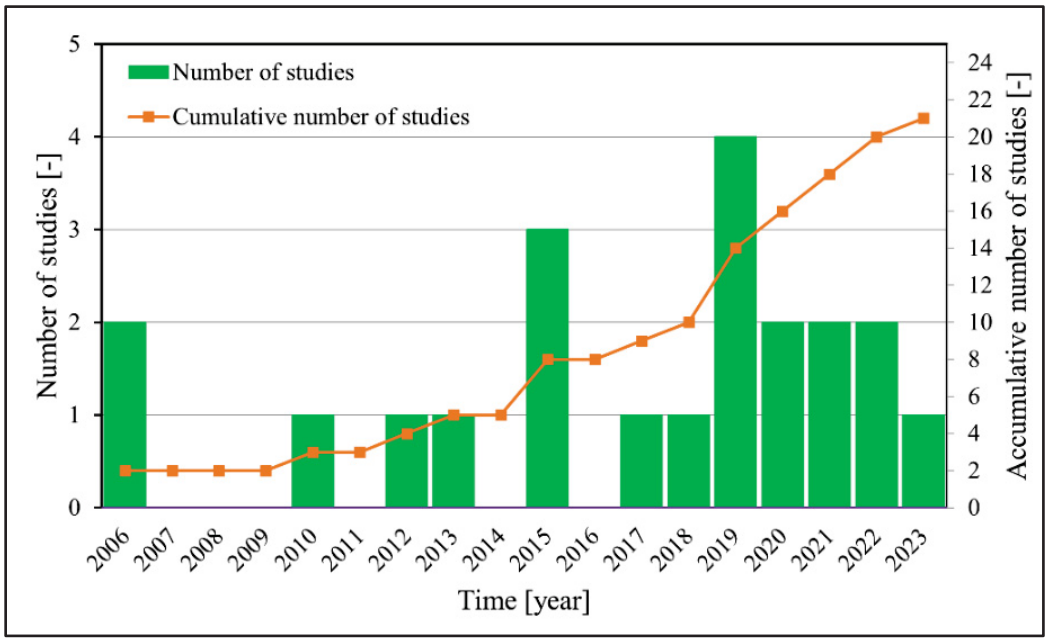

Figure 1.9 Number of studies in PVWPS in Iran

Table 1.5 Summary of studies regarding solar water pumping in Iran.

-Author(s) **-Location** **-Year**	- Abdolzadeh et al. (Abdolzadeh et al., 2011) - Kerman - 2006	- Abdolzadeh et al. (Abdolzadeh et al., 2009) - Kerman - 2006	- Kordzadeh (Kordzadeh, 2010) - Kerman, Kerman - 2010
Application or study type	Efficiency improvement of SWPS by cooling	Effect of operating head on PVWPS	To increase the efficiency of the panel through thermal management.
Methodology	Experimental setup	Experimental setup	Experimental setup
-Battery **- Cooling**	- No - Water spray	- No - No	- No -Thin continuous water film
PV: **- Efficiency** **- Panel model** **- Nominal power**	- 13.5 % - Not provided - 3 panels each 45W	- 12.5% - Not provided - 2 or 3 panels each 45W	- Not provided - Not provided - 2 or 3 panels each 45 W

Motor-pump: **- Efficiency** **- Model** **- Head** **-Flow rate**	- Not provided - PS150 Boost - 45 m (max) - 850 L/h (max)	- Not provided - PS150 Boost - 45 m (max) - 850 L/h (max)	- Not provided - PS150 Boost Lorentz - 45 m (max) - 1000 L/h (max)
Highlights	Maximum improvement in pumping volumetric flow rate of around 40% in the case with three PV panels (135 W) with 25 L/h per module water spray at a head of 16 m.	Two essential factors for the design of PVWPS are achieving the maximum power relevant to the chosen operating head and meeting the consumer needs. Successfully considering both criteria contribute to the design of systems with minimized capital costs.	Decrement of nominal power and increment of system head positively impact the PV efficiency and the system. Thin water layer on the panel enhances the efficiency of the panel and consequently the system especially in low nominal powers of the panel.

-Author(s) **-Location** **-Year**	- Tabaei & Ameri (Tabaei & Ameri, 2012) - Kerman, Kerman - 2012	- Rezae & Gholamian (Rezae & Gholamian, 2013) - Golestan, Gorgan - 2013
Application or study type	To improve the performance of the SWPS system by using booster reflectors	Farmland irrigation.
Methodology	Experimental setup	Numerical (RETScreen)
-Battery **- Cooling**	- No - No	- ATLAS BX (12 V-100 Ah) - No

PV: **- Efficiency** **- Panel model** **- Nominal power**	- Not provided - Not provided - Not provided	- 16.4 % - SANYO HIT Power 195 BA20 - 15 panels each 195 W
Motor-pump: **- Efficiency** **- Model** **- Head** **-Flow rate**	- Not provided - PS150 Boost - 45 m (max) - 1000 L/h (max)	- 62 % (motor-pump) - MOTOGEN- CR90L2A electromotor - 16 m - 200 m^3 per day
Highlights	Increase in output power of the panel by about 14% for aluminum foil reflector and 8.5% for stainless steel 304 reflector. Furthermore, 18% increase in pump flow rates with the aluminum foil reflector and a 9% increase for the stainless-steel reflector. The superiority of aluminum foil was due to its higher reflectivity characteristics	Adoption of solar water pumping systems for irrigation can result in considerable cost savings in the long term; however, incentives are necessary. The payback period was 14 and 6 years for subsidized gasoil and FOB Persian Gulf price, respectively

-Author(s) **-Location** **-Year**	- Habiballahi et al. (Habiballahi et al., 2015) - Kerman, Kerman - 2015	- Tabaei & Ameri (Tabaei & Ameri, 2015) - Kerman, Kerman - 2015	- Mohammadi (Mohammadi, 2015) - South of Iran - 2015
Application or study type	Efficiency improvement of SWPS by cooling	Improving the effectiveness of a SWPS by cooling & booster reflector.	Irrigation and drinking for remote areas
Methodology	Experimental setup	Experimental setup	Mathematical optimization
-Battery **- Cooling**	- No - Collectors beneath the panel	- No - Continuous film of water	- No - No
PV:	- 13.5 %	- Not provided	- Not provided

- Efficiency **- Panel model** **- Nominal power**	- Not provided - 3 panels each 45 W	- Not provided - 3 panels each 45 W	- Not provided - 2-5 panels each 55 W
Motor-pump: **- Efficiency** **- Model** **- Head** **-Flow rate**	- Not provided - PS150 Boost - 45 m (max) - 850 L/h (max)	- Not provided - PS150 Boost - 45 m (max) - 1000 L/h (max)	- Not provided - Not provided - Not provided - 56 m^3 per day
Highlights	About 20% improvement in mean power and 29% increase in mean water flow rate occurred due to cooling by collectors beneath the panels at Head=16m and a collector mass flow rate of 310 L/h.	Applying both booster reflector and PV cooling with a film of water for a SWPS revealed a maximum of 50.4 % increment in output power of the panels at a head of 16 m.	Finding an optimized solution for two factors of loss of load probability and life cycle cost of the system with pareto solutions that provides flexibility for the user to choose between different plans.

-Author(s) **-Location** **-Year**	- Niajalili et al. (Niajalili et al., 2017) - Gilan, Rasht - 2017	- Shirinabadi et al. (Shirinabadi et al., 2018) - Tabriz - 2018
Application or study type	Rice paddy	800 kW water pumping power plant.
Methodology	Experimental	Numerical (PVSYST)
-Battery **- Cooling**	- L16RE-B (6V-370 Ah) - No	- No - No
PV: **- Efficiency** **- Panel model** **- Nominal power**	- 13.7% - LG220P1C - Two panels each 220 W	- Not provided - YL300P-35b - 2670 panels each 300 W

Motor-pump: **- Efficiency** **- Model** **- Head** **-Flow rate**	- Not provided - Pedrollo, Centrifugal pump HFm 50B - 10 m (max) - 300 L/min (max)	-Not provided - Horizontal centrifuge - Not provided - 342 L/second
Highlights	SWPS is a good option in Gilan since there are enough water and irradiation. The field area mandates the size of the system in terms of panel area and pumping power. SWPS becomes feasible after 9 years compared to conventional gasoline-powered pumping systems. Conventional pumping systems cost 1.5 times SWPS in the project lifetime (25 years).	Feasibility of replacing a conventional grid-based water pumping station with 1000W pumping capacity with PVWPS was evaluated successfully. It was shown that the proposed system can avoid emission of approximately 509 tons of CO_2_eq per year.

-Author(s) **-Location** **-Year**	- Parvaresh Rizi et al. (Parvaresh Rizi et al., 2019) - Fars, Jahrom & Khorasan Razavi, Kashmar - 2019	Chahartaghi and Hedayatpour Jaloodar (Chahartaghi et al., 2019) - Mazandarn, Gharakhil - 2019
Application or study type	Citrus orchard and Vineyard.	Drip irrigation
Methodology	Mathematical modeling	Mathematical modeling
-Battery **- Cooling**	- Yes - No	- No - No
PV: **- Efficiency** **- Panel model** **- Nominal power**	- Not provided - Not provided - Between 56 to 90 panels each 80.5 W	- 15% - Not provided - Not provided

Motor-pump: **- Efficiency** **- Model** **- Head** **-Flow rate**	Solar pump: - Not provided - DC - 40m (max) - 23 m^3/h (max) Diesel: - Not provided - RobinPKX320 - 28m (max) - 66 m^3/h (max) Electric: - 56% - WKL50 - 28m (max) - 20 m^3/h (max)	- Not provided - Not provided - 12m (static head) - Not provided
Highlights	The financial analysis of three different sources of energy for irrigation (i.e., solar, electricity, diesel) showed that the economic viability depends on different parameters of annual electricity cost, distance from the electricity grid, availability of pumps and other instruments, irrigation power required, fuel supply and its price, etc. Due to subsidies for electricity and fuel, solar pumping would be feasible through incentives.	The system achieved its maximum water discharge when the solar panels were tilted at angles close to the latitude. More specifically, at a tilt angle of 41 degrees

-Author(s) **-Location** **-Year**	- Zamanlou and Iqbal (Mohammad Zamanlou;Tariq Iqbal, 2019) - West Azarbaijan, Urmia - 2019	- Nikzad et al. (Nikzad et al., 2019) - Mazandaran, Sari - 2019
Application or study type	Grape garden irrigation	Rice paddy irrigation
Methodology	Numerical (CropWat, Lorentz Compass 3, HOMER Pro, MATLAB Simulink)	Numerical (PVSYST) Experimental (noise measurements)
-Battery **- Cooling**	- Trojan SAGM 12V 105Ah - No	- Trojan SAGM 12V 205Ah - No
PV: **- Efficiency**	- 13% - Canadian Solar 300CS6X	- 15.13% - Lorentz, LCM100-M36

- Panel model **- Nominal power**	- 300 W	-100 W
Motor-pump: **- Efficiency** **- Model** **- Head** **-Flow rate**	- 63% (max) - Lorentz PS2-1800 C-SJ8-7 - 40 m (max) - 13 m^3/h (max)	Solar pump: - 48% (motor-pump) - Lorentz PS2e600C-SJ8-5 - 15m (max) - 12 m^3/h (max) Diesel engine: - Not provided - KUBOTA RT100 DI - Not applicable - Not applicable
Highlights	-Feasibility study showed the successful application of PV-Battery-MPPT system for irrigation of 2.36-hectare grape garden to total dynamic head of about 27m with 24000 CAD total cost.	The CAPEX of the on-grid system is 2.41 times that of the conventional one. While over the 20-year operational period, the life cycle cost of the conventional system is more than that of the on-grid one by a factor of 2.89. on the contrary, the CAPEX of the off-grid model is 2.14 times that of the conventional one. In addition, over 20 years of operation, the life cycle cost of the conventional system is only 1.30 times that of the off-grid model.

-Author(s) **-Location** **-Year**	- Shayeteh and Kardehi Moghaddam (Shayeteh et al., 2020) - Bojnurd, North Khorasan - 2020	- Ghasemi- Mobtaker (Ghasemi-Mobtaker et al., 2020) - Central part of Hamedan province - 2020
Application or study type	Water supply for irrigation and drinking	Use of PVWPS in two irrigation scenarios: surface irrigation (SFI) and sprinkler irrigation (SPI)
Methodology	Numerical (MATLAB)	Numerical (TRNSYS)
-Battery **- Cooling**	- No - No	- No - No
PV:	- 12.56%	- Not provided

- Efficiency **- Panel model** **- Nominal power**	- TDB 125X125-72-P - 160 W	- ND AH325 - 325 W
Motor-pump: **- Efficiency** **- Model** **- Head** **-Flow rate**	- 51% pump, 82% motor - URD 152.9 PUMPIRAN - 45m (max) - 12.6 m^3/h (max)	- Overall efficiency of 18-22 % - Not provided - Not provided - Not provided
Highlights	The optimized configuration based on tilt angle and azimuth angle showed about 19% lower total cost of the project compared to an existing system without optimization.	The maximum photovoltaic power needed for replacement in SFI and SPI systems are 4.55 and 5.20 kW, respectively, for a 100-hectare barley farm in Hamedan. SPI resulted in substantial CO_2 emissions equal to 1184 kg/ha compared to 425 kg/ha for SFI. Furthermore, the SFI method paired with PV panels emerged as the most favorable technique due to its minimum environmental damage.

-Author(s) **-Location** **-Year**	- Chahrtaghi and Nikzad (Chahartaghi & Nikzad, 2021) - Isfahan, Isfahan - 2021	- Heiydari et al. (Heydari et al., 2021) - North/Razavi/South Khorasan - 2021
Application or study type	Potato farm irrigation	Solar water pumping station
Methodology	Numerical (COMPASS, RETScreen, PVsyst)	Numerical
-Battery **- Cooling**	- Battery - Natural convection by free air	- No - No
PV: **- Efficiency** **- Panel model** **- Nominal power**	- 15.46% - Polycrystalline silicon - 300 W	- Not provided - Not provided - Not provided

Motor-pump: **- Efficiency** **- Model** **- Head** **-Flow rate**	- Pump:85% (max), Motor: 64% (max) - Not provided - 80 m (max) - 25 m^3/h (max)	- Not provided - Not provided - Not provided - Not provided
Highlights	The maximum and minimum exergy efficiencies were 3.56 and 0.27 %. Furthermore, the use of PVSWP could avoid the emission of 4.8 tons of CO_2 per year for a 1-hectare potato farm in Isfahan. Finally, the use of a sun tracker was not suggested due to its high capital and operational costs and due to adding to the complexity of the system.	Selection of a solar water pumping station among 93 sites in the northeast and east of Iran based on 15 criteria provided a practical framework for selecting the most suitable site for implementing a PVWPS project.

-Author(s) **-Location** **-Year**	- Jahanfar and Tariq Iqbal (Jahanfar & Iqbal, 2022a) - Near Mashhad -2022	- Jahanfar and Tariq Iqbal (Jahanfar & Iqbal, 2022b) - Near Mashhad - 2022
Application or study type	Irrigation of a 2.2-ha cherry and apple farm	Irrigation of a 2.2-ha cherry and apple farm
Methodology	Numerical (HOMER Pro)	Numerical (MATLAB Simulink)
-Battery **- Cooling**	- Yes - No	- Yes - No
PV: **- Efficiency** **- Panel model** **- Nominal power**	- Not provided - JC-340-72P - 340 W	- Not provided - JC-340-72P - 140 panels each 340 W

Motor-pump: **- Efficiency** **- Model** **- Head** **-Flow rate**	- Not provided - Lorentz PSK2-40 - 170 m (Total dynamic head) - 27 m^3/hour	- Not provided - Lorentz PSK2-40 - 170 m (Total dynamic head) - 27 m^3/hour
Highlights	Feasibility study and optimization of a hybrid PV-battery-tank solar water pumping analysis led to a cost-effective system with 40 batteries (each 100Ah) and 140 cubic meters of water tank with around 20000 CAD total cost.	Dynamic analysis of a hybrid PVWPS with battery bank and water tank with MATLAB Simulink for a garden showed the stability of the system in different weather conditions and different load demands. It was shown that temperature variations do not change the stability of the system and the proposed hybrid PVSWP can be used for any city in the country.

-Author(s) **-Location** **-Year**	- Irandoostshahrestani and Rousse (Irandoostshahrestani & R. Rousse, 2023) - Bandar Abbas - 2023
Application or study type	Irrigation of a citrus farm
Methodology	Numerical (MATLAB)
-Battery **- Cooling**	- 8A31DT-DEKA (12 V 104 Ah) - No
PV: **- Efficiency** **- Panel model** **- Nominal power**	- CS3K-305MS - 18.36% - 305 W
Motor-pump: **- Efficiency** **- Model** **- Head** **-Flow rate**	- Pump (90%) - Not provided - 8m (Total head) - Not provided
Highlights	A small increase in tolerance of power loss can decrease the size of system, its CAPEX, and LCOE, with limited impact on WSP. This means that users with limited economic resources should find alternatives to prevent water shortage.

1.7 Conclusions

In this study, the current status of research related to PVWPS in Iran was evaluated. In spite of Iran's considerable solar potential, there has been limited research in solar water pumping systems. The existing studies involve numerical, experimental, and theoretical techniques. The findings of the study can be summarized as:

- This review shows the interest and the potential of solar energy use for agricultural purposes.
- One main finding is the reduction in CO_2 emissions, noise pollution, and savings in fossil fuel consumption. This shows their positive impact on the environment.
- The fact that there is currently research being done in various provinces of Iran shows the adaptability of this renewable energy-based system in various locations, from high solar potential regions of the south to the less irradiated provinces in the north.
- While the CAPEX of SWPS can be more than conventional systems, the sustained economic efficiency and savings over the lifetime of the project show their financial practicality.
- Since Iran is investing in the infrastructure of renewable energy systems, challenges like subsidies, interest rates, and exchange rate fluctuations are effective in promoting the PVWPS utilization.
- The recent enhancement in the number of studies done on SWPS shows an increasing acknowledgment of the advantages of this system.
- This study provides understanding for researchers, policy-makers, and farmers, highlighting the advantages of SWPS and giving ideas for innovation and utilization of this system in the country.

CHAPTER 2

PHOTOVOLTAIC ELECTRIFICATION AND WATER PUMPING USING THE CONCEPTS OF WATER SHORTAGE PROBABILITY AND LOSS OF POWER SUPPLY PROBABILITY: A CASE STUDY

M. Irandoostshahrestani[a], and D. R. Rousse[a]

[a] Industrial Research Group in Technologies of Energy and Energy Efficiency (t3e), École de technologie supérieure (ÉTS), University of Quebec, Montreal, Canada

Paper published in energies, December 2022

NOTE: This paper is originally published under the following information: Irandoostshahrestani, M.; R. Rousse, D. Photovoltaic Electrification and Water Pumping Using the Concepts of Water Shortage Probability and Loss of Power Supply Probability: A Case Study. Energies 2023, 16, 1. https://doi.org/10.3390/en16010001. The content of this section is adjusted slightly to make sure it is consistent, and it respects regulations and formatting standards.

Abstract

In this paper, a techno-economic investigation of a small-scale solar water pumping system combined with power generation is conducted numerically. Irrigation and power production for a typical small-sized citrus farm located in southern Iran are simulated. The system consists of monocrystalline photovoltaic panels (CS3K-305MS, 305 W), absorbent glass material batteries (8A31DT-DEKA, 104 Wh), inverters (SMA Sunny Boy 2.0, 2000 W), and a pumping storage system. The key concepts of water shortage probability (WSP) and loss of power supply probability (LPSP) are used in conjunction with users' tolerances and sizing of the system. A genuine MATLAB code was developed and validated before the simulations. A specific electricity consumption pattern for a rural home and a variable irrigation water profile were considered. The main objective of the study is to size a system that provides both electricity for domestic use of a home as well as the energy required for running the irrigation pumps with respect to investment cost, LCOE, WSP, and LPSP. The main findings of the

research are that LPSP and WSP threshold tolerances can have a preponderant effect on the cost and sizing of the system. Interestingly, results reveal that there is a minimum variation of the capital expenditure (CAPEX) versus the number of PV panels. For the optimal configuration, the study indicates that shifting from an LPSP of 0% to 3% (or about ten days of potential yearly shortage) makes the LCOE drop by about 55%, while the WSP decreases by about 36%.

Keywords: PV-powered system; electrification; water pumping; water shortage probability; loss of power supply probability; battery storage; irrigation

2.1 Introduction

Worldwide, the need for energy is expanding globally as the population and average energy consumption per capita are both increasing (‘Key World Energy Statistics’, 2021). Nowadays, both the private and public sectors are trying to use renewable and sustainable energy sources to meet their needs. Among other renewable sources, the solar photovoltaic system has been used since 1954 when Chapin, Fuller, and Pearson developed the silicon photovoltaic (PV) cell (Chapin, Fuller, & Pearson, 1954). Lots of studies have been done since then to increase the efficiency of PV panels. Nevertheless, the turning point in using this energy source is the drastic drop in the technology cost along with the increase in reliability and durability of systems (Gualteros & Rousse, 2021; International Renewable Energy Agency, 2022). Since 2020, several calls for tenders for power production have been won by bids involving solar PV, thus dethroning fossil fuel power plants. More than ever, this makes PV panels an attractive alternative for energy supply.

2.1.1 Photovoltaic water pumping

In this context, various studies are conducted in the field of solar photovoltaic water pumping systems all around the world. For instance, a photovoltaic solar electrification system for a rural home was studied by Bhayo et al. (Bhayo et al., 2019). A bank of batteries was used for

the days with low irradiation or overnight. A specific uneven electricity consumption profile was considered. It was shown that there are times with a surplus of energy, and this excess energy is used for pumping water. In addition to sizing and other technical aspects of the project, they also evaluated the levelized cost of energy of the system as an economic parameter. In another study by Vishnupriyan et al. (Vishnupriyan et al., 2022), the variation of the tilt angle effects on electricity production, the efficiency of the system, and energy loss were investigated. The study was numerically conducted with PVsyst software, and the best tilt angle of the system was determined. Tiwari et al. (Tiwari et al., 2020) studied solar water pumping by using MATLAB. To evaluate the performance of the system, different parameters of the pump head, PV panel configuration, and radiation were considered. They also studied optimized performance and sizing of the system. Raza et al. (Raza et al., 2022) investigated the social-economical-environmental impacts of using a photovoltaic-based high-efficiency irrigation system in Punjab, Pakistan. Half of the rural community relies on agriculture for a living and the energy crisis in Pakistan has adverse effects on people's lives. The results of the study showed that more people adopted high-efficiency irrigation systems, and this led to lower operational costs compared to conventional fossil-based systems, and consequently led to up to a 100% increase in farmers' net income. Furthermore, it was shown that more than 17 kilo tons of CO_2 emissions reduction per year, and 41% of water savings occurred. In another study in Quetta city, Pakistan (Khan et al., 2021), the effect of running water wells with a photovoltaic water pumping system on the water table and discharge of its valley aquifer was investigated. RETScreen software was used to perform a financial cost-benefit analysis. The results led to recommendations for using two lower-capacity pumps for shallow wells and one higher-capacity pump for deeper wells.

2.1.2 The concept of Water Shortage Probability (WSP)

In a study by Gualteros and Rousse (Gualteros & Rousse, 2021), an open-access software was developed that assists in different aspects of pre-feasibility study, sizing, and optimization as well as maintenance and financial evaluations. The goal of the study was to help people with limited awareness about photovoltaic solar water pumping systems in off-grid rural areas. The

concept of water shortage probability was introduced, as a special case of the loss of power supply probability to establish water shortage tolerance of the community, and it was shown that the tolerance to water shortage has a considerable effect on the size and price of the system. In another investigation by Lunel and Rousse (Lunel & Rousse, 2020), a Python code was developed with the aim of solving the problem of expensive and less available for poor communities of commercial packages such as PVsyst or hard-to-handle tools such as the online tool, SISIFO. Their package is open source with the scope of modeling and sizing small solar photovoltaic water pumping systems for rural communities.

2.1.3 Photovoltaic electricity in Iran

Despite having immense potential, a clean renewable energy industry is not yet well-developed in Iran. The reluctance to use renewable energy has been due to the low price of energy carriers in this country. However, nowadays this trend is changing. The change in Iran's policy toward renewable energy can mainly be attributed to unstable energy prices, the necessity for greenhouse gas emissions reduction, the creation of job opportunities, and relief from international sanctions (Gorjian et al., 2019). The government has implemented incentive policies to use and invest in renewable energy. For example, the minister of energy of Iran has announced guaranteed purchase prices (feed-in-tariffs) for renewable electricity. This includes diverse types of renewable energy, including solar PV, biomass, hydropower, geothermal, wind, and so on (SATBA Iran, 2022).

In 2016, Iran's agriculture industry consumed more than 36 GWh of electricity which represent more than 15% of the country's total power consumption (Nikzad et al., 2019), and it still has about 14–15% of the country's power consumption in 2020 (Iran's Ministry of Energy-Tavanir Holding Company of Iran, 2022). In a study by Nikzad et al. (Nikzad et al., 2019), a solar water pumping system for irrigation of rice paddies in a northern province of Iran, i.e., Mazandaran, was investigated. The authors conducted both a technical and economic study, while the environmental aspects were investigated as well. Noise and CO_2 emissions were complementary to the environmental parameters of their study. To enhance the reliability of

the system, backup battery banks were considered. The idea of selling electricity in non-irrigation months of the year was then considered. The economic and environmental advantages of replacing a conventional diesel pump with a photovoltaic water pumping system were discussed. In another study by Niajalili et al. (Niajalili et al., 2017), the feasibility of a solar water pumping system in the northern province of Gilan was investigated for a typical rice paddy. Sizing of PV panels, as well as a comparison of the lifecycle cost of the solar water pumping system with that of the conventional ones were performed. It was shown that the initial cost of the solar water pumping system could be up to nine times that of a conventional system. However, the total lifecycle cost of this solar system is in turn, about 33% lower than its conventional counterpart. In a numerical study by Shahverdi et al. (Shahverdi et al., 2021), a parabolic trough collector was considered as the heat source for an organic Rankine cycle. The cycle was designed for a pressurized irrigation system and eight different organic fluids were tested. The cycle produced the required electricity for the water pumping system. It was shown that the maximum efficiency of the Rankine cycle was 12.19%, with 47.85% of corresponding collector efficiency. In another study, a comparative financial investigation was conducted by Parvaresh Rizi et al. (Parvaresh Rizi et al., 2019) for pressurized irrigation water pumping systems with both conventional (fuel and on-grid) and solar systems. The study revealed that in general, when the required pumping power is more than 3 kW and the transmission electricity line is less than 2 km, it is more affordable to supply the required energy from a private power transmission line. The authors mentioned that Iran is highly dependent upon its subsidized fossil fuels and that new policies are required to finance solar water pumping projects. Chahartaghi and Nikzad (Chahartaghi & Nikzad, 2021) studied energy, exergy, and greenhouse gas emission reduction of a photovoltaic water pumping system for a potato farm in Isfahan, Iran, at different ambient temperatures and irradiations. The minimum and maximum exergy efficiency of the PVWPS were shown to be 0.27 and 3.56%, respectively. The proposed system could avoid the emissions of 4.8 tons of CO_2 annually, which is equal to 11.1 barrels of crude oil.

2.1.4 Aim of this study

In the context of this specific review, the goal of this study is to investigate the techno-economic parameters of a small-scale PV-battery solar electrification and water pumping system for a typical citrus farm located in the Hormozgan province of Iran by considering the LPSP and WSP concepts. It is aimed to show how selecting appropriate (or tolerable) values of LPSP and WSP can affect the overall cost of the system and thus show that the capital cost (CAPEX) and LCOE totally depend on the user's threshold selected for these two parameters. In fact, the original idea is to link the performance of the system in terms of CAPEX and LCOE to the concepts of WSP and LPSP tolerances by a population when it comes to proposing systems that provide both electricity and water. Initially, the optimum fixed tilt angle of the PV panels is determined. Based on the profile of the crop's water requirements in different months and the corresponding electricity load, the sizing of PV panels and the battery bank backup system is performed to enhance the reliability of the system.

2.1.5 Principal contributions of this study

Several preponderantly interesting results were found here:
A comparison of different LPSPs shows that a small increase in tolerance for power loss can considerably lower the size, the CAPEX, and the LCOE of the system with limited change in water shortage probabilities. This suggests that communities and/or dwellings with limited financial capabilities should consider complementary strategies to avoid running out of water for irrigation.

- The WSP could go lower with higher LPSP because more water could be pumped into the tank when people can tolerate power shortages.
- There is a minimum in the curve that plots the CAPEX with respect to the number of PV panels in the system where limited variations of WSP and LCOE happen with further increases in the number of PV panels and that for any LPSP. This is due to the battery bank requirement rapidly increasing below the minimal number of panels which are less expensive. For the current study, this is about 5 to 6 panels.

- Overall, the main findings are that the success of a project will depend on the resilience of the population combined with its financial capacity.

2.2 Methodology

In this section, only the preponderant elements of mathematical modeling, along with the schematic of the investigated system, are outlined to avoid making the paper overly lengthy. Afterward, the specific configuration of the benchmark problem used for the validation is depicted. Then, the genuine algorithm used to simulate the problem is depicted and briefly discussed. Afterward, specifications of the main components of the system are provided in the form of tables and validation is provided against a specific benchmark problem. Finally, the case study is investigated, and it involves the same components used in the benchmark reference. It is worth specifying that the rationale behind the choices embedded in configuration and components comes from the need to validate the whole model against results available in the literature, according to the study of Bhayo et al. (Bhayo et al., 2019). A different topology could be implemented, and different components could be used in further studies.

2.2.1 Mathematical modeling

In order to estimate the total amount of solar irradiation on a tilted surface, the hourly values of global horizontal, direct normal, and diffuse horizontal irradiance should be used. Data provided by the National Solar Radiation Database (NSRDB) (NREL, 2022a) for Indian Ocean Data Coverage (IODC) by the Meteosat satellite with Physical Solar Model Version 3 (PSM-v3) are used in this study. Currently, it provides mean Direct Normal Irradiation (DNI) for the years 2017– 2019. The values for the last available year, i.e., 2019, are considered herein. It is worth noting that using average values for these years could be questionable since averaging eliminates the extrema in irradiance. This can negatively affect the reliability and accuracy of system sizing. Of course, selecting a particular year involves limitations, too, but it reduces the possibility of underpredicting required capacity.

To obtain an estimate of the total amount of energy that strikes a surface with a given slope and orientation, one needs to determine and calculate several variables, mainly times and angles, hereafter defined in the nomenclature.

Most of the material presented in this section is based on the classical textbook by Duffie and Beckman (Duffie & Beckman, 1982). The basic concepts are provided with the aim of recalling the main steps that make it possible to determine the angle of incidence of direct radiation on a surface necessary to obtain the irradiance. First, the declination angle of the sun is obtained with (Ibrahim, Khatib, & Mohamed, 2017; P. Cooper, 1969):

$$\Delta = 23.45 \times \sin\left(360 \times \frac{284 + n}{365}\right) \tag{2.1}$$

where n is the number of the current day starting from the first of January (n = 1) to 31 December (n = 365). The sunset hour angle is (Duffie & Beckman, 1982):

$$\omega_{ss} = \arccos\left(-\tan(\varphi) \times \tan(\delta)\right) \tag{2.2}$$

where φ is the latitude of the city under study. Sunrise hour angle, ω_{sr} equals $-\omega_{ss}$. Sunrise and sunset hour angle are used to calculate sunrise and sunset. The hour angle is defined as:

$$\omega = 15 \times (12 - ST) \tag{2.3}$$

where ST is solar time obtained with:

$$ST = LT + \frac{(EOT + 4 \times (LL - LSTM))}{60} \tag{2.4}$$

where LT is local time, EOT is the equation of time, LL is local longitude, and LSTM is the local standard time meridian. For LSTM, 15 degrees should be multiplied by the difference from Greenwich time. EOT is obtained from:

$$EOT = 9.87 \times \sin(2 \times \Gamma) - 7.53 \times \cos(\Gamma) - 1.5 \times \sin(\Gamma) \tag{2.5}$$

$$\Gamma = 360 \times \frac{(n - 81)}{365} \tag{2.6}$$

The zenith angle θ_z is defined as (Duffie & Beckman, 1982):

$$\theta_z = \arccos\left(\sin(\delta) \times \sin(\varphi) + \cos(\delta) \times \cos(\varphi) \times \cos(\omega)\right) \tag{2.7}$$

And finally, the required angle of incidence is defined as (Duffie & Beckman, 1982):

$$\theta = \arccos(A + B + C) \tag{2.8}$$

where:

$$A = (\sin(\varphi) \times \cos(\beta) - \cos(\varphi) \times \sin(\beta) \times \cos(\gamma)) \times \sin(\delta) \quad (2.9)$$

$$B = (\cos(\varphi) \times \cos(\beta) + \sin(\varphi) \times \sin(\beta) \times \cos(\gamma)) \times \cos(\delta) \times \cos(\omega) \quad (2.10)$$

$$C = \cos(\delta) \times \sin(\beta) \times \sin(\gamma) \times \sin(\omega) \quad (2.11)$$

where φ, δ, β, γ, and ω are the latitude of the location, the declination angle, the tilt and azimuth angles of the surface, and the hour angle, respectively. Hourly global solar radiation on an inclined surface is composed of three terms: direct beam, diffuse, and ground reflected radiation (Duffie & Beckman, 1982):

$$I_\beta = I_b R_b + I_d \frac{1 + \cos(\beta)}{2} + I \times \mu \times \frac{1 - \cos(\beta)}{2} \quad (2.12)$$

where I_b, R_b, I_d, I, and μ are the direct beam radiation, a geometric factor, the diffusive radiation, the global horizontal radiation, and the albedo coefficient, respectively. R_b is defined as (Duffie & Beckman, 1982):

$$R_b = \frac{\cos(\theta)}{\cos(\theta_z)} \quad (2.13)$$

It is worth noting that $R_b = 0$ between sunset and sunrise.

In order to obtain the output power of the PV panel, following equations are used (Bhayo et al., 2019; Bukar, Tan, & Lau, 2019; Ibrahim et al., 2017):

$$P_{PV}(t) = N_{PV} \times I_{PV}(t) \times V_{PV} \quad (2.14)$$

where N_{pv} and V_{PV} are the number and voltage of the panels. I_{PV}, the current of the panel is:

$$I_{PV}(t) = I_{PV,r} \times \left(\frac{G(t)}{G_{STC}}\right) \times (1 + \alpha \times (T_C(t) - T_{C,STC})) \quad (2.15)$$

$I_{PV,r}$ is the panel's rated current, and G(t) is the surface incident solar irradiation. Similarly, G_{STC} is the incident solar irradiation on the surface under standard test conditions, and α is the temperature coefficient. Furthermore, T_C is the temperature of the panel, and it increases as the incident irradiation on the surface increases. $T_{C,STC}$ is the temperature of the cell under standard test conditions. The following equation is utilized to consider the effect of irradiation of temperature:

$$T_C(t) = T_{amb} + \left(\left(\frac{NOCT - 20}{800}\right) \times G(t)\right) \quad (2.16)$$

NOCT is the nominal operating cell temperature. It is worth noting that T_{amb} is the ambient temperature, and it is available for each hour of the year. The charging and discharging states of the batteries are calculated through the following equations, respectively (Bukar et al., 2019):

$$SOC_{Charging}(t) = SOC(t-1) \times (1-\sigma) + \left(P_{PV}(t) - \left(\frac{P_l(t)}{\eta_{inv}}\right)\right) \times \eta_{bc} \quad (2.17)$$

$$SOC_{Disharging}(t) = SOC(t-1) \times (1-\sigma) - \frac{\left(\left(\frac{P_l(t)}{\eta_{inv}}\right) - P_{PV}(t)\right)}{\eta_{bd}} \times \eta_{bd} \quad (2.18)$$

where σ is the hourly self-discharge rate, and P_l denotes load power. Furthermore, η_{bc} and η_{bd} represent the efficiency of the battery at charge and discharge modes, respectively. Values of σ, η_{bc}, and η_{bd} are 0, 0.97, and 1, respectively (Bhayo et al., 2019; *Valve-Regulated Lead-Acid (VRLA) Gelled Electrolyte (Gel) and Absorbed Glass Mat (AGM) Batteries*, 2004). Finally, to complete the model, η_{inv} is the efficiency of the inverter.

Now, when it comes to simulating pumping, one needs to calculate π, the pumping power of the system. The following equation is then used (Bhayo et al., 2019):

$$\pi = \rho \times g \times \dot{V} \times H \quad (2.19)$$

where ρ, g, $\dot{V}$, and H are the density of water, gravitational acceleration, volumetric flow rate, and total dynamic head. In the following simulations, the total head of the pumping system is set to be 8 m to allow a direct comparison with the benchmark study. The efficiency of the pump is considered 90%, which should be taken into consideration in Equation (19).

In order to assess the reliability of the system, two terms, LPSP and WSP, are considered. LPSP is defined as:

$$LPSP\ (\%) = \frac{\sum_{t=1}^{t=8760} LPS(t)}{\sum_{t=1}^{t=8760} P_l(t)} \times 100 \quad (2.20)$$

where LPS(t) is loss of power supply at time t and is considered as the difference of demand and supply at that instance of time. WSP can be considered a special case of LPSP. It is then defined as:

$$\text{WSP}\ (\%) = \frac{\sum_{d=1}^{d=365} \text{WS(d)}}{\sum_{d=1}^{d=365} \text{IWR(d)}} \times 100 \tag{2.21}$$

It is worth noting that WS(d) is the deficiency of water on day d, which analogously accounts for the difference in water supply and water demand on that specific day. The selection of hours or days for the definition of WSP is based on the required precision of the system. Since the hourly definition of WSP is strict and unnecessary, it is considered based on its daily definition.

For the financial analysis, the levelized cost of energy (LCOE) is investigated. LCOE shows the unit price of energy per kWh by applying the current value of total cost over the project's lifetime (Bhayo et al., 2019). The general form of LCOE is then given by:

$$\text{LCOE} = \text{Life Cycle Cost/Lifetime Energy Production} \tag{2.22}$$

The simplified discounting form of LCOE is used in this study, as described in (Bhayo et al., 2019):

$$\text{LCOE}_{\text{Discounting}} = \frac{\text{CAPEX}_0 + \text{OPEX}_t}{\sum_{t=0}^{\text{Lifetime}} (\frac{\text{EP}_t}{(1+r)^t})} \tag{2.23}$$

where EP_t is electricity production in year t and r is the real discount rate which is considered 15% (Nikzad et al., 2019). $CAPEX_0$ and $OPEX_t$ are the investment or capital expenditure of components and total operational annual expenditures, respectively.

The total capital expenditure involves the PV, pump, and other parts of the system such that:

$$\text{CAPEX}_0 = \text{CAPEX}_{0-\text{PV}} + \text{CAPEX}_{0-\text{pump}} + \text{CAPEX}_{0-\text{else}} \tag{2.24}$$

while $OPEX_t$ is obtained from the following equation:

$$\text{OPEX}_t = O_t + M_t + R_t + F_t \tag{2.25}$$

where O_t, M_t, R_t, and F_t are operational, maintenance, replacement, and fuel costs, respectively. The operational cost is assumed to be zero as there is no need to "operate" anything (Bhayo et al., 2019). The maintenance cost M_t is assumed to be two percent of the PV and pumping investment costs (Bhayo et al., 2019; H. Li & Sun, 2018). In this study, only PV-system-related costs, pumps, and storage-related costs are accounted for in M_t. The salvage values of the components are neglected because they are assumed to be used over their lifetime (Bhandari & Stadler, 2009; Ndwali, Njiri, & Wanjiru, 2020; Numbi & Malinga, 2017). The other related capital expenditures i.e., $CAPEX_{0-else}$ are assumed to imply no maintenance. Therefore:

$$M_t = 0.02 \times CAPEX_0 = 0.02 \times [CAPEX_{0-pv} + CAPEX_{0-pump}] \quad (2.26)$$

In the present study, the PV system unit capital cost is assumed to be 0.93 IRR/W (Bhayo et al., 2019), which includes 40 percent of the installation costs. At the same time, the pump storage system is considered to have a unit capital cost of 2.4 IRR/W (R. Komiyama & Fujii, 2015; Ryoichi Komiyama & Fujii, 2014; Y. Li, Gao, Ruan, & Ushifusa, 2018).

The lifetime of the project is fixed at 30 years. It is also assumed that the annual electricity yield EP_t will be constant every year during the project's lifetime and that there is no output energy degradation during the lifetime of the project. Based on the life span of components, the replacement cost is defined as:

$$R_t = R_{battery} + R_{inverter} \quad (2.27)$$

$$R_{battery} = CAPEX_{0-battery} \times \left(\frac{1}{(1+r)^5} + \frac{1}{(1+r)^{10}} + \frac{1}{(1+r)^{15}} + \frac{1}{(1+r)^{20}} + \frac{1}{(1+r)^{25}}\right) \quad (2.28)$$

$$R_{inverter} = CAPEX_{0-inverter} \times \left(\frac{1}{(1+r)^{10}} + \frac{1}{(1+r)^{20}}\right) \quad (2.29)$$

Here F_t equals zero as transportation in internal combustion engine's vehicles and other fossil fuel-based maintenance costs are embedded in M_t.

2.2.2 Schematic of the solar irrigation system

The schematic of the solar irrigation system is depicted in Figure 2.1. The DC electricity produced by the PV Array is converted to AC through a solar Inverter, and it is conducted to a switchboard that supplies either the Residence Load or a Bi-directional Inverter. This Bi-directional Inverter is responsible for both Battery Bank charging/discharging and supplying electricity to the Motor-Pump which in turn fills the Water Tank of the pumping system, enabling irrigation of the Farm.

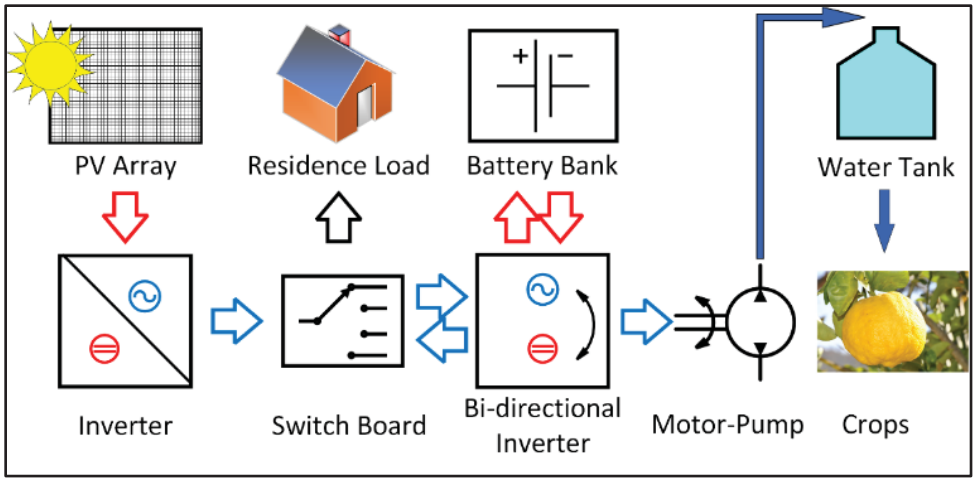

Figure 2.1 Schematic of the electrification-water pumping system with DC/AC conversion directly after the PV panels

Figure 2.1 clearly indicates that an inverter is inserted between a switchboard and the PV array itself, thus readily converting DC to AC. A different choice could be made, according to the pump type (AC or DC), for instance. However, the justification for this choice stems from the requirements for validating the formulation and implementation of the model, which is then validated against the model proposed in (Bhayo et al., 2019). This configuration is also used for the simulation discussed in Section 3.2 without loss of generality.

2.2.3 Algorithm of the prediction model

Figure 2.2 shows the first part of the algorithm of the prediction model for the system. In brief, the system mandates when to charge the batteries, when to supply electricity to the residents, and finally, when to run the pump depending on the availability of sun and the state of charge of the batteries. First, inputs such as GHI, DHI, DNI, ambient temperature, longitude, latitude, etc. are used to calculate total irradiation on the tilted surface. Then, the maximum annual total irradiation on tilted surfaces is calculated, and the angle relevant to the maximum value is selected for investigations. Subsequently, global tilted irradiation, power load profile, irrigation water requirement, specification of components, and an initial PV array size are computed, and an initial value for system size is considered for calculations of PV power output.

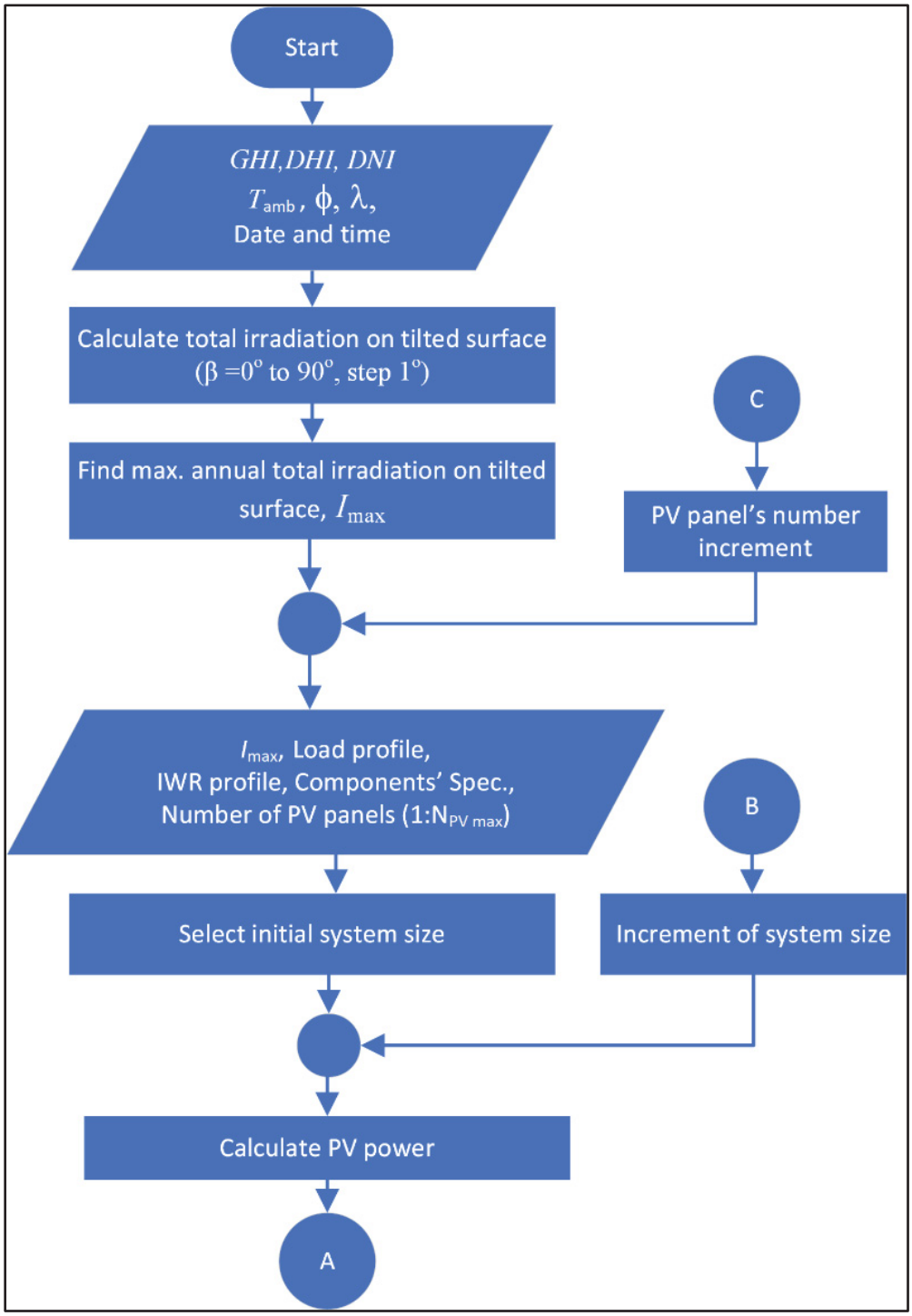

Figure 2.2 The first part of the electrification-pumping algorithm of the study

Figure 2.3 shows the iterative procedure. The algorithm verifies whether or not the PV power generation matches the load at a given time. On the one hand, when the available power is higher than the load, then the algorithm verifies the SOC of the batteries: when the battery pack is not fully charged, priority is given to charging; when the battery pack is full, the pump starts and fills the reservoir. On the other hand, when the load exceeds the PV power, then the algorithm still verifies the SOC of the batteries: when the battery pack SOC is lower than SOC_{min}, the algorithm goes back to increasing the size of the battery pack and other relevant components (B in Figure 2.2, and Figure 2.3). Hence, the algorithm calculates water pumping values, SOC for charging or discharging states, and ultimately the LPSP. When the LPSP tolerance is met, the sizing is favorable and the LCOE, CAPEX, and WSP are calculated; when the LPSP is higher than the maximum allowed $LPSP_{max}$, the loop recalculates the above-mentioned parameters by increasing the size of the battery and other components in order to reach the favorable LPSP (B in Figure 2.2, and Figure 2.3). It is worth noting that the program is repeated for N_{PVmax} of 1 until the maximum number of PV panels which is considered by the user (C in Figure 2.2, and Figure 2.3).

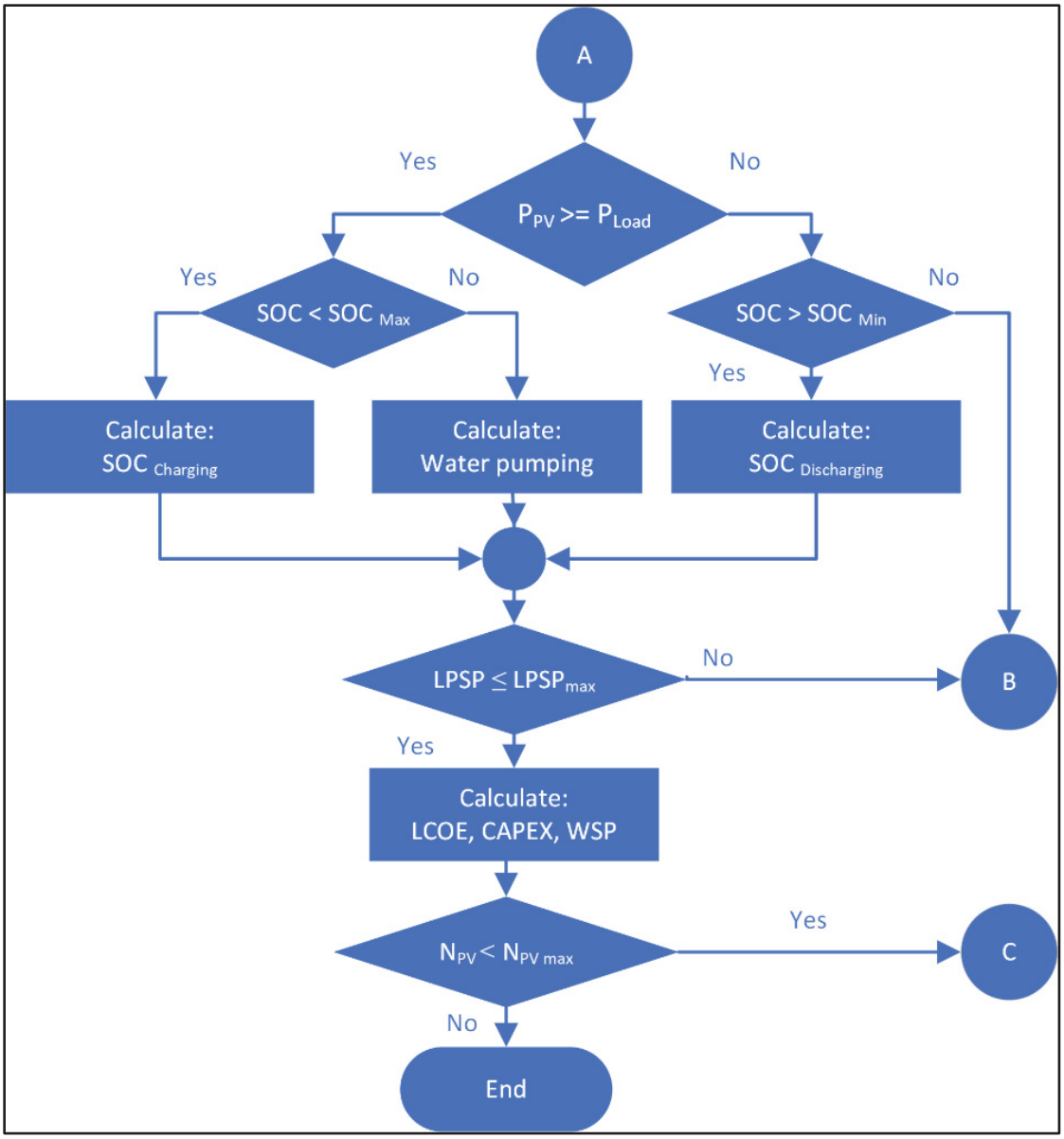

Figure 2.3 The second part of the electrification-pumping algorithm of the study

2.2.4 Specification of components

The specifications of all components including PV panel, battery, solar inverter, Bi-directional inverter, and pumping storage system are succinctly shown in the following Tables. These components were chosen in order to benchmark outgoing predictions with respect to the relevant study of Bhayo, Kayem, and Gilani (Bhayo et al., 2019) shown in the following tables.

It is worth noting that for a better life expectancy for batteries, their minimum and maximum SOC are considered as 35 and 90% of their maximum capacity, respectively. The lifespan of batteries is five years. After that period, they are considered to have no residual value and hence no salvage value. On the other hand, the inverters are assumed to work for 10 years, although they could last longer. The panels are considered to work for the whole duration of the project, i.e., 30 years, without loss of performance, which could be interpreted as a strong assumption.

Table 2.1 PV panel specifications

PV Model	**CS3K-305MS**
Type	Mono-crystalline
Power at STC, P_{mp}	305 W
Optimum operating Voltage at STC	32.7 V
Optimum operating Current at STC	9.33 A
Module Efficiency	18.36%
Temperature Coefficient (α)	−0.37% per °C
Nominal Module Operating Temperature	42 °C
PV lifespan	30 years
Price	201.31IRR

Table 2.2 Battery specifications

Battery Model	**8A31DT-DEKA**
Battery Technology	Absorbent Glass Mat.
Nominal Voltages	12 V
Battery Capacity	104.0 Ah
Battery life span	5 years
Depth of discharge	60%
Price	362.25IRR

Table 2.3 Solar inverter specifications

Model	**SMA Sunny Boy 2.0**
Continuous AC Output Power	2000 W
Min/Max Input DC Voltages	80/600 V
Max Input DC Current per string	10 A
Max. short circuit current per string	18 A
Power consumption while operating	2 W
Efficiency	97%
Life span	10 years
Price	867IRR

Table 2.4 Bi-directional inverter specifications

Model	**Multi-Grid**
Type	VDE-AR-N 4105
Power Output from 25 °C to 40 °C	2400 to 2200 W
Maximum efficiency	94%
Rated Input Voltage DC/AC	19–33/187–265 V
Rated Output Voltage DC/AC	24/230 V
Rated Output DC	70 A
Life span	10 years
Unit Price	992IRR

Table 2.5 Pumping and storage system specifications

Yearly Operation and Maintenance Cost	**2% of Investment Cost**
Pump Efficiency	90%
Total head	8 m
Life span	30 years
Investment cost	2.4IRR/W

2.2.5 Specification of components

To validate the correct formulation and implementation of the proposed genuine algorithm, the results are tested against those found in reference (Bhayo et al., 2019). In this study, Bhayo et al. used a site located in Malaysia, and hence, for the validation process, the same site with the same demand is used, but here, of course, the genuine part of the algorithm (the bottom part) is not explicitly employed.

First, in Figure 2.4, the installed battery capacity (IBC) in Wh, the daily average power generation in kWh/day, and the water pumped to provide storage in m^3/day are presented as a function of the number of PV panels installed in the installation. In Figure 2.4, as the number of PV panels increases, the required capacity of the battery decreases. This is due to the fact that the battery is supposed to compensate for the lack of energy supply. As the PV panel capacity increases, less electricity deficiency happens, leading to more system reliability; hence less battery capacity is required. On the other hand, an increase in PV panel number leads to more power generation during the lifetime of the project and more water pumping. In Figure 2.4 the current predictions are found to accurately reproduce the results proposed in the benchmark publication.

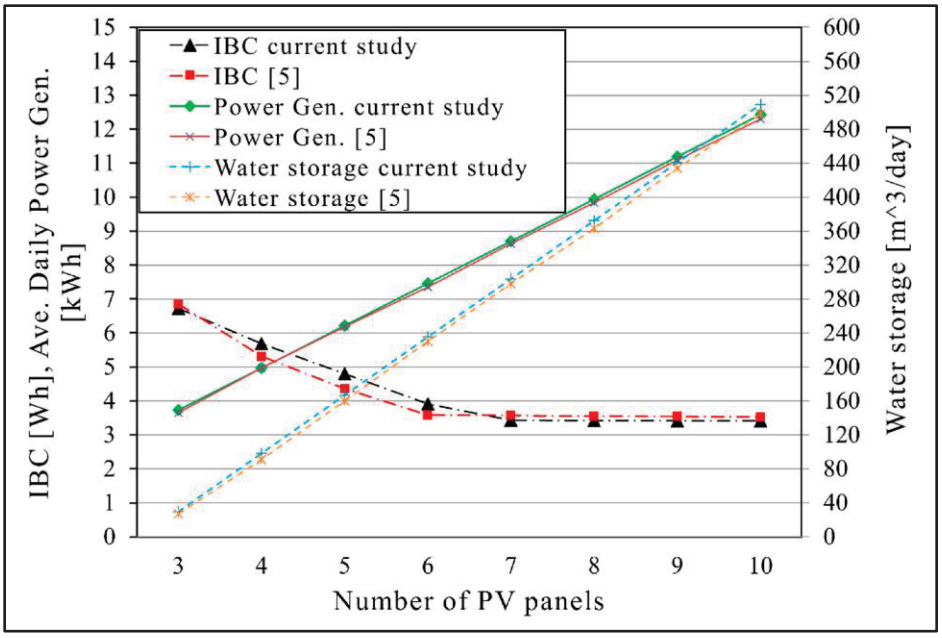

Figure 2.4 Validation of technical results of the current study with Reference (Bhayo et al., 2019)

Figure 2.5 presents the lifetime power generation of the system in kWh, the lifetime cost in IRR, and the LCOE in IRR/kWh. It shows that increasing the number of PV panels makes the LCOE decrease, especially below seven panels. This is because, as the number of PV panels increases, more power is produced during the lifetime of the project and because the first increase in the number of panels does not affect the lifetime cost too much. Based on the definition of LCOE, the cumulated generated power is the denominator of LCOE, while the cost is the numerator. Then, as increasing PV panels above six leads to an increment of the lifetime cost of the system (or the numerator of Equation (2.23)) simultaneously with the denominator, Figure 2.5 indicates a more or less stabilization of the LCOE above seven panels for this specific simulation. Here again, the agreement with the predictions found in (Bhayo et al., 2019) for the same problems is excellent.

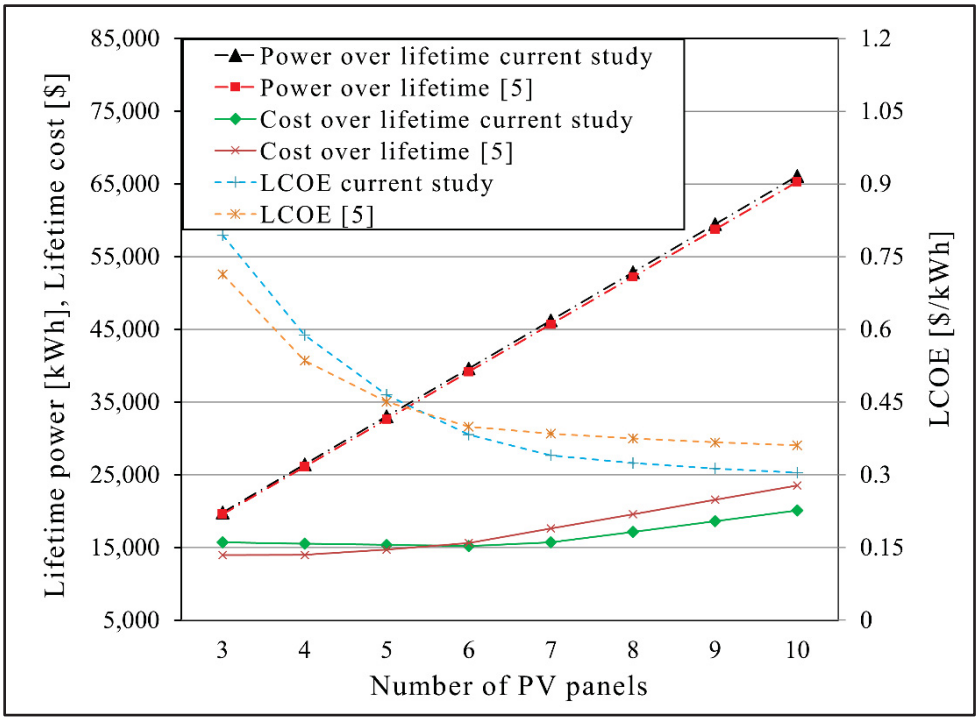

Figure 2.5 Validation of economic results of the current study with reference (Bhayo et al., 2019)

The above results provide confidence in the ability of the proposed model to simulate the citrus farm of Bandar-Abbas presented next.

2.2.6 Case study

Iran has a great potential for solar energy use, especially in central and southern parts of the country (Besarati, Padilla, Goswami, & Stefanakos, 2013; Chandler, Whitlock, & Stackhouse, 2022). The capital of Hormozgan province, i.e., Bandar Abbas, is considered for investigation. This city has a latitude and longitude of 27.17 degrees North and 56.26 degrees East, respectively. The amount of daily average global horizontal insolation as well as the ambient temperature for Bandar Abbas for each month of the year is shown in Figure 2.6. From April to the end of September, the average daily insolation on a horizontal surface is above 5 kWh/m^2 while the ambient temperature is above 25°C. On the one hand, the higher the irradiation, the better the electricity production. On the other hand, ambient temperatures above 25°C will necessarily lead to lower cell efficiencies as the surface temperatures will impair production.

The maximum daily average is 6.5 kWh/m^2 in June, while the maximum average temperature reaches 36°C in June, July, and August.

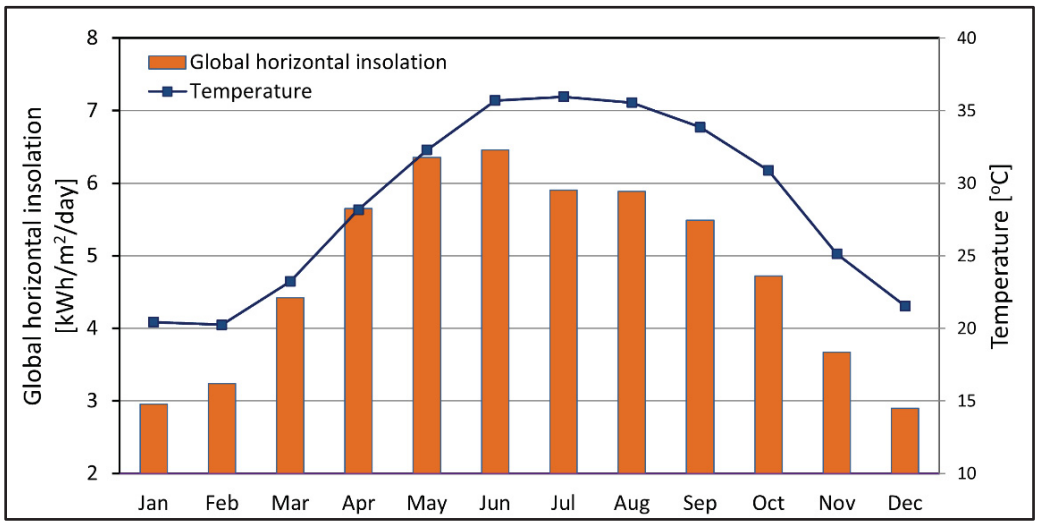

Figure 2.6 Monthly average Global horizontal insolation as well as ambient temperature for Bandar Abbas; data from (NREL, 2022a)

The hourly diagram of the global horizontal irradiation for one year is very noisy, as evidenced by the profile depicted in Figure 2.7, from (NREL, 2022a). Calculations are based on this profile. In Figure 2.7, sudden drops in GHI values mainly correspond to clouds and/or rainy periods.

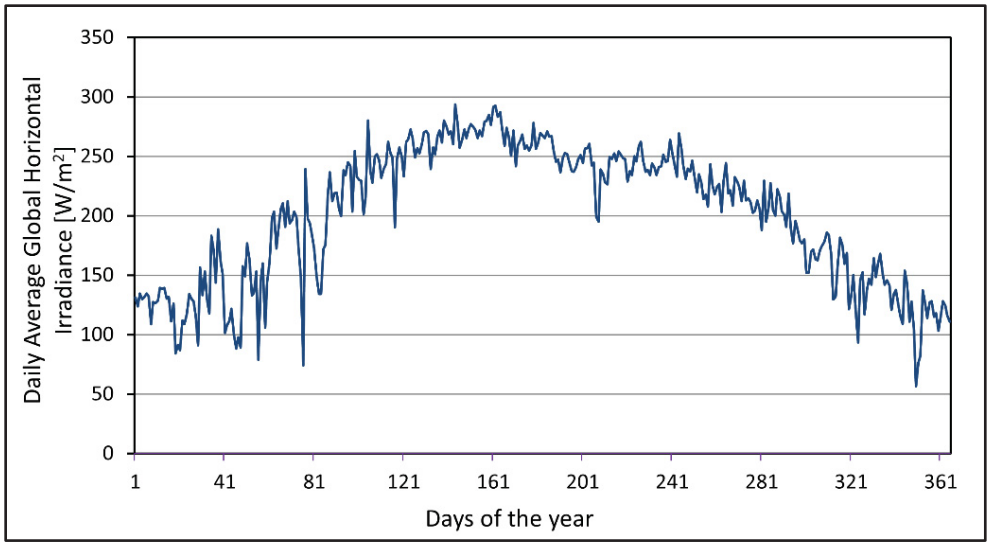

Figure 2.7 Daily average global horizontal irradiance (GHI) for Bandar Abbas, data from (NREL, 2022a)

Irrigation water requirement (IWR) and crop water requirement (CWR) are terms mostly used in agricultural water management topics. IWR is the net depth of water needed for a crop to satisfy its water requirement (in mm). In fact, IWR is the fraction of CWR not supplied through rainfall, groundwater, and storage of water in soil (Pereira & Alves, 2005). Figure 2.8 depicts IWR and CWR for citrus farms at the Hormozgan provincial level (Bazrafshan, Zamani, Ramezani Etedali, & Dehghanpir, 2019). To obtain an average daily irrigation water requirement, a trendline is fitted with a polynomial regression of order 6. The equation is:

$$IWR = -0.0091 \times m^6 + 0.3545 \times m^5 - 5.1071 \times m^4 + 32.086 \times m^3 - 81.701 \times m^2 + 91.436 \times m - 4.4536 \quad (2.30)$$

where m is the month number. Here, order six ensures that $R^2 = 0.9948$. The unit for IWR is mm and it should be multiplied by the area of the farm (1 hectare) to obtain the total volume of water required for irrigation.

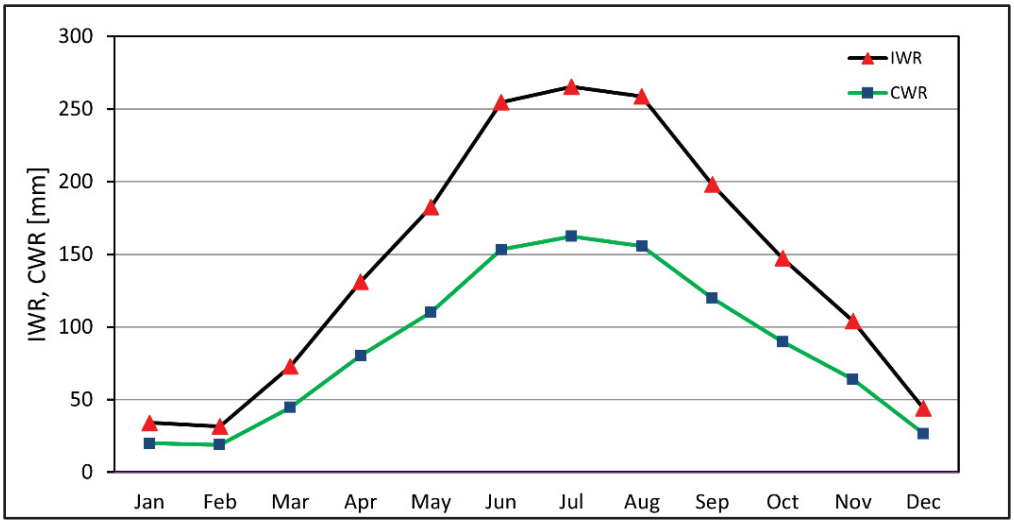

Figure 2.8 Irrigation and crop water requirement for a citrus farm in Hormozgan province, data from (Bazrafshan et al., 2019)

To complete the description of the total electrical load of a typical installation, the hourly average electricity load for a typical house, constructed from several different profiles, is depicted in Figure 2.9. In the proposed profile, reasonable increases in electricity demand, with respect to the basic load, are considered for the morning (from 6 to 8), noon (from 13 to 14), and night (from 19 to 23). The profile also shows a 50% increase in the basic 100 W load between the afternoon peaks (from 15 to 18). It is worth mentioning that different shapes can be used as load profiles based on appliance users' profiles, as long as they reflect a reasonable pattern for a residential house.

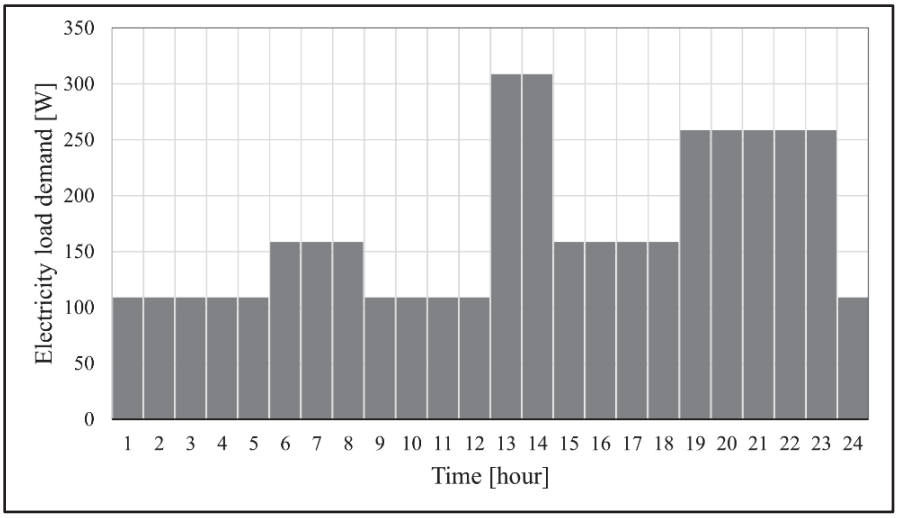

Figure 2.9 Hourly electricity load for a typical rural house

2.3 Results and discussions

In this section, the results obtained in an attempt to optimize a citrus farm located in Bandar-Abbas in terms of LCOE, CAPEX, and WSP for three different LPSPs are presented.

The first concern is to determine the most suitable fixed tilt angle for the PV array (oriented due South). Despite simple rules of thumb considerations for the best PV tilt angle, the problem of panel slope for yielding the maximum solar energy collection can be complex and it is a function of various parameters such as local latitude, surface azimuth, and clearness index (Memme & Fossa, 2022). The variation of the yearly average daily irradiation with respect to the slope of the array was calculated for $0 \leq \beta \leq 90°$. The optimal tilt angle that leads to the maximum power generation of PV panels for one year is about $\beta = 17°$ for this city. These results for the optimum tilt angle were confirmed with respect to the cumulative electricity production in a year (not explicitly presented). It is worth mentioning that, although the maximum value of average daily irradiation occurs at 17°, limited reductions were found in the range of 10 to 28 degrees. Therefore, construction of the structures (not considered herein) could be much easier at 20°, for instance, without substantial losses in performance.

In Figure 2.10, Figure 2.11, and Figure 2.12, the results of the study in terms of the variations of WSP, LCOE, and CAPEX with respect to the number of PV panels are presented for three different thresholds for LPSP. It is assumed that the residents need different reliabilities for their electricity demand, leading to LPSP values of 0, 1%, and 3% in Figure 2.10, Figure 2.11, and Figure 2.12, respectively. One should note that despite similar shapes, the y-axes of these figures involve different scales. The lower the value of LPSP, ceteris paribus, the higher the corresponding values of all three other parameters.

In Figure 2.10, LPSP = 0 simply means 100% reliability of the system in providing electricity for the residence, 365 days per year. Therefore, based on the algorithm used in the study, LPSP is fixed to the desired value (or tolerance of a customer or community), and the minimum PV panel and battery capacity are obtained accordingly. In Figure 2.10, the capital cost of a 4-panel system (left in Figure 2.10) reaches 66 thousand IRR, while the WSP peaks at more than 28% and the LCOE exceeds 7 IRR/kWh as there is a major requirement for batteries. However, a slight increase in the number of panels produces a rapid decline in both the WSP and LCOE. Nevertheless, the symbolic threshold of 1 IRR/kWh reaches around 10 panels and further increases do not change the LCOE significantly while the CAPEX increases.

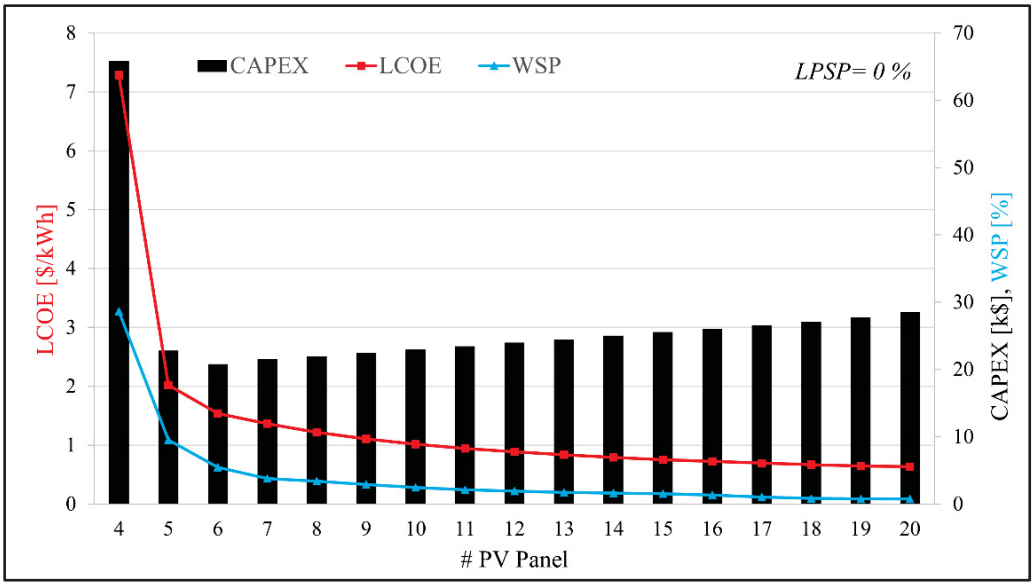

Figure 2.10 The number of PV panels versus LCOE, CAPEX, and WSP for LPSP = 0%

It is obvious that as the number of PV panels increases, the water shortage probability will decrease since the system is capable of producing more electricity. This is mostly at the expense of an increment in the capital cost of the project (CAPEX). Moreover, this is true for the three values of LPSP.

In Figure 2.11, similar trends are observed. However, 10 panels with LPSP = 1% will lead to an LCOE of about 33% less than that calculated in Figure 2.10. Logically, a higher LPSP has an important effect on the capital cost. CAPEX drops from about 23 thousand IRR (Figure 2.10) to 15 thousand IRR (Figure 2.11) for a 10-panel system.

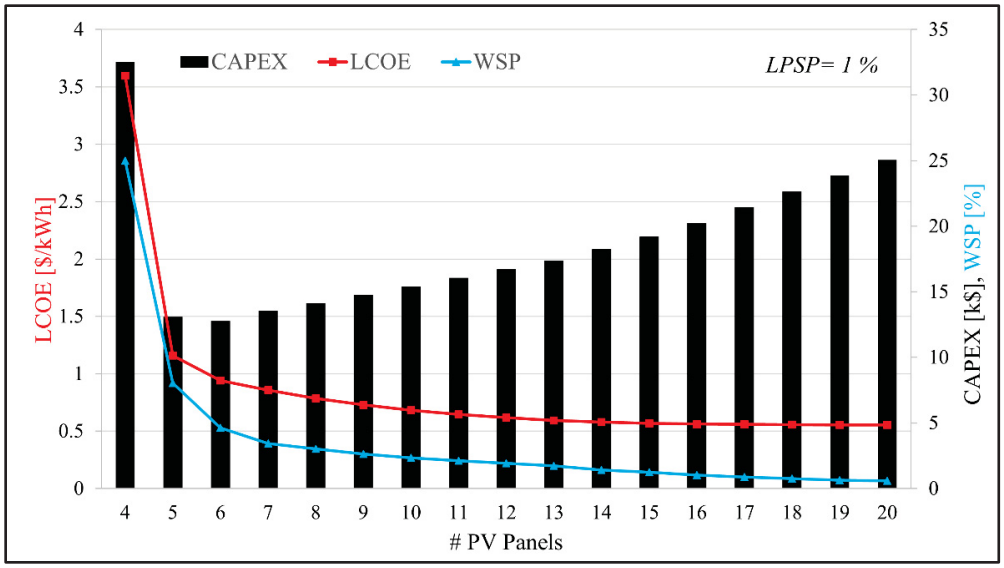

Figure 2.11 Number of PV panels versus LCOE, CAPEX, and WSP for LPSP = 1%

As the LPSP has such an influence, simulations were also carried out for a 3% LPSP and the results are reported in Figure 2.12 . Here again, similar trends are observed. However, 10 panels with LPSP = 3% will lead to an LCOE drop of about 40% while the CAPEX reaches as low as 14 thousand IRR for the 10-panel system.

From Figure 2.10, Figure 2.11, and Figure 2.12, it can be seen that there is a minimum value for the capital cost of the system at different LPSP values. This minimum value happens for 6, 6, and 5 PV panels and for LPSPs of 0, 1%, and 3%, respectively. This is due to the fact that generally, increasing PV panels means making the system bigger, and hence more investment is needed. However, as mentioned earlier, at the extremely low number of PV panels, considerable amounts of battery bank capacity are required for the system to guarantee the threshold values for LPSPs, and consequently, in this case, the battery price dictates the high values of the CAPEX.

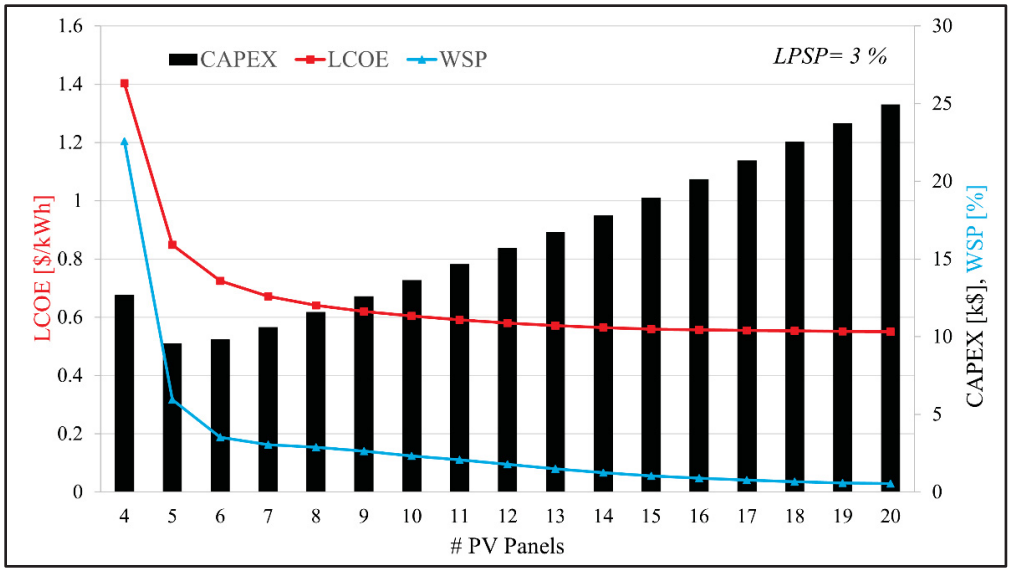

Figure 2.12 Number of PV panels versus LCOE, CAPEX, and WSP for LPSP = 3%

The variation of the system's capital cost at PV panel numbers of 4 to 5 or 6 is considerable in all cases of LPSPs. For LCOE trends, the same as the explanations provided in the previous section, i.e., validation section, LCOE decreases by increasing the number of PV panels, since the production of electricity is much higher than the increment in investment cost of the system. At a fixed LPSP value, the selection of the best sizing of the system in terms of the number of PV panels and battery bank capacity depends on the tolerance of WSP and the capability of the user to pay the investment cost of the system. In fact, this is the end user who decides which system size is compatible with their needs. Here, it is worth noting that WSP = 1% means that there is a yearly average of about 3.6 days for which there could be a water shortage, not a guaranteed shortage. In these periods, the requirement for irrigation could also be less, thus modifying the water demand, as the WSP is correlated to irradiation. Nevertheless, several strategies could be considered to solve this problem, such as personal water storage by individuals during sunny days, prior to critical periods of the year, or variable prices of water per liter with weather predictions. Yet these strategies are not reviewed here.

For instance, Figure 2.13 shows that at LPSP = 0, for a PV panel number of five, the LCOE is about 2 IRR/kWh and reduces to about half at 10 PV panels and to 0.75 IRR per kWh at 15

PV panels. This suggests that there should not be much gain in terms of LCOE to increase the number of panels above 10. Furthermore, at LPSP = 0, WSP values for these panel numbers are 9.5%, 2.4%, and 1.5%, respectively (Figure 2.14). This reinforces the previous conclusion. Accordingly, still at LPSP = 0, CAPEX equals 22.8 thousand IRR for 5 PV panels, 23.0 thousand IRR at 10 PV panels, and 25.5 thousand IRR at 15 PV panels. Additionally, this also confirms that 10 panels would be enough.

As another example, at LPSP of 3%, for 5 PV panels, the LCOE is 0.85 IRR/kWh and reduces to 0.60 IRR/kWh for 10 PV panels and to 0.56 IRR/kWh at 15 PV panels (Figure 2.13). Furthermore, WSP values for these panel numbers are 6.0%, 2.3%, and 1.0%, respectively (Figure 2.14). Additionally, finally, CAPEX (Figure 2.15) equals 9.6 thousand IRR, 13.6 thousand IRR, and 18.9 thousand IRR for 5, 10, and 15 PV panels, respectively. Here, we see that a higher tolerance to a loss of power could lead to substantial savings: the LCOE could be reduced by more than 50% when LPSP increases from 0 to 3%, especially for small systems, and the WSP would also drop. This could sound counterintuitive, but when people accept several potential periods without electricity (higher LPSP), this provides energy to fill the water tank and thus reduces the WSP. Finally, the CAPEX also drops with higher LPSP.

These graphs (Figure 2.13, Figure 2.14, and Figure 2.15) provide a clear picture of the effect of LPSP and WSP tolerances on sizing and the cost of the system. For instance, if investment cost is a concern of the user of the system, selecting a system with PV panels of 6 to 9 would be reasonable since, in these sizes, CAPEX does not increase considerably, but WSP reduces from 5.5% up to 2.9% at LPSP of 0. Additionally, similarly, from 4.6% up to 2.6% at LPSP of 1%, and from 3.5% up to 2.6% at LPSP of 3%.

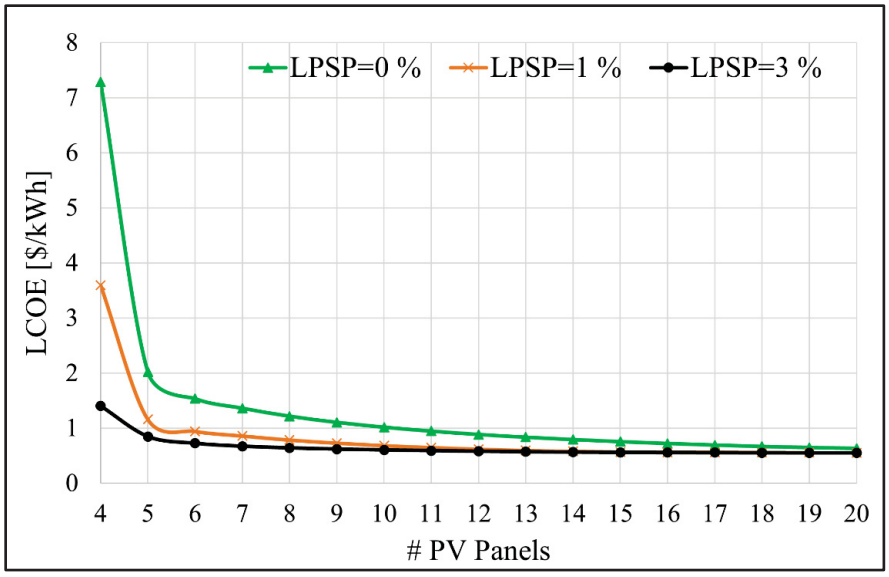

Figure 2.13 Comparison of different LCOE values for three LPSP tolerances of 0, 1%, and 3%

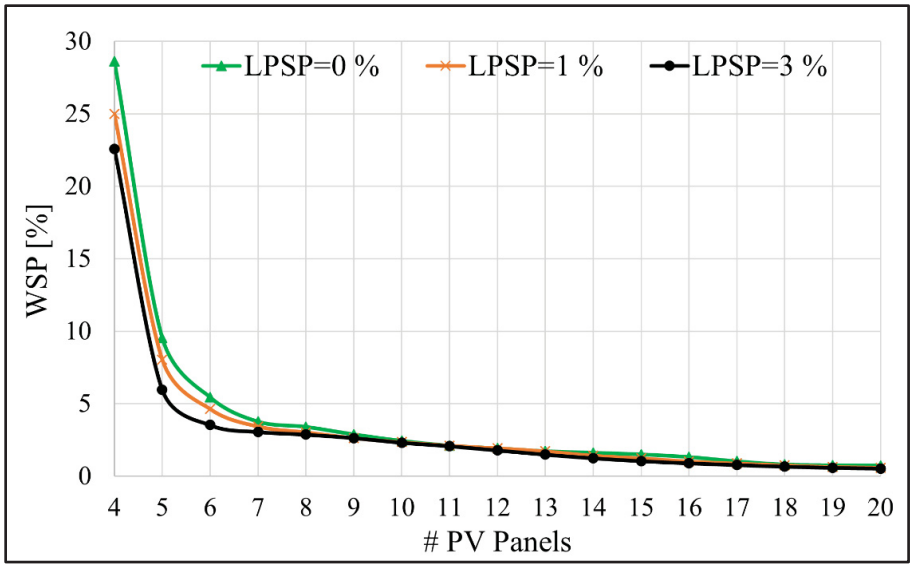

Figure 2.14 Comparison of different WSP values for three LPSP tolerances of 0, 1%, and 3%

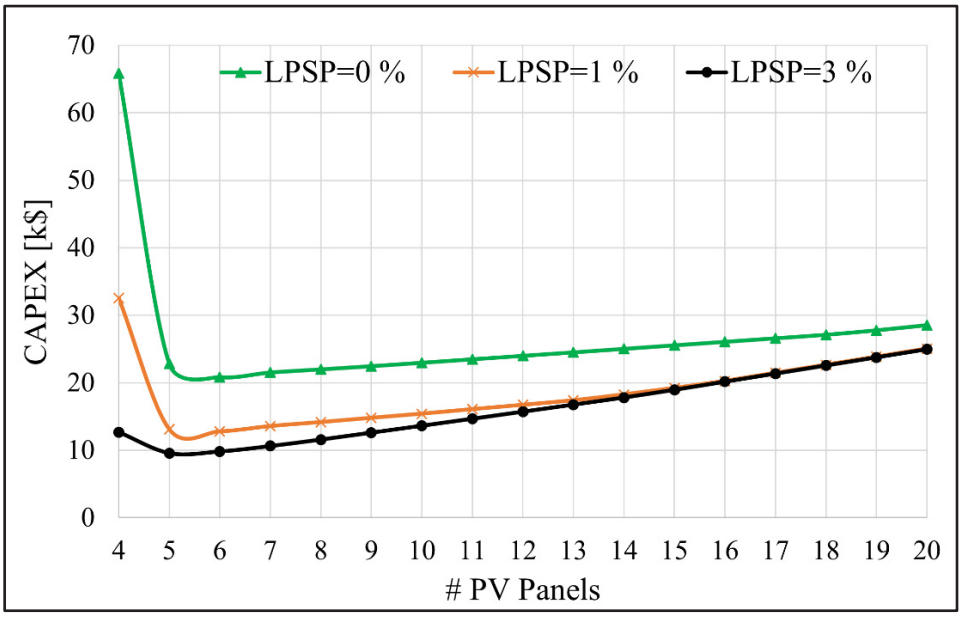

Figure 2.15 Comparison of different investment costs for three LPSP tolerances of 0, 1%, and 3%

2.4 Conclusions

In this study, photovoltaic electrification and water pumping based on a PV-battery system were investigated for a city located in southern Iran, i.e., Bandar Abbas. Two specific concepts that influence the size and cost of the system were used herein: (1) the water shortage

probability (WSP) for the evaluation of drought tolerance in the context of irrigation; and (2) the loss of power supply probability (LPSP) as a tolerance threshold for lack of access to electricity of a rural home. Moreover, a simplified expression for the levelized cost of energy (LCOE) was also implemented to evaluate the financial viability of systems with more than the sole capital expenditure (CAPEX). A genuine MATLAB implementation of a particular electrification/pumping algorithm was carried out. Then, the correct formulation and implementation were validated against a benchmark solution. Additionally, finally, a case study involving parametric variations was undertaken.

The investigations were carried out to determine the appropriate size of the system (in terms of the number of PV panels and the battery capacity required) for selected values of LPSP and to find the corresponding values of WSP, LCOE, and CAPEX.

The results, not surprisingly, revealed that increasing the number of PV panels leads to more energy production and consequently lower WSP. This, however, is at the expense of more investment in the system (CAPEX). However, the effect of increasing energy production may increase the capital cost, but leads to the reduction of the LCOE.

Several preponderantly interesting results were found here:

- A comparison of different LPSPs shows that a small increase in tolerance for power loss can considerably lower the size, cost, and LCOE of the system with limited change in water shortage probabilities. This suggests that communities and/or dwellings with limited financial capabilities should consider complementary strategies to avoid running out of water for irrigation.
- The WSP could go lower with a higher LPSP because more water could be pumped into the tank when people can tolerate power shortages.
- There is a minimum in the curve that plots the CAPEX with respect to the number of PV panels in the system, where limited variations of WSP and LCOE happen with further increases in the number of PV panels and that for any LPSP. This is due to the

battery bank requirement rapidly increasing below the minimal number of panels which are less expensive. For the current study, this is about 5 to 6 panels.

2.5 Perspectives

The current work undertaken in the t3e group and ÉTS Montreal now is concerned with electrification/pumping and treating/heating water for the domestic needs of a small-sized remote community. Namely, the investigation aims at defining the appropriate size of a system with respect to community size, needs, budget, and tolerances to water and power shortages.

Another crucial work that remains to be done is to determine the influence of two different business models to satisfy the same needs: (1) the individual or the community owns the system; or (2) a company installs a system and sells electricity and water to consumers. These two diametrically opposed models could lead to very different systems for the same communities because low LPSPs imply that a large amount of water could be pumped unnecessarily due to too limited reservoirs. This remains to be explored.

Finally, if the conventional battery is appropriate for small-scale systems, when the irrigation component becomes more important, it would be interesting to consider other energy storage modes, both in terms of their technical and environmental performance.

.

CHAPTER 3

OPTIMIZING RELIABILITY, COST, AND WATER ACCESS: A MULTI-OBJECTIVE FRAMEWORK FOR OFF-GRID SOLAR/WIND HYBRID SYSTEMS WITH BATTERY AND WATER STORAGE FOR ENERGY AND WATER NEEDS OF A RURAL COMMUNITY

M. Irandoostshahrestani[a], D. R. Rousse[a]

[a] Industrial Research Group in Technologies of Energy and Energy Efficiency (t3e), École de technologie supérieure (ÉTS), University of Quebec, Montreal, Canada

Paper submitted for publication, April 2025

NOTE: This paper is submitted at the Energy Conversion and Management journal on April 29th, 2025 with manuscript number of ECM-D-25-05407 under the following information: Irandoostshahrestani, M.; R. Rousse, D.; Optimizing Reliability, Cost, and Water Access: A Multi-Objective Framework for Off-Grid Solar/Wind Hybrid Systems with Battery and Water Storage for Energy and Water Needs of a Rural Community. Furthermore, the Python code used for this study is provided in the Appendix.

Abstract

This study presents a multi-objective optimization framework for improving affordability, reliability, and water access in standalone off-grid energy systems integrating photovoltaic (PV) panels, wind turbines (WT), battery storage, and water reservoirs. The system is designed to meet both residential load demand and water needs. A mathematical model and a novel Energy Management System (EMS) algorithm optimize power generation, energy storage, and water pumping. The EMS prioritizes residential electricity supply, ensuring battery charging for nighttime and low-irradiation periods, while excess power is used for water storage. Main performance parameters including Loss of Power Supply Probability (LPSP), Water Shortage Probability (WSP), and Capital Expenditure (CAPEX) are optimized using a genetic algorithm

(GA)-based multi-objective technique in order to enhance reliability, water availability, and cost efficiency of the system. A detailed financial model and reliability analysis evaluate system performance, with a case study in a remote island in Quebec demonstrating the feasibility of an autonomous, off-grid energy solution. The results show that the optimized system could effectively supply residential electricity while utilizing surplus power for water pumping, thus, reducing reliance on diesel generators (DG) or grid electricity. The proposed solutions showed a payback period of 8 to 12 years with LCOE in the range of 16.3 ¢/kWh to 23.4 ¢/kWh.

Keywords: Water pumping systems; Wind turbine; Loss of power supply probability; Water shortage probability; Multi-objective optimization; Solar energy

3.1 Introduction

Around 750 million people in the world have no access to electricity in 2023, and they are mostly located in sub-Saharan Africa (Cozzi, Wetzel, Tonolo, Diarra, & Roge, 2023). Solar power systems are crucial in solving global warming, and to secure the energy supply, and helping economic growth. Affordability, scalability, and environmental sustainability are the main factors that justify their extensive use (IRENA, 2021).

Based on the importance of solar power systems, studies have investigated their use in water supply for off-grid communities. Meunier et al. (Meunier et al., 2019) studied a PV water pumping system (PVWPS) designed to supply water for a rural, off-grid community in a village in Burkina Faso. The model was validated through experiments and it considered users' water consumption patterns and climatic data of ambient temperature and solar irradiance. The model calculates the discharge rate of the pump and the water level in the water storage system. The study focused on the architecture of the PVWPS and the water tank and its control loop that determines the starting and stopping of the pumping system based on water height in the reservoir. The study also investigates a methodology for evaluating coefficients related to system performance. It was revealed that the proposed model can predict the water level and

the discharge rate in different solar and weather conditions with good accuracy. The authors concluded that their model can be reliably applied in sub-Saharan Africa for performance evaluation and sizing of PVWPS projects.

In another study, Bakelli et al. (Bakelli, Hadj Arab, & Azoui, 2011) analyzed a PV water pumping system for supplying drinking water to remote villages in Ghardaia, Algeria. The study considered a daily water requirement of 6 cubic meters. The optimization model developed in the study employed the LPSP concept to evaluate the reliability of the system and the life cycle cost for economic assessment. The LPSP values were in the range of 0% to 9% which shows different levels of reliability. The model discusses the configurations of the system leading to these reliability values at the minimum life cycle cost while considering CAPEX, replacement costs, and operations and maintenance costs in the lifetime of the project. This study shows the effect of the nominal power of PV modules and the water storage tank size on the reliability of the system and its cost. The life cycle cost analysis was done for pump heads of 6, 14, and 26 meters at different LPSP values. The results showed that making a balance between PV panel numbers and water storage capacity is important for minimizing costs with regard to reliability parameters. For example, for LPSP of 0, the study showed that the optimal system configuration is different based on head and reliability criteria. This shows that it is necessary to evaluate each application individually based on the approach proposed in the study. This case study shows the importance of a comprehensive strategy to design and optimize a PVWPS and it also reveals the need for balancing reliability with economic parameters.

In another study by Bhayo et al. (Bhayo et al., 2019), a standalone PV-battery system for a water pumping application was investigated. The goal was to optimize power generation and utilization of surplus energy for a rural housing unit in Malaysia with a daily load requirement of 3.2 kWh. Utilizing real-time weather data and residential load requirements, the study developed an algorithm to lower the Levelized Cost of Energy (LCOE) while ensuring system reliability (LPSP= 0) and using the excess power for water pumping. The investigation evaluates the adaptability of the system to varying weather conditions, and shows its potential

for rural electrification. By finding optimal PV and battery configurations, the importance of integrated renewable energy systems in finding economic and reliable energy solutions for rural communities is shown. The results revealed that the selected PV-battery system includes 2.44 kWp PV system and 3.55 kWh battery backup capacity. This system could produce approximately 9.8 kWh of electricity and pump 363 cubic meters (m^3) of water daily.

In a multi-objective optimization study by Muhsen et al. (Muhsen, Ghazali, & Khatib, 2016), three parameters: life cycle cost, loss of load probability, and amount of excess water, were taken into consideration for a PVWPS designed to provide a constant daily water volume of 30 m^3 for the typical consumption of 120 people, based on meteorological data from Kuala Lumpur, Malaysia. A constant static head of 20m was assumed for water pumping. A wide range of weighting factor sets was used to address the challenge of initializing weights for the objective functions. The study showed that the optimized configuration consisted of 20 PV modules and a maximum water reservoir capacity of 52 m^3, which resulted in a loss of load probability of approximately 0.5% and achieving an average water flow rate of 3.3 m^3/h during pumping.

In our recent study (Irandoostshahrestani & R. Rousse, 2023), a techno-economic analysis was conducted on a small-scale PVWPS. The study focused on a farm in Bandar Abbas, a city located in the south of Iran. The system involves PV panels, batteries, inverters, and a water-pumping system. The research used the WSP and LPSP concepts for sizing of the system. The findings showed the considerable impact of LPSP and WSP values on both system size and cost. For example, LPSP increase from 0 to 3% resulted in 55% reduction in the LCOE and a decrease of about 36% in WSP. In addition, it was shown that changing the PV panel nominal capacity can considerably affect the reliability of the system and its costs. Therefore, the paper concludes that it is essential to evaluate each project based on user requirements, including water access, power reliability and capital expenditures.

A recent study explored the use of hybrid photovoltaic/wind turbine (PV/WT) energy systems to provide affordable and reliable power. El-Maaroufi et al. (El-Maaroufi, Daoudi, & Ahl

Laamara, 2024) studied an off-grid PV/WT system with battery and hydrogen storage for Laayoune city, Morocco. They used HOMER Pro to find the best system design that reduces costs and improves reliability. Their results showed that a 100% renewable energy system is possible without relying on fossil fuels. The optimized system produced steady electricity at a low cost of $0.0477/kWh. Furthermore, the study evaluated GHG emissions and concluded that integrating various energy sources with storage systems makes the system reliable, economic, and sustainable.

In another research, Al-Omari et al. (Al-Omari, Khlaifat, & Haddad, 2024) conducted a feasibility study for a hybrid PV/WT system for electrifying a water pumping system in a village in Jordan, aiming to replace expensive and polluting conventional diesel generators. Here again, HOMER was used for the optimization of this off-grid system with the objectives of reducing environmental impact and cost, and improving reliability. They showed that the hybrid system could achieve an LCOE of $0.241/kWh with a payback period of less than seven years, demonstrating that the system is feasible and sustainable for a rural community.

This review indicates that, to the best knowledge of the authors, no studies have yet specifically examined a dual-application hybrid PV/WT small-scale autonomous system integrating battery and water storage, designed to supply both residential electricity and drinking water. In this context, this study proposes to extend our previous study (Irandoostshahrestani & R. Rousse, 2023) by integrating complementary wind energy production, to satisfy both needs (power and water). Moreover, the proposed combined system incorporates an innovative EMS that prioritizes electricity demand while utilizing excess power for water pumping. Therefore, the goal of this study is to evaluate the feasibility of these systems while considering their reliability, water accessibility, and system cost. Here, a remote island in Quebec, Canada is chosen to evaluate the concept. The system is designed to operate entirely on renewable energy, and to eliminate reliance on conventional fossil fuel-based systems. It is obvious that if a community uses such a project, it is required to keep auxiliary equipment for maintenance periods or when the system is damaged, but the design implies a penetration rate of 100%.

3.2 Schematic of the system and energy management algorithm

The system's schematic is illustrated in Figure 3.1. The PV panels and the WTs generate the required electricity for the residents, and when the load demand is met, the excess power is used for battery charging. When the batteries are fully charged, the remaining excess power is directed to the pumping system, and the pumped water is stored in reservoirs.

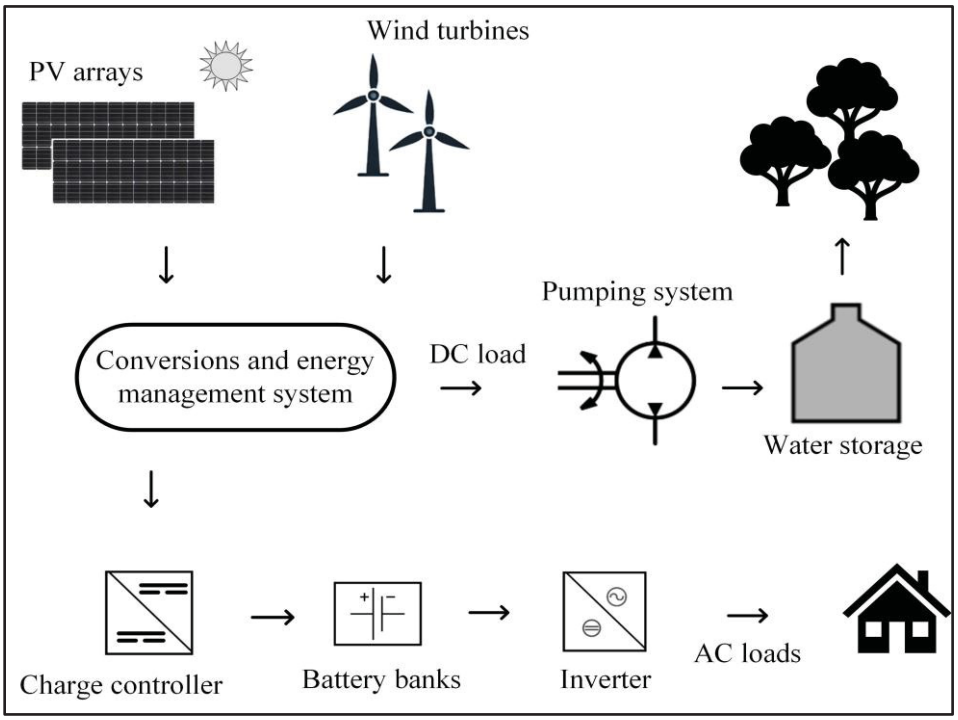

Figure 3.1 Schematic of the system

The algorithm of the genuine methodology is shown in Figure 3.2. As shown, the best tilt angle for maximum annual total irradiation is determined. Then, when the power load demand is met, the battery banks are charged and finally, the water pumping system is run when there is an excess power produced by the panels and the wind turbines, i.e., when the load demand is met, and the batteries are fully charged. The algorithm incorporates loops to calculate various PV, WT, and battery capacities together with appropriate water tank volumes. Finally, using the Non-dominated Sorting Genetic Algorithm II (NSGA-II), the optimized PV/ WT and battery bank nominal capacities and water storage tank volumes are selected based on minimized LPSP, WSP, and CAPEX.

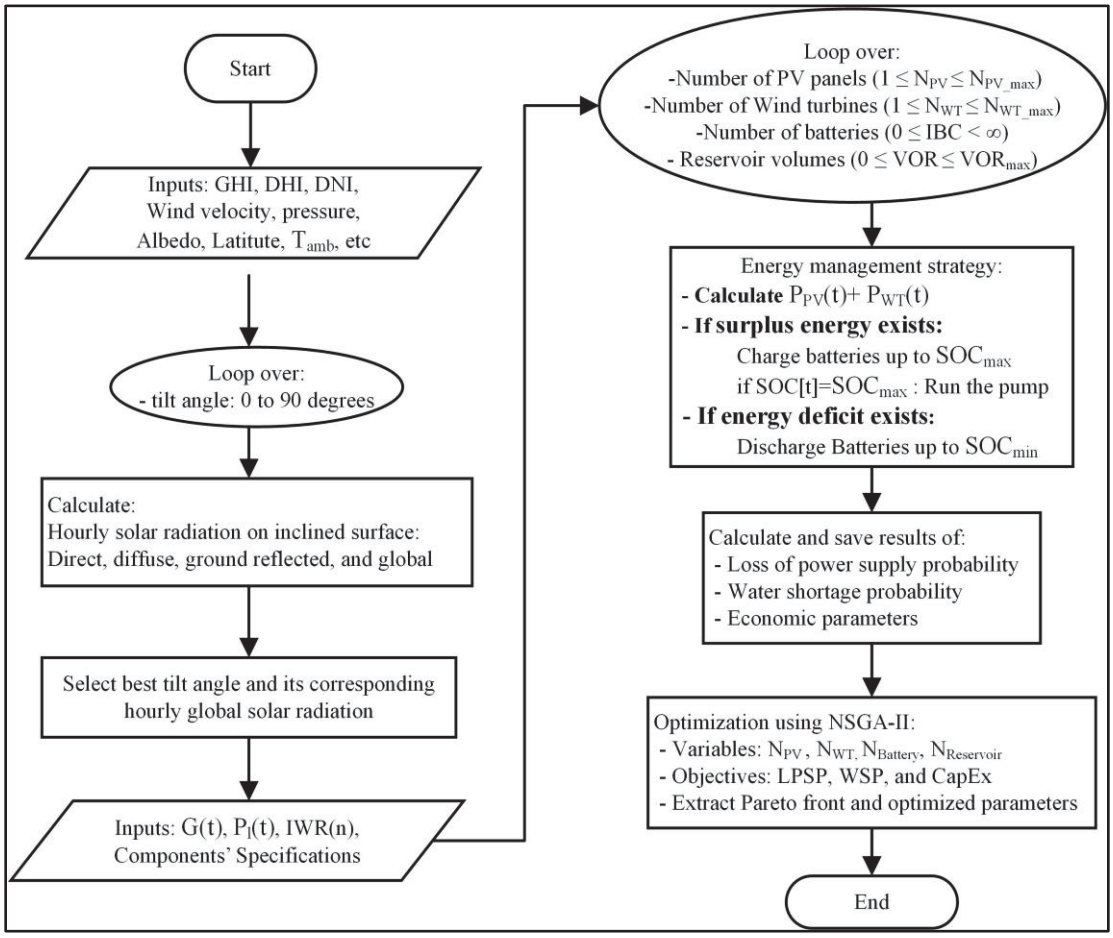

Figure 3.2 Algorithm used in the study

3.3 Case study

Îles-de-la-Madeleine, located in the Gulf of Saint Lawrence, Quebec, Canada, at a latitude of 47.40°N and a longitude of 61.77°W, was selected for this case study. Data from the NSRDB (NREL, 2022a) for the most recent available year, i.e., 2023, was used. Figure 3.3 shows the monthly average variations in GHI, ambient temperature, and albedo coefficient. As shown, the minimum monthly average temperature is -4.9°C in February, while the maximum is 17.8°C in July. The albedo coefficient is higher in winter because the ground is snow-covered. Furthermore, the monthly average of GHI ranges widely from 0.58 kWh/m²-day in December to 5.96 kWh/m²-day in July. In addition, wind speed variation throughout the year at hub height is shown in Figure 3.4.

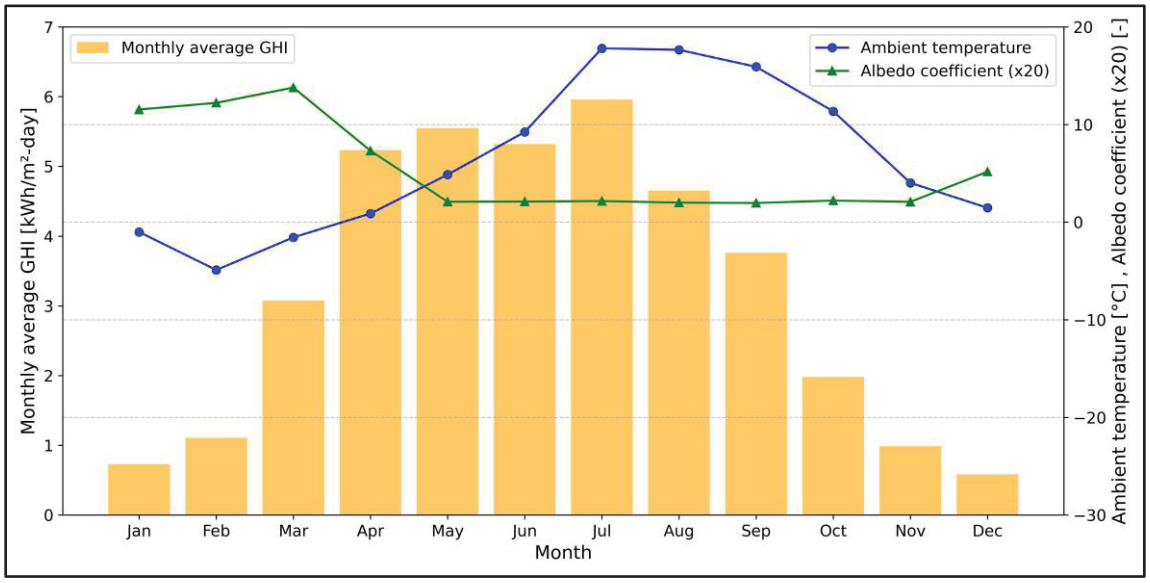

Figure 3.3 Monthly averages of GHI, ambient temperature, and albedo coefficient for Îles de-la-Madeleine, QC. Data from the NSRDB (NREL, 2022a)

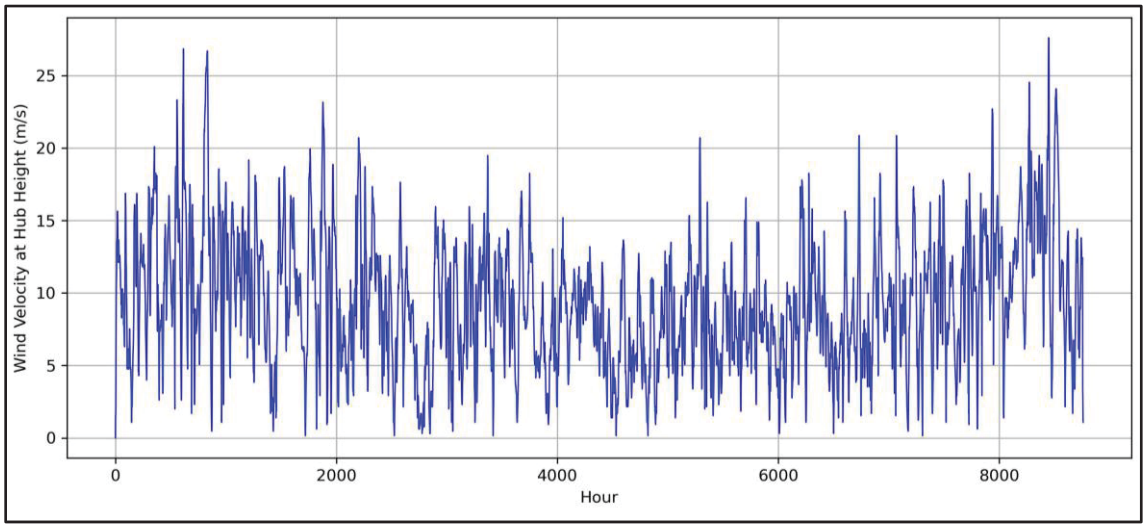

Figure 3.4 Typical windspeed at hub height for Îles-de-la-Madeleine, QC (NREL, 2022a)

There are several small communities in the Îles-de-la-Madeleine, the archipelago has a total population of about 13 thousand people, spread across several villages and hamlets. Among these places, some are particularly small and isolated. For example, Grosse-Île is a unique English-speaking community in the region, with a relatively small population. Hence, in this

case-study, a small community of 100 people with a constant daily water requirement of 260 liters per person (Gouvernement du Québec, 2025) (i.e., a total amount of 26 m^3/day) is considered. The electricity consumption is obtained from the Canadian Centre for Energy Information database (Energy Information Canada, 2025). Since this data reflects the average of all electricity-consuming sectors, including residential, commercial, and industrial, it is scaled with respect to the annual consumption of households in Quebec, which equals 17 thousand kWh/year (Hydro Quebec, 2024), Figure 3.5.

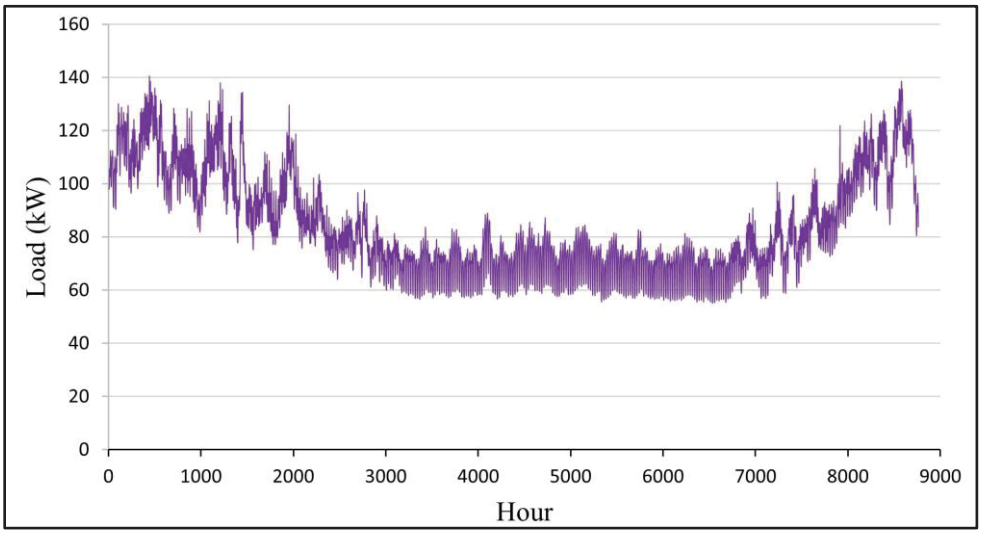

Figure 3.5 Electricity load demand profile

3.4 Methodology

In this section, the mathematical models are presented. Python is used to solve the mathematical model. Basic solar radiation models are provided in Appendix II. In the following sections, PV, WT, battery, water pumping and storage, reliability, and financial models, as well as the optimization procedure, are explained.

3.4.1 Solar PV system

To determine the power generated by the PV panels at each time step, the following equation is used (Bhayo et al., 2019; Bukar et al., 2019; Ibrahim et al., 2017):

$$P_{PV}(t) = N_{PV} \times P_{PV,r} \times \left(\frac{G(t)}{G_{STC}}\right) \times [1 + \alpha \times (T_C(t) - T_{C,STC})] \quad (3.1)$$

where N_{PV} is the total number of PV panels, $P_{PV,r}$ is the rated power of each panel under Standard Test Conditions (STC), G(t) is global solar radiation on the inclined surface at time t, G_{STC} is the solar irradiance under STC (equal to 1000 W/m²), α is temperature coefficient of power (usually provided in the PV datasheet), $T_{C,STC}$ is cell temperature under STC (equal to 25 °C). The cell temperature at time t is calculated using the following equation (Ibrahim et al., 2017):

$$T_C(t) = T_{amb} + (NOCT - 20) \times \left(\frac{G(t)}{G_{NOCT}}\right) \quad (3.2)$$

where NOCT is the Nominal Operating Cell Temperature, which should be obtained from the PV datasheet, T_{amb} is the ambient temperature, and G_{NOCT} is the reference radiation at nominal conditions (equal to 800 W/m^2). Due to the area limitations for the PV panels, the maximum allowable PV panel number ($N_{PV,max}$) is set to 600:

$$1 \leq N_{PV} \leq N_{PV,max} \quad (3.3)$$

3.4.2 Wind turbine system

In this section, the output power of the wind turbine is described. The following equation is used to calculate the output power at standard temperature and pressure (STP) conditions (Das et al., 2021; Fagbenle, Katende, Ajayi, & Okeniyi, 2011) as described by (Shah Irshad et al., 2024):

$$P_{WT,STP} = \begin{cases} 0, & V \leq V_{c-in} \\ \dfrac{V^3 - V_{c-in}^3}{V_r^3 - V_{c-in}^3}, & V_{c-in} < V < V_r \\ P_r, & \leq V < V_{c-out} \\ 0, & V \geq V_{c-out} \end{cases} \quad (3.4)$$

where V_{c-in}, V_{c-out}, and V_r are the cut-in, cut-out, and rated windspeed. P_r is the rated power of the WT. The values of these parameters are given in Section 5. Specifications of the components. The wind speed at hub height should be obtained. As mentioned previously, wind speed data from NSRDB (NREL, 2022a) were used, and the data is given for a height of 2m.

The following equation (Das, Hoque, Mandal, Pal, & Raihan, 2017) is used to scale the windspeed to the WT's hub height:

$$V = V_{ref} \times (\frac{H}{H_{ref}})^{\alpha} \quad (3.5)$$

where the exponent (α), an empirical coefficient, is assumed to be 1/7 (Islam, Saidur, & Rahim, 2011). Finally, the actual output power of a WT is calculated using the following equation:

$$P_{WT} = \left(\frac{\rho}{\rho_0}\right) \times P_{WT,STP} \quad (3.6)$$

where ρ_0 is the air density at STP conditions, which equals 1.225 kg/m^3. The actual density of air is derived from the ideal gas law. It is also assumed that the maximum number of wind turbines ($N_{WT,max}$) could be 26, i.e.:

$$0 \leq N_{WT} \leq N_{WT,max} \quad (3.7)$$

3.4.3 Battery storage system

The following equations define the dispatch strategy for PV, WT, and batteries:

$$P_b(t) = P_{PV}(t) + P_{WT}(t) - P_{l,real} \quad (3.8)$$

$$P_{l,real} = \frac{P_l(t)}{\eta_{inv}} \quad (3.9)$$

where $P_{l,real}$ is the power passing through the inverter (Al-Buraiki & Al-Sharafi, 2022), and $P_l(t)$ is the load demand at each hour. When $P_b(t) > 0$, surplus energy is available, and the batteries' State of Charge (SOC) is determined using the following equation (Al-Buraiki & Al-Sharafi, 2022):

$$SOC_{Charging}(t) = SOC(t-1) \times (1-\sigma) + (P_b(t) \times \eta_{bc}) / IBC \quad (3.10)$$

On the other hand, when $P_b(t) < 0$, there is an energy deficit, and the State of Charge (SOC) is determined using the following equation (Al-Buraiki & Al-Sharafi, 2022):

$$SOC_{Discharging}(t) = SOC(t-1) \times (1-\sigma) + (P_b(t) \times \eta_{bd}) / IBC \quad (3.11)$$

where σ, η_{bc}, and η_{bd} represent the self-discharge rate and the battery efficiency under charging and discharging conditions, respectively. For simplicity, self-discharge rate is

assumed to be 0 and the efficiency of 1 was considered in this study. The nominal installed battery capacity (IBC) is calculated using the following equation:

$$\mathrm{IBC} = \mathrm{N_{Battery}} \times \mathrm{C_{Battery}} \tag{3.12}$$

where $\mathrm{C_{Battery}}$ is the nominal capacity of each battery in Wh. Unlike the PV panels, no limitation on the number of batteries was considered; therefore:

$$0 \leq \mathrm{IBC} < \infty \tag{3.13}$$

A very large number of battery banks was considered as the upper bound. In addition, it is assumed that the initial SOC of the batteries is equal to 50%, i.e.:

$$\mathrm{SOC}(0)=0.5 \tag{3.14}$$

It should be noted that lower and upper bounds for the SOC of the batteries must be considered during system design to prevent overcharging or over-discharging, which helps extend battery lifespan. The SOCmin and SOCmax values are set at 10% and 90%, respectively:

$$0.1 \leq \mathrm{SOC}(t) \leq 0.9 \tag{3.15}$$

3.4.4 Water pumping system

A centrifugal pump (Lorentz PS2-4000 C-SJ17-4) with a DC motor and a nominal power of 4 kW is selected. Its characteristic curve was derived from the manufacturer's datasheet (BERNT LORENTZ GmbH & Co. KG, 2022). The Curve Fitter tool in MATLAB (The MathWorks Inc., 2022) was used to derive the characteristic curve equation. The pump's flow rate (Q [m^3/h]) at different heads (H [m]) and input powers (P [W]) are calculated as follows:

$$Q = Q_{00} + Q_{10} \times H + Q_{01} \times P + Q_{20} \times H^2 + Q_{11} \times H \times P + Q_{02} \times P^2 \tag{3.16}$$

where Q_{00} = 3.276, Q_{10} = -0.6048, Q_{01} = 0.01748, Q_{20} = -0.0007923, Q_{11} = 0.0001245, and Q_{02} = -3.137 × 10-6. The goodness of the fitted curve was evaluated using R2, which was equal to 0.9935. The curve and the residual values are shown in Figure 3.6. Using this equation, the amount of pumped water throughout the day can be calculated. It is worth noting that, based on the datasheet, the pumping system has a minimum power requirement below which the pump cannot operate (see Table 3.1). Furthermore, the system limits the input power of the pumping system and this power is different for each head. In this study, a total head of 45 m was assumed for the pumping system.

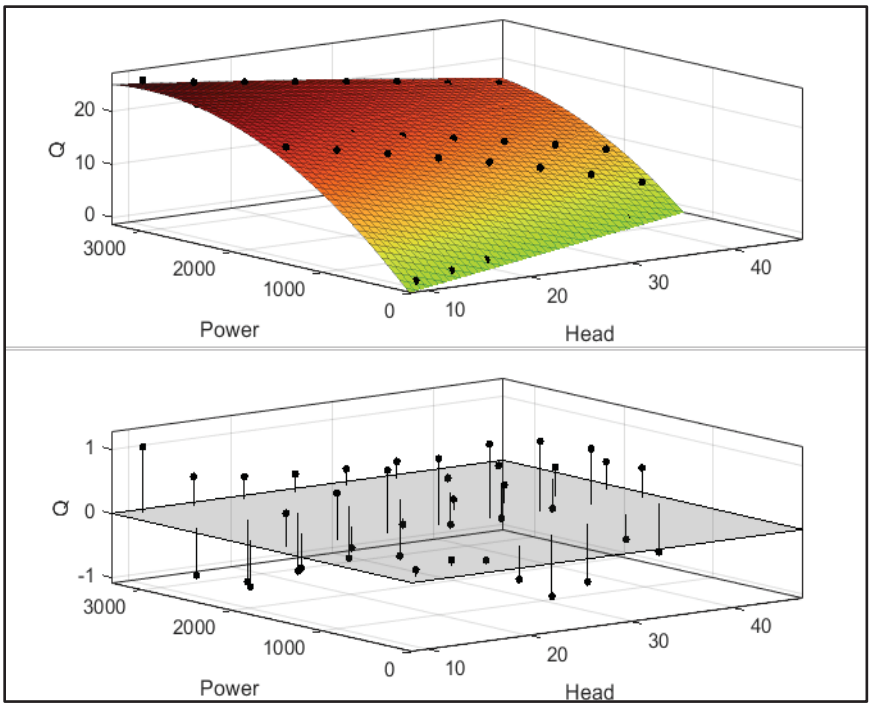

Figure 3.6 The fitted pump characteristic curve (top) and its residual values (bottom)

Table 3.1 Minimum and maximum power ranges for the Lorentz PS2-4000 C-SJ17-4 pump at different heads (BERNT LORENTZ GmbH & Co. KG, 2022)

Head [m]	10	15	20	25	30	35	40	45
Minimum input power [kW]	0.15	0.32	0.50	0.70	0.90	1.07	1.21	1.41
Maximum input power [kW]	3.50	3.50	3.50	3.50	3.40	3.35	3.35	3.30

3.4.5 Water pumping system

Considering an analogy between the battery storage system and water storage tanks, the Volume Of Reservoirs for each day (VOR(n)) is calculated based on the difference between daily pumped water (V(n)) and daily Water Requirement (WR(n)):

$$\mathrm{VOR(n)} = \mathrm{VOR(n-1)} + \sum_{t=1}^{t=24} \mathrm{Q(t)} - \mathrm{WR(n)} \tag{3.17}$$

As mentioned in Section 3. Case study, a constant daily water requirement of 26 m³ was considered for the community. Each water storage tank occupies a certain area, and this necessitates putting a limit on the maximum number of water storage tanks. Based on the type of water storage selected and area limitations, a maximum reservoir volume VOR_{max} of 87 m^3 was considered:

$$0 \leq VOR < VOR_{max} \tag{3.18}$$

3.4.6 Reliability models

LPSP is used as a criterion for assessing the reliability of electricity supply for the community. The LPSP is defined as follows (Al-Buraiki & Al-Sharafi, 2022):

$$\mathrm{LPSP} = \frac{\sum_{t=1}^{t=8760} \mathrm{LPS(t)}}{\sum_{t=1}^{t=8760} \mathrm{P_l(t)}} \times 100 \tag{3.19}$$

Based on the users' tolerance, a maximum allowable power loss will be considered:

$$\mathrm{LPSP} < \mathrm{LPSP_{max}} \tag{3.20}$$

The WSP percentage which is a measure of water access reliability (Irandoostshahrestani & R. Rousse, 2023) is defined as:

$$\mathrm{WSP\ (\%)} = \frac{\sum_{d=1}^{d=365} \mathrm{WS(d)}}{\sum_{d=1}^{d=365} \mathrm{WR(d)}} \times 100 \tag{3.21}$$

Similarly, a maximum value for the maximum WSP will be considered:

$$\mathrm{WSP} < \mathrm{WSP_{max}} \tag{3.22}$$

3.4.7 Economic model

The life cycle cost of the project was analyzed in this study. It is defined as follows:

$$\text{Life Cycle Cost} = \mathrm{CAPEX} + \mathrm{OPEX_t} \tag{3.23}$$

where CAPEX and $OPEX_t$ are the capital expenditure and total annual operational expenditures, respectively, and are defined as follows (Bhayo et al., 2019):

$$\mathrm{CAPEX} = \mathrm{CAPEX_{PV}} + \mathrm{CAPEX_{WT}} + \mathrm{CAPEX_{Battery}} + \mathrm{CAPEX_{Pumping}} + \mathrm{CAPEX_{Inverter}} + \mathrm{CAPEX_{MPPT}} + \mathrm{CAPEX_{Reservoir}} \quad (3.24)$$

Similar to WSP_{max} and $LPSP_{max}$, a maximum value is considered for CAPEX:

$$\mathrm{CAPEX} < \mathrm{CAPEX_{max}} \quad (3.25)$$

The total annual operational expenditures are defined as follows (Bhayo et al., 2019):

$$\mathrm{OPEX_t} = M_t + R_t + O_t + F_t \quad (3.26)$$

The operational cost (O_t) and fuel cost (F_t) are assumed to be zero. Furthermore, the maintenance cost (M_t) is considered to be 2% of the initial costs of the pumping system and PV panels each year throughout the project's lifetime (Bhayo et al., 2019; H. Li & Sun, 2018) and a constant value of $600 is considered for WT maintenance. The components' salvage values are disregarded, assuming they will be utilized throughout their entire lifespan (Bhandari & Stadler, 2009; Ndwali et al., 2020; Numbi & Malinga, 2017). Furthermore, the lifetime of the project was assumed to be 30 years. The replacement cost is determined based on the components' lifespan as follows:

$$R_t = (\mathrm{CAPEX_{Battery}} + \mathrm{CAPEX_{Inverter}} + \mathrm{CAPEX_{MPPT}} + \mathrm{CAPEX_{Pump}}) \times \left(\frac{1}{(1+r)^{10}} + \frac{1}{(1+r)^{20}}\right) + \left(\mathrm{CAPEX_{WT}} \times \frac{1}{(1+r)^{15}}\right) \quad (3.27)$$

The discount rate (r) is assumed to be 4% based on the reports of Bank of Canada (Bank of Canada, 2024). Furthermore, payback period is also considered to assess the feasibility of the project (Das et al., 2017), (Hossain Mondal, 2010):

$$\text{Payback period} = \frac{\text{Investment}}{\text{Annual net saving}} = \frac{\text{CapEx}}{\text{Return} - \text{Annualized OPEX}_t} \quad (3.28)$$

Return represents the cost savings from avoiding diesel generator fuel and its corresponding costs and is calculated as:

$$\text{Return} = [\text{Annual Energy Consumed} \times \text{Fuel price} \times \text{DG Efficiency}] + \mathrm{DG_{OM}} + \mathrm{DG_{Price}} \quad (3.29)$$

where Annual Energy Consumed is the total residential load and power required for pumping water. Diesel fuel price is considered to be equal to 1.78 C$/L ('Diesel Prices: Global Petrol Prices', 2025) and a mean value of 0.71 L/kWh is considered for the diesel generator efficiency, assuming a 50% capacity utilization for the DG (Fleck & Huot, 2009). Furthermore, its O&M costs estimated from available DGs on the market are assumed to be C$200 per year.

The optimization problem in the study is of a multi-objective type. As shown in the algorithm chart, there are four design variables (N_{PV}, N_{WT}, $N_{Battery}$, VOR_{max}) and three objectives (LPSP, WSP, and CAPEX). The goal is to minimize these objectives, which results in higher reliability in load and water demand, as well as lower costs. A multi-objective framework is used to minimize the objectives. The optimization is based on real data and configurations; therefore, a large dataset of different possible combinations of design is used. In this approach, only combinations meeting the defined constraints are considered in the optimization:

$$LPSP < LPSP_{max} , WSP < WSP_{max} , CAPEX < CAPEX_{max} \quad (3.30)$$

The NSGA-II method (Deb, Pratap, Agarwal, & Meyarivan, 2002) is used to solve this multi-objective problem by using DEAP algorithm (Fortin, Rainville, Gardner, Parizeau, & Gagné, 2017) of Python's NumPy package (van der Walt, Colbert, & Varoquaux, 2011). This algorithm assesses each solution by evaluating the degree it minimizes the objectives. Finally, a Pareto front solution is obtained while respecting the defined constraints of the project.

3.5 Specifications of the components

In this section, the specifications of the main components (i.e., PV panels, wind turbines, batteries, inverter, pumping system, water storage system, and solar charge controller) are summarized in Table 3.2. The project duration is set at 30 years, and the lifespans of the batteries, inverter, and charge controller are assumed to be 10 years. The PV panels and water storage system are assumed to operate for the lifetime of the project. The price of each component listed in the table is presented in Canadian dollars and estimated from the market.

Table 3.2 Specifications of the components

PV model	**RESTAR RTM-100M** (https://www.restarsolar.com/mono-crystalline-panel/mono-crystalline-pan-rtm-100m.html, 2025)
Type	Mono-crystalline
Power at STC, P_{mp}	100 W
Voltage at P_{mp}	17.90 V

Current at P_{mp}	5.59 A
Module Efficiency	15.44 %
Temperature Coefficient of P_{mp}	−0.39 %/°C
NOCT	45 °C
Lifespan	30 years
Dimensions	1200 × 540 × 35 mm
Price	C$150
Wind turbine	**Bergey windpower Excel 10** (*BERGEY EXCEL 10 Datasheet*, 2012)
Type	Horizontal axis with 3 blades
Rated Power	8.9 kW
Rated Windspeed	11 m/s
Cut-in Windspeed	2.5 m/s
Cut-out Windspeed	N.A. (assumed to be 20)
Lifespan	15 years
Price	C$40000
Battery model	**DC HOUSE** ('12V 200Ah Deep Cycle LiFePO4 Lithium Battery', 2025)
Type	Deep cycle lithium
Battery Capacity	2.56 kWh
Lifespan	10 years
Price	C$550
Inverter	**Generic model**
Type	Pure sine wave
Maximum Efficiency	92 %
Lifespan	10 years
Price	20% of PV+WT system
Charge controller	**Generic model**
Type	MPPT
Lifespan	10 years
Price	20% of PV system
Pumping system	**Lorentz PS2-4000 C-SJ17-4** (BERNT LORENTZ GmbH & Co. KG, 2022)
Type	Submersible
Maximum Power	4 kW
Maximum Flow Rate	26 m^3/h
Maximum Head	45 m
Lifespan	10 years
Price	C$10000
Water storage	**VT1650-86** ('ONTARIO AGRA: Vertical Liquid Storage Tanks', 2025)

Type	Vertical liquid storage tank
Volume	6246 Liters
Dimensions	86″ Diameter x 74″ Height
Lifespan	30 years
Price	C$2500

3.6 Results and discussions

The study by Bhayo et al. (Bhayo et al., 2019) was used for validation purposes, and the details of the validation process were provided in our previous study (Irandoostshahrestani & R. Rousse, 2023), ensuring the validity of the results for basic solar geometric equations, PV/battery calculations, and the developed economic model. Initially, it is important to find the most appropriate tilt angle for the PV array. Although there are general guidelines for finding the best tilt angle, various factors like the location's latitude, surface azimuth angle, clearness index, etc. affect the optimal slope (Memme & Fossa, 2022). Three different modes were considered to determine the best angle: (1) a fixed tilt angle throughout the year, (2) a seasonal adjustment of the tilt angle to its optimal value, and (3) a monthly adjustment of the tilt angle to its best value for each month. In all different modes, various tilt angles from 0° to 90° were evaluated to obtain the optimum angle in terms of the average global solar radiation on the inclined surface. Figure 3.7 shows the result of solar insolation and the optimized tilt angle for the mentioned modes. Section (a) shows that the optimal tilt angles vary considerably during the year, and they range from 10° in June to 65° in January. As shown in Figure 3.3, July has the highest GHI values, making it the month with the greatest solar insolation among other months in section(a). Similarly, solar insolation is generally higher in spring and summer but significantly weaker in fall and winter due to lower GHI values, as shown in section (b). This figure shows that a fixed tilt angle of 28° results in a maximum annual insolation of 3.50 kWh/m²-day. For monthly and seasonally changing tilt angle modes, the best tilt angles are shown in section (c). Figure 3.8 depicts the daily average of solar insolation for the three modes, showing that the annual average of daily solar insolation for a fixed 28° tilt angle (3.50 kWh/m²-day) is only slightly lower than that of the seasonal (3.56 kWh/m²-day) and monthly (3.59 kWh/m²-day) adjustment modes. This corresponds to a maximum reduction of 2.6% in annual insolation for the fixed tilt angle strategy. To avoid complexity, the fixed tilt strategy is

used. Figure 3.8 shows that solar insolation is considerably lower in fall and winter, and it emphasizes the importance of wind turbine contributions during low-irradiation months.

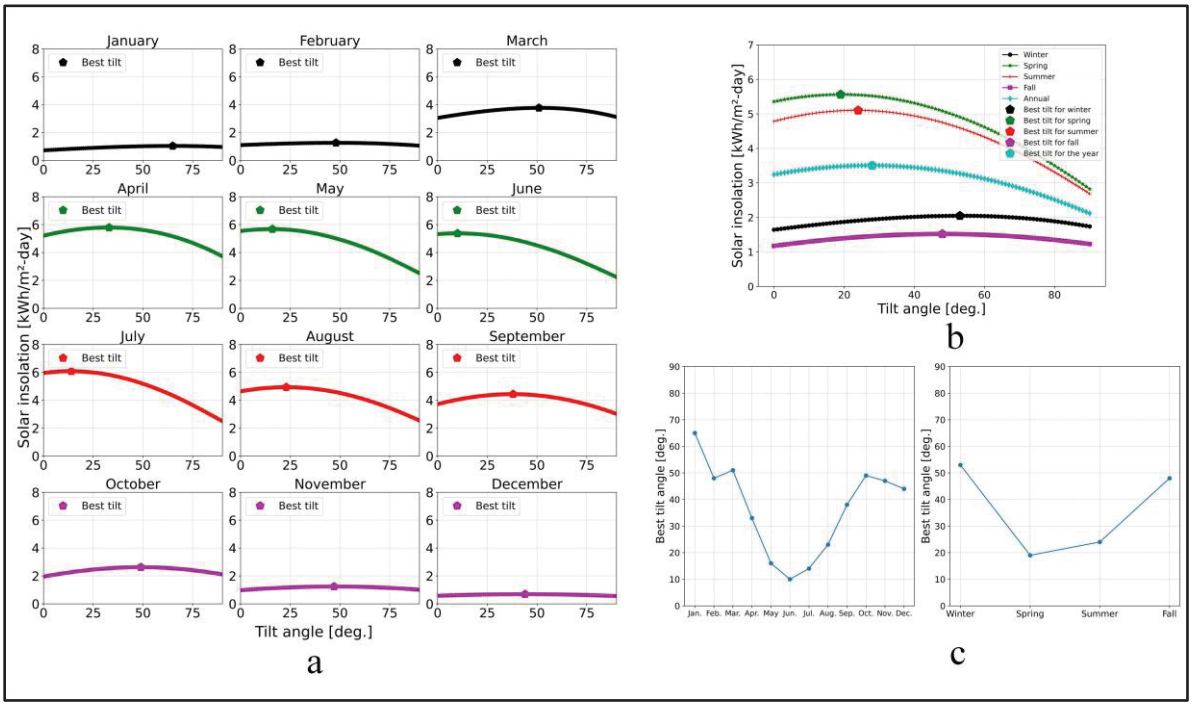

Figure 3.7 (a) Monthly solar insolation and optimal tilt angles.
(b) Seasonal and annual tilt optimization.
(c) Optimized monthly and seasonal tilt angles

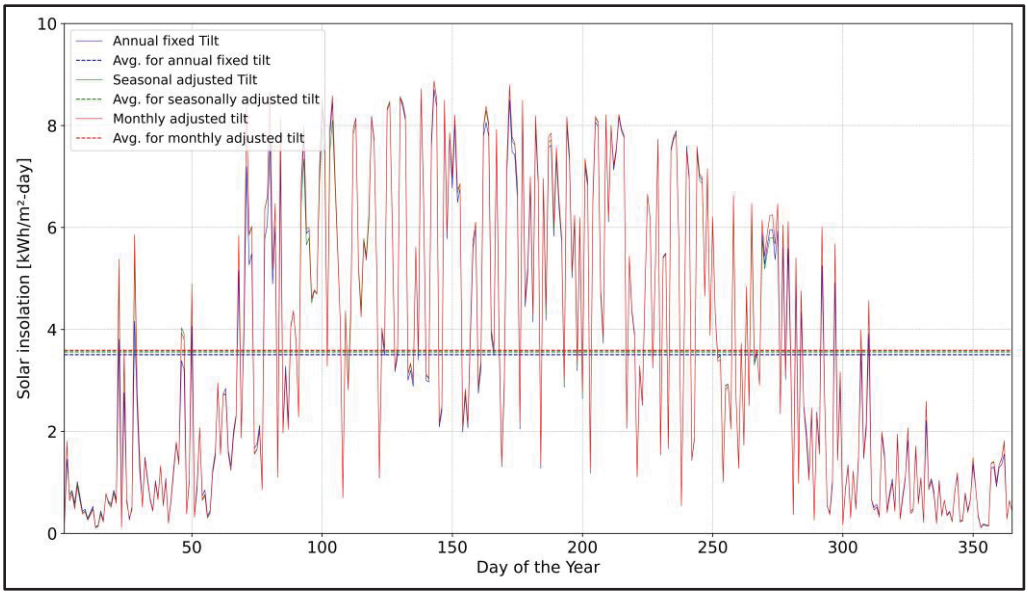

Figure 3.8 Comparison of solar insolation for fixed, seasonal, and monthly tilt adjustment strategies throughout the year

The results of the optimization, with constraints of $LPSP_{max}$ and WSP_{max} set at 15% and $CAPEX_{max}$ set at C$3 million, are shown in Figure 3.9. All the solutions correspond to systems with 200 to 260 kW of wind turbine rated power, 30 to 60 kW capacity of PV panels, and 1 to 3.6 MWh battery storage and 68-87 m^3 of water storage system (not shown in the figures). Furthermore, most of the optimized systems feature the maximum possible number of PV panels and battery capacities up to 3.6 MWh although there were no constraints for battery capacity. This is because batteries impact the system's CAPEX more than other components due to their higher prices; therefore, the optimized systems tend to include a limited capacity for battery banks.

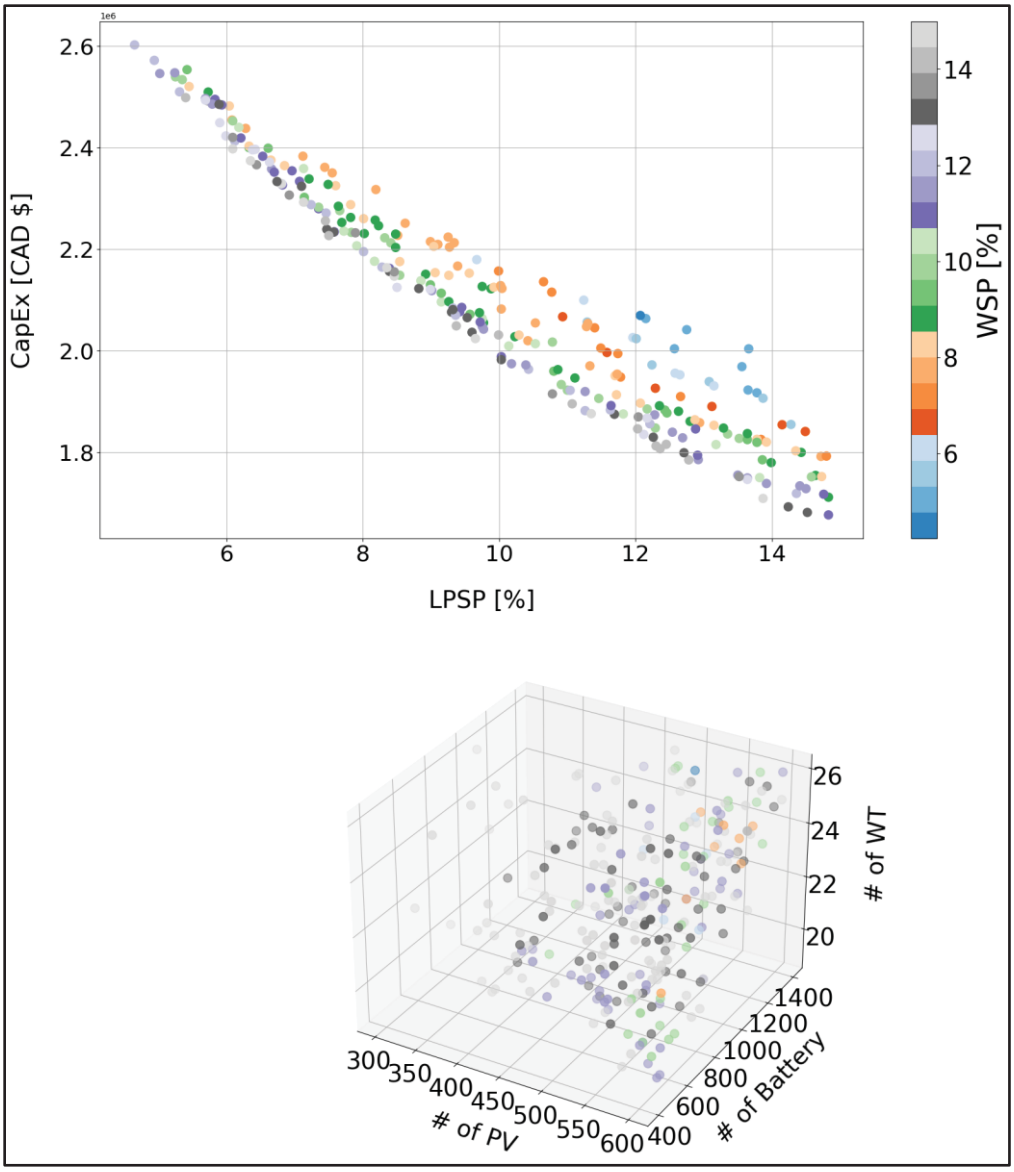

Figure 3.9 Optimized objectives (top) and the corresponding system configuration (bottom) for $LPSP_{max}$ and WSP_{max} of 15% and $CAPEX_{max}$ of 3 M$

To demonstrate the performance of the designed system, a system configuration of interest with 60 kW PV panel capacity, 260 kW nominal power of WT, 1.54 MWh battery storage capacity, and a water storage volume of 87 cubic meters, resulting in an LPSP of 9.9%, WSP of 5.4%, and a CAPEX of C$2.2 million is selected. The system performance is shown in Figure 3.10. Despite low solar insolation in cold seasons and low WT power generation on some days, the system remains reliable by means of the battery storage systems, which leads

to minimum SOCs for the batteries for many hours of the year. Furthermore, the daily water requirement, pumped water, reserved water, and water deficit throughout the year are shown in Figure 3.11. It is evident that there is abundant excess power in most of the year with a maximum potential pumped water of 384 m^3 as the pumping system has a maximum water pumping rate of 16 m^3 per hour at full load. Here, the WSP is mainly limited by the maximum water storage capacity, as there is considerable excess power, and increasing storage capacity can help mitigate water shortages.

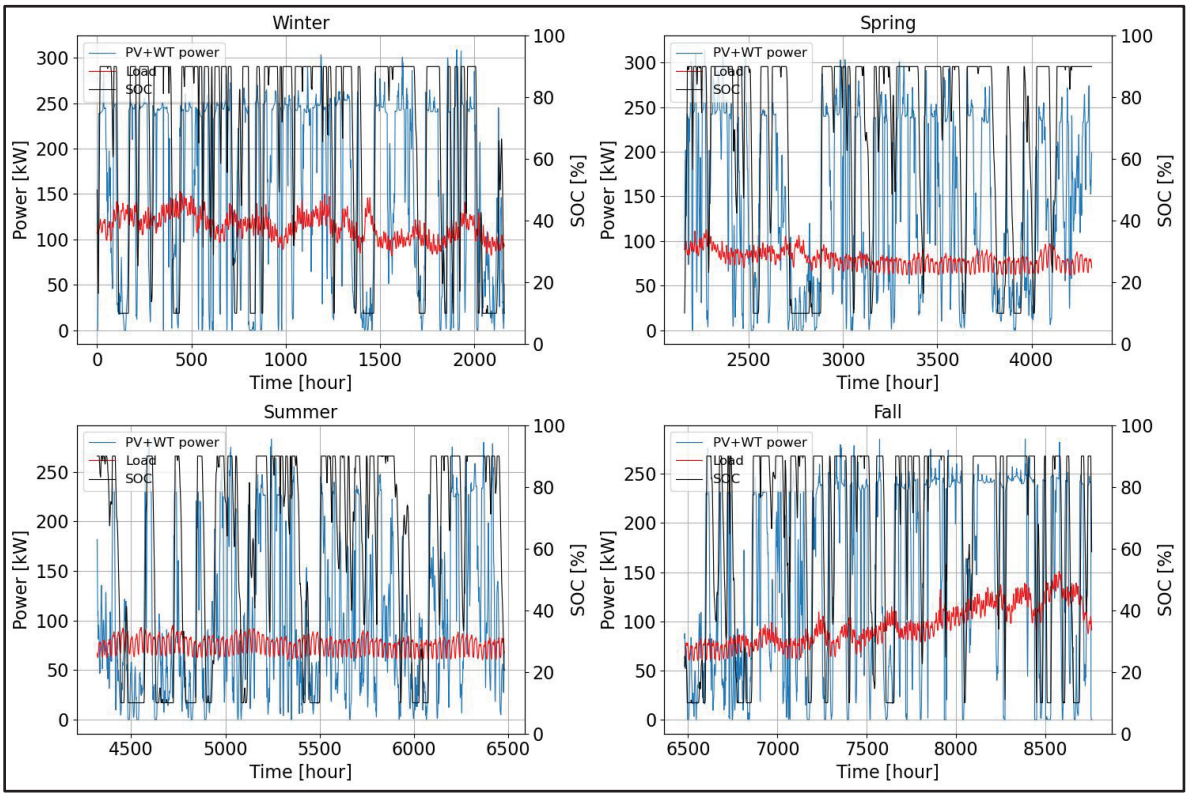

Figure 3.10 SOC, PV and WT generated power,
and load demand over the course of a year
for a specific system

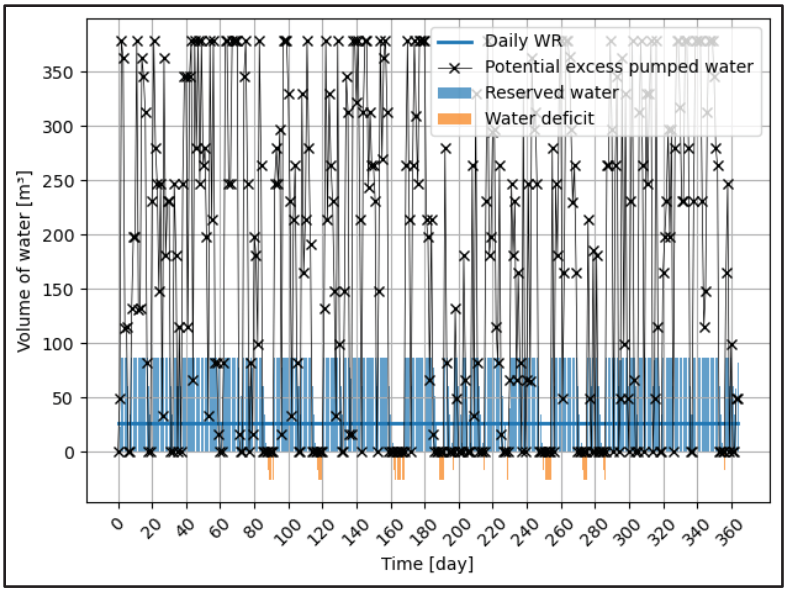

Figure 3.11 Water volume dynamics during the year for a specific system

To better understand the contribution of each energy production source, Figure 3.12 depicts the daily average energy production for the mentioned system (i.e., a system with a 260 kW wind turbine and 60 kW PV capacity with 1.54 MWh battery storage and a 87 m³ water tanker). The blue bars represent wind turbine production, while the yellow sections indicate solar PV generation. The red dashed line is the average daily energy consumption. There are times when total renewable generation is more than consumption, and also other times when production is low, which shows the variability of these energy sources. In summer, when wind speeds are low (see Figure 3.4), solar PV production compensates for the low wind energy production. On the other hand, in seasons with less sunlight, wind production is higher and it makes up for the low solar energy generation. It demonstrates how wind and solar energy complement each other throughout the year, and they create a more balanced and reliable system compared to systems relying only on PV or WT generation. It is worth mentioning that the nominal power of PV systems is lower than WT installations as they occupy more area. Systems with a single electricity source can only operate effectively when the source is stable and the demand is lower than the generation capacity. This is evident in the study by Bhayo et al. (Bhayo et al., 2019), where the maximum hourly load was less than 300 W, and there were no consecutive days of very low irradiation in the case study of Malaysia. It is worth noting that the system

corresponding to Figure 3.12 has an LPSP of 9.9% and a WSP of 5.4%, with a CAPEX of C$2.2 million. The mentioned complementary behavior of PV and WT relatively minimizes the need to oversize the system with excessively large PV panels, wind turbines or storage. It is obvious that it is possible to design a system with LPSP of zero but it requires a larger system size. However, the goal of this study is to show the feasibility of increasing renewable energy penetration while keeping in mind that an auxiliary power generation system should be considered to enhance system reliability.

In order to evaluate the economic feasibility of the project, the payback period is plotted for the optimized solutions, Figure 3.13. It can be seen that the system with the lowest LPSP has a payback period of 12.0 years, while systems with an LPSP of 15% have payback periods of about 8.0 years. It should be mentioned that these payback period values are obtained based on scenarios where a diesel generator is used as an alternative to the renewable PV/WT system and the land price is not included in the calculations. However, when access to the grid is available, the payback period for renewable systems increases, making them unfeasible due to the considerably low electricity price in Quebec (Hydro Quebec, 2023), which is around 6.7 cents per kWh. The proposed systems of the study have LCOE in the range of 16.3 ¢/kWh to 23.4 ¢/kWh which are not competitive with grid power in Quebec. However, Îles-de-la-Madeleine has no grid access as it is located more than 100 kilometers away from the coast of Quebec.

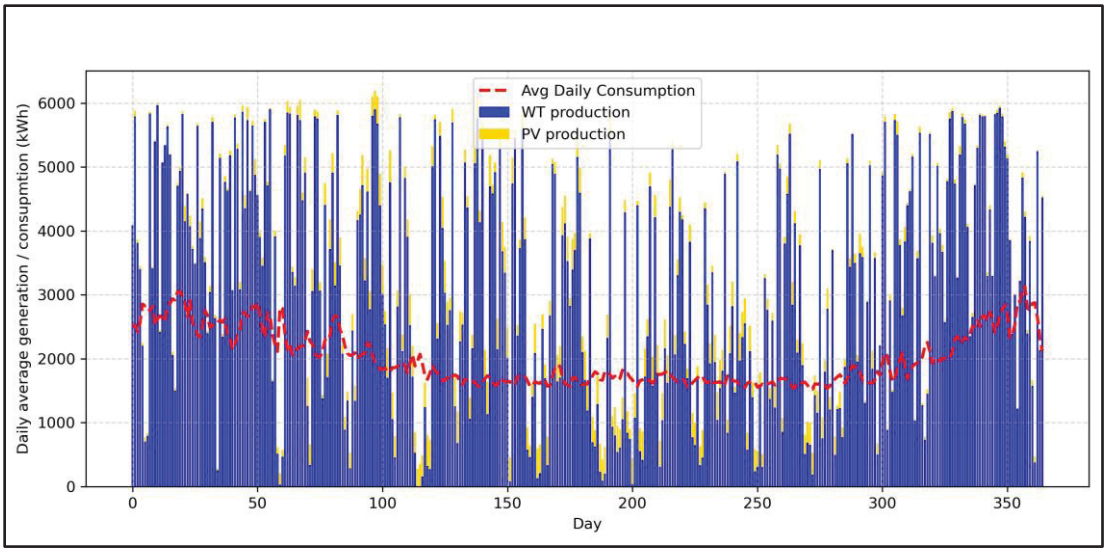

Figure 3.12 Daily total energy production from PV and WT over a year for a specified configuration

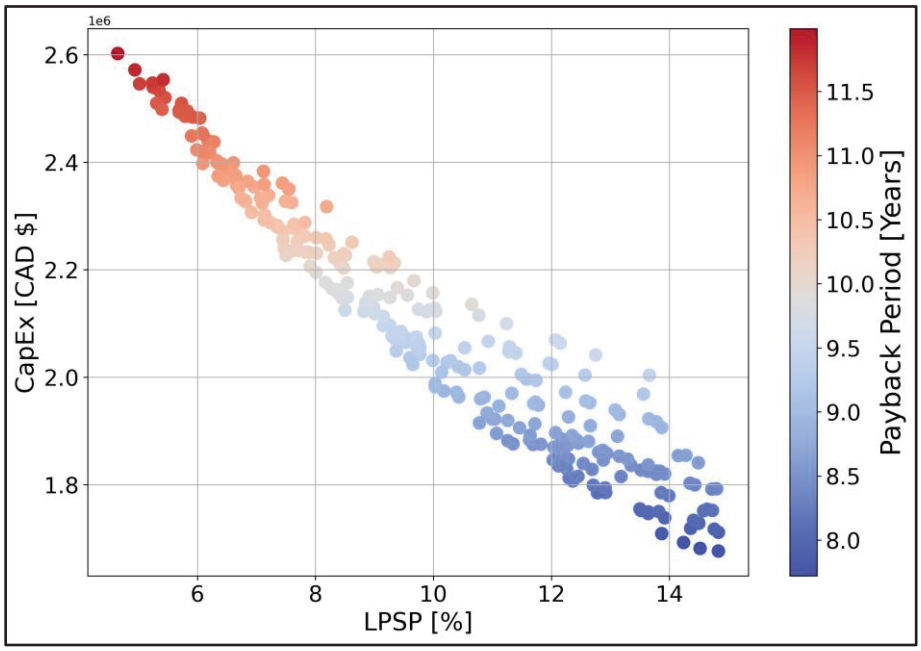

Figure 3.13 Payback period for proposed systems

3.7 Conclusions

In this study, an off-grid PV-WT-battery and water storage system is designed to meet the residential load demand and provide water for a community in Îles de la Madeleine, Quebec,

Canada. The EMS used in the study prioritizes residential load demand over water pumping. The EMS mandates that the system charge the batteries when excess power is available after meeting the residential load. Furthermore, if surplus energy still remains, the pumping system is activated to store water in reservoirs. The concepts of LPSP and WSP are employed to evaluate system reliability, and the system is optimized using the GA with these reliability objectives, as well as CAPEX. Due to land area limitations, the system design imposes a maximum allowable number of PV panels and wind turbines. It was shown that the electricity production of PV and WT exhibits complementary behavior across different seasons, enhancing system reliability. It was demonstrated that LPSP and WSP significantly influence system size and, consequently, its CAPEX. Furthermore, the system has considerable excess power during the year which can be used for a water pumping system for the community. The goal of this study was to show the feasibility of increasing renewable energy systems in remote areas with no grid access in order to lower dependency to conventional diesel generator power generation. The proposed optimized systems had a payback period in the range of 8.0 to 12.0 years with LCOE in the range of 16.3 ¢/kWh to 23.4 ¢/kWh.

CHAPTER 4

DISCUSSIONS

In chapter 2, a PV-battery storage system designed for a house with low electricity consumption was studied for a location with high solar potential. In this section, the effects of wind turbine integration to a PV system for a location with limited solar irradiation were studied. The dispatch algorithm, methodology and components are similar to those discussed in Chapter 3. The village of Kuujjuaq, located in the Nunavik region of Quebec, Canada, at a latitude of 58.09°N and a longitude of 68.42°W, was selected for this evaluation.

It should be noted that the village of Kuujuaq was chosen with the sole aim of demonstrating that the proposed methodology can be used in a wide range of sites on land and because data is easily accessible. It must be admitted, however, that water pumping could not be carried out easily from ground water due to the average temperature of the site. In addition, the idea of preheating the water pumped from the reservoir to avoid freezing would consume a preponderant amount of energy. In fact, water in Kuujuaq is transported to homes by truck, not by an aqueduct as in the south. However, there are facilities like the water supply infrastructure with 825 m^3 reservoir in the village (‘Water Supply Infrastructure in the Northern Village of Kuujjuaq’, 2025).

Data from the NSRDB (NREL, 2022a) for the most recent available year, i.e., 2023, was used. Figure 4.1 shows the monthly average variations in GHI, ambient temperature, and albedo coefficient. As shown, the minimum monthly average temperature is -28.3°C in February, while the maximum is 15.1°C in July. The albedo coefficient is notably high in late fall and winter because the ground is snow-covered. Furthermore, the monthly average of GHI ranges widely from 0.26 kWh/m^2-day in December to 6.2 kWh/m^2-day in June.

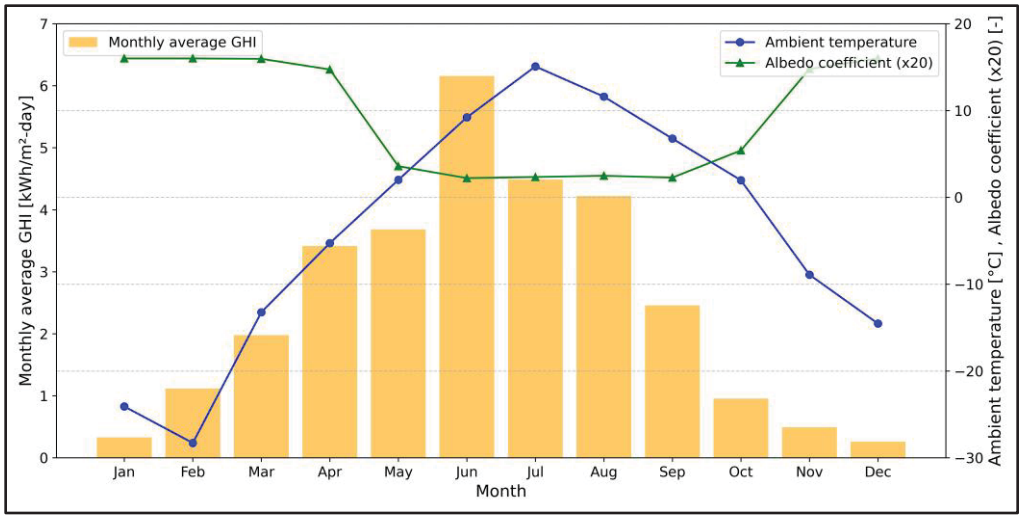

Figure 4.1 Monthly averages of GHI, ambient temperature, and albedo coefficient for Kuujjuaq

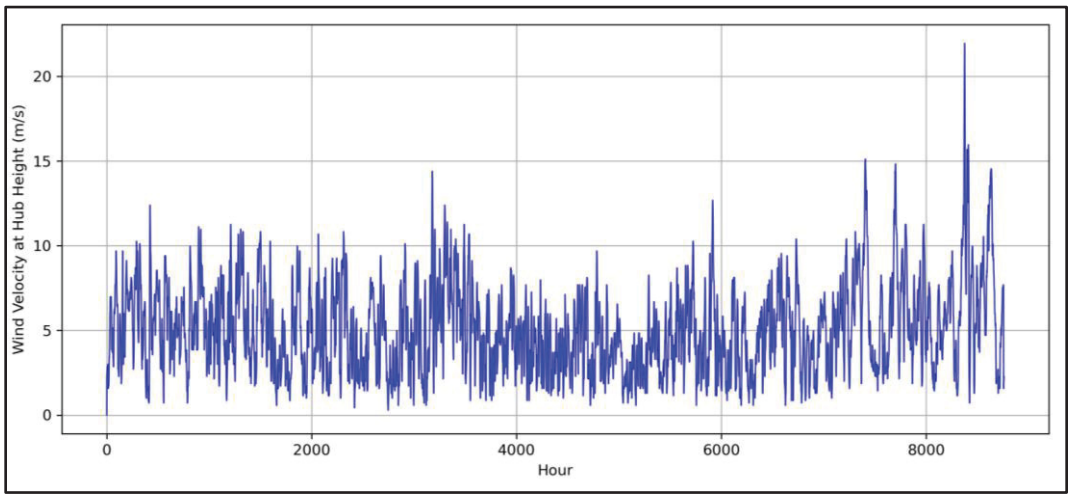

Figure 4.2 Windspeed at hub height for Kuujjuaq village, QC

For estimating theoretical irrigation values, a total annual net water requirement of 550 mm is considered for an equivalent potato farm, as obtained from a report by Alberta Agriculture and Rural Development (Mckenzie & Shelley A. Woods, 2011). As shown in Figure 4.3, the farm needs irrigation from May to September. These figures are transposed to Kujjuuaq, although there is no farming possibility in this area of the country. Therefore, the theoretical pumping system should provide the average daily irrigation equal to these monthly amounts. The proposed farm area is 1 hectare (ha), and the irrigation water requirement (IWR) is calculated by multiplying the net water requirement by the farm area. This results in average monthly

needs of 26.2, 98.8, 170.4, 179.9, and 74.9 cubic meters of water from May to September. It is worth noting that the average ambient temperature remains above 0 °C during these months (Figure 4.1), with minimal risk of water freezing.

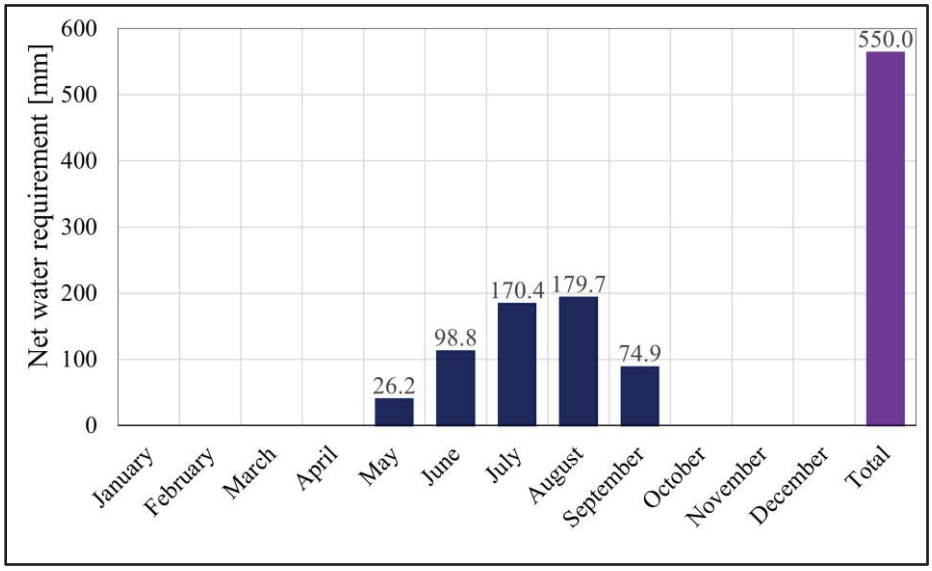

Figure 4.3 Annual irrigation water requirement for a typical farm (Mckenzie & Shelley A. Woods, 2011)

Furthermore, the electricity demand of a typical rural home is shown in Figure 4.4, with a daily consumption of 13 kWh. This should be noted that this location requires a conventional heating system (like a diesel-based furnace) to be used in winters as the weather conditions are very harsh in cold seasons, and the current electricity consumption excludes heating loads.

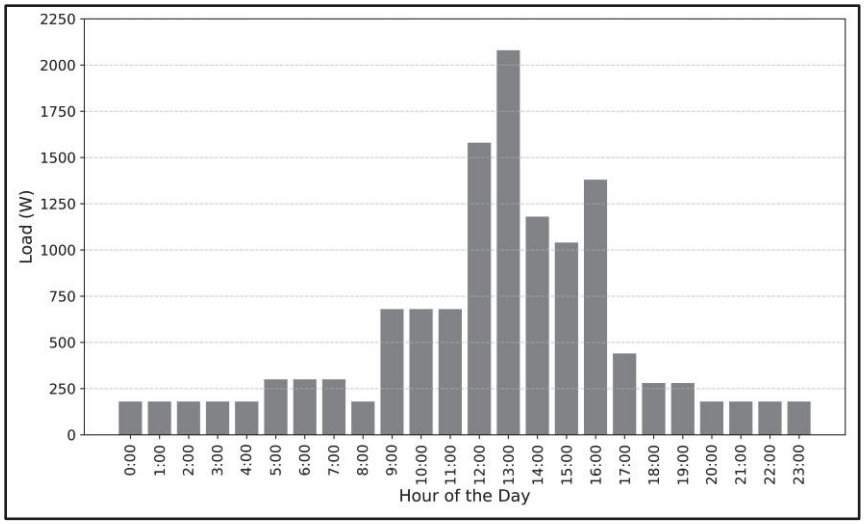

Figure 4.4 Hourly pattern of daily electricity consumption for a house

Figure 4.5 shows the result of solar insolation and the optimized tilt angle for the mentioned modes. Section (a) illustrates that the optimal tilt angles vary significantly throughout the year, ranging from 18° in July to 90° in December. As shown in Figure 4.1, June has the highest GHI values, making it the month with the greatest solar insolation among other months in section (a). Similarly, solar insolation is generally higher in spring and summer but significantly weaker in fall due to lower GHI values, as shown in section (b). This figure shows that a fixed tilt angle of 42° results in a maximum annual insolation of 2.89 kWh/m²-day. For monthly and seasonally changing tilt angle modes, the best tilt angles are shown in section (c). Figure 4.6 depicts the daily average of solar insolation for the three modes, showing that the annual average of daily solar insolation for a fixed 42° tilt angle (2.89 kWh/m²-day) is only slightly lower than that of the seasonal (3.05 kWh/m²-day) and monthly (3.10 kWh/m²-day) adjustment modes. This corresponds to a maximum reduction of 7% in annual insolation for the fixed tilt angle strategy. To avoid the inconvenience of adjusting the panel each month or each season, the fixed tilt angle strategy is considered. Figure 4.6 shows that solar insolation is considerably lower in cold seasons, and this shows the importance of wind turbine integration during these months.

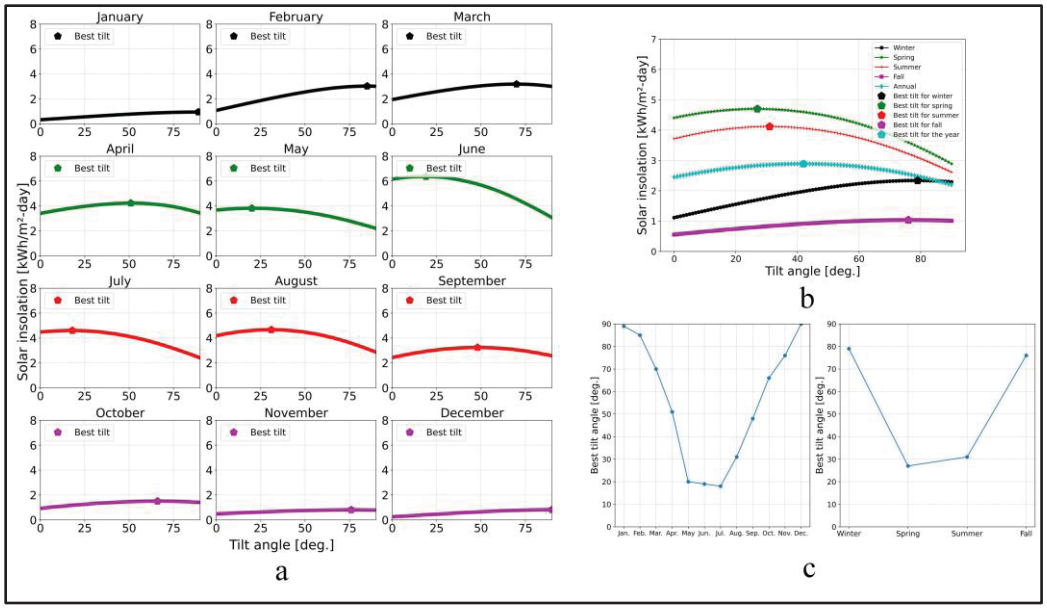

Figure 4.5 (a)Monthly solar insolation and optimal tilt angles.
(b) Seasonal and annual tilt optimization.
(c) Optimized monthly and seasonal tilt angles

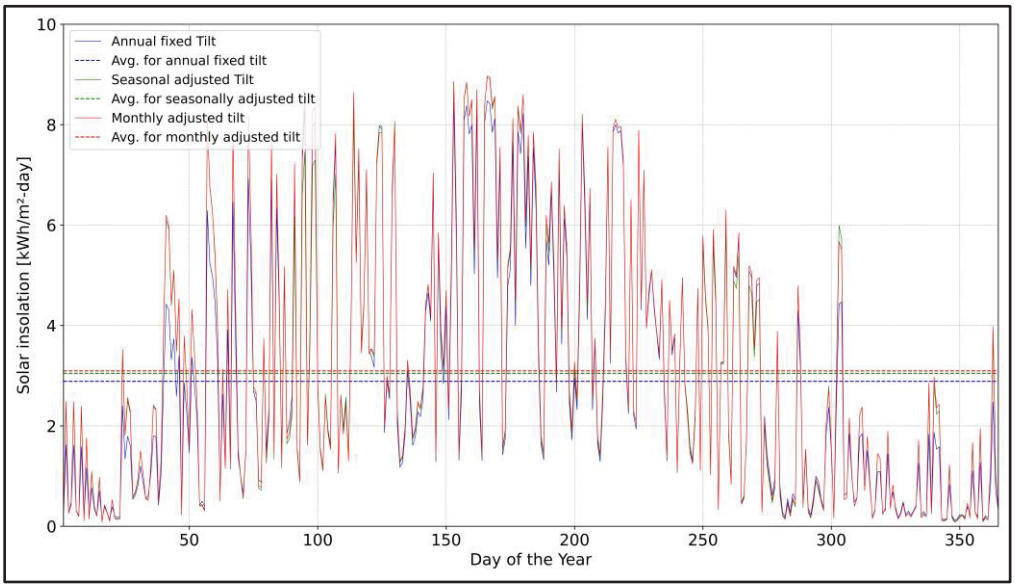

Figure 4.6 Comparison of solar insolation for fixed, seasonal and monthly tilt adjustment strategies throughout the year

4.1 PV- BESS system with no wind turbine integration

Initially, no wind turbine contribution was assumed to show the deficiencies in the system design. The results of the optimization, with constraints of $LPSP_{max}$ of 15%, WSP_{max} set at 25% and $CAPEX_{max}$ set at C$80 thousand, are shown in Figure 4.7. These constraints are based on practical limitations, such as budget considerations or performance thresholds. In the top subplot, the objective functions are shown, and the bottom subplot shows the system configuration in terms of N_{PV}, $N_{Battery}$, and VOR_{max}. It can be seen that systems with lower WSP and LPSP values correspond to higher CAPEX values. This is due to the fact that larger systems have higher nominal capacities for batteries, PV panels, and water storage systems. Clearly, all optimized solutions correspond to configurations with the maximum possible number of PV panels (i.e., 60), resulting in a nominal PV capacity of 6 kW. It can be concluded that if there are no land area limitations for PV panels, it is advisable to remove the constraint on the maximum PV panel capacity in the system design procedure. In addition, as evident from the figure, the optimized solutions correspond to systems with battery capacities below 340 kWh (i.e., a maximum of 186 batteries). It should be noted that battery capacity, as one of the design parameters, had no maximum value constraint as its upper bound. However, due to the higher cost of batteries compared to water storage systems and PV panels, no optimized solution includes battery capacities above 340 kWh for the defined objective limits. It is evident from Figure 4.7 that although the selected systems are large (263- 283 battery banks with a capacity of 316-340 kWh and 60 PV panels with a nominal power of 6 kW), the system lacks reliability (LPSP in the range of 14.3-15% and WSP in the range of 22-24%) with CAPEX of approximately C$76-80 thousand. This is justified by the fact that GHI values are very low in fall and early winter (less than 2 kWh/m^2-day), leading to consecutive days of low PV production, affecting system reliability.

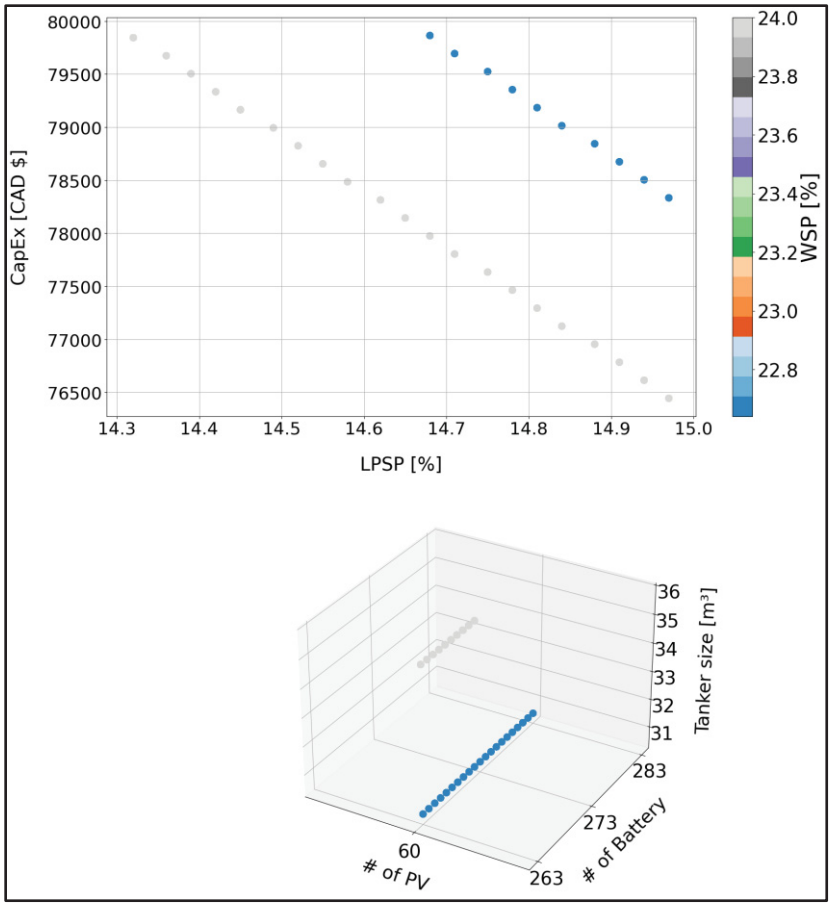

Figure 4.7 Optimized objectives (top) and the corresponding system configuration (bottom) for system with no WT contribution

To demonstrate the performance of the designed system, we selected a system configuration of interest with 60 PV panels (6 kW capacity), 263 batteries (316 kWh storage capacity), and a water storage tank of 35.7 cubic meters, resulting in an LPSP of 14.97%, WSP of 22.64%, and a CAPEX of C$78,334. The system performance is shown in Figure 4.8. During fall and early winter, PV power is very low (due to low GHI values), and the PV panels cannot meet the residential load. As a result, the batteries discharge until they reach their minimum SOC, set to 10% of IBC. During these hours, the system experiences energy deficits, leading to a considerable loss of power supply. Conversely, during most hours of the hot seasons, excess power fully charges the batteries to their maximum SOC of 90% of IBC. Notably, the EMS for the electricity dispatch strategy used in the algorithm, which runs the pumps when the batteries

are fully charged, aligns with the simultaneous availability of high solar irradiation and water demand in the hot season months.

Additionally, the daily irrigation water requirement, pumped water, reserved water, and water deficit throughout the year are shown in Figure 4.9. It is evident that there is abundant excess power in the hot seasons, whereas the system is unable to run the pumps in fall and winter, leading to water deficits and low reliability for the water pumping system, although the farm does not need water for irrigation. The goal of this section was to show how much unreliability arises in terms of LPSP and WSP when only PV is used as the supply source. In the next section, WT is integrated to the system, resulting in better power supply and consequently water access for irrigation.

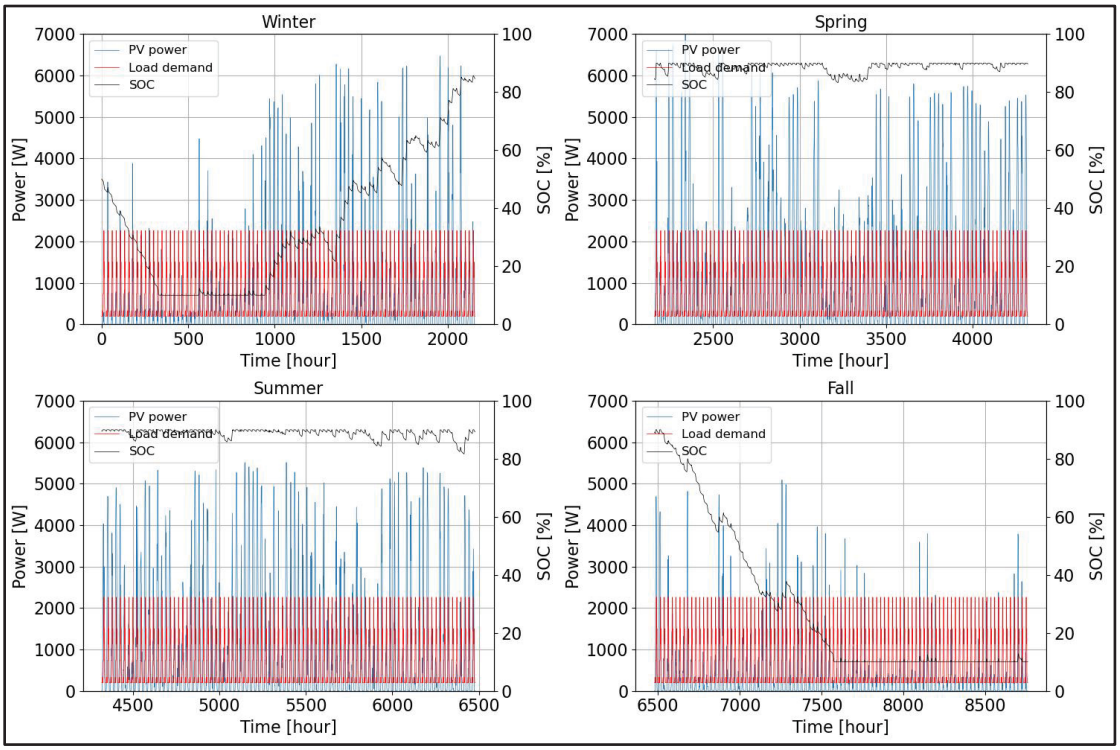

Figure 4.8 SOC, PV-generated power, and load demand over the course of a year for a specific system configuration with no WT contribution

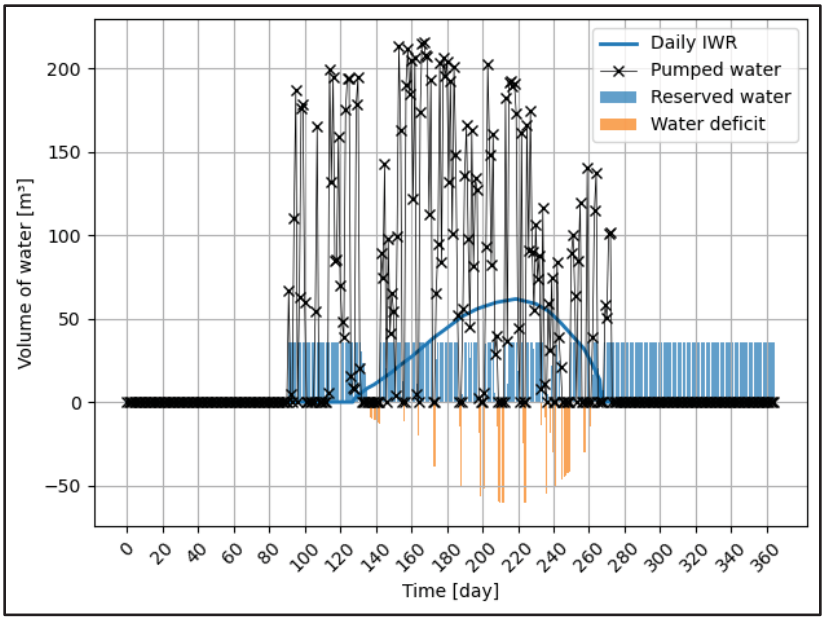

Figure 4.9 Water volume dynamics during the year
for a specific system with no WT contribution

4.2 PV- BESS system with wind turbine integration

In this section, it is assumed that the system can integrate wind turbines up to $N_{WT,max}$. The results of the optimization, with constraints of $LPSP_{max}$ and WSP_{max} set at 6% and $CAPEX_{max}$ set at C$80 thousand, are shown in Figure 4.10. All optimized systems correspond to those with the maximum possible WT nominal power, i.e., four wind turbines with a total capacity of 4 kW (not included in this figure). Furthermore, almost all optimized systems feature the maximum possible number of panels (60), the maximum possible water storage capacity (40.8 m^3), and relatively low battery capacities (up to 36 batteries with a total nominal capacity of 43.2 kWh). This is because batteries impact the system's CAPEX more than other components; therefore, the optimized systems tend to include fewer battery banks. This system is more reliable in terms of LPSP and WSP compared to a system with no wind turbine while maintaining a similar CAPEX range. The system can achieve an LPSP as low as 0 and a WSP as low as 6%.

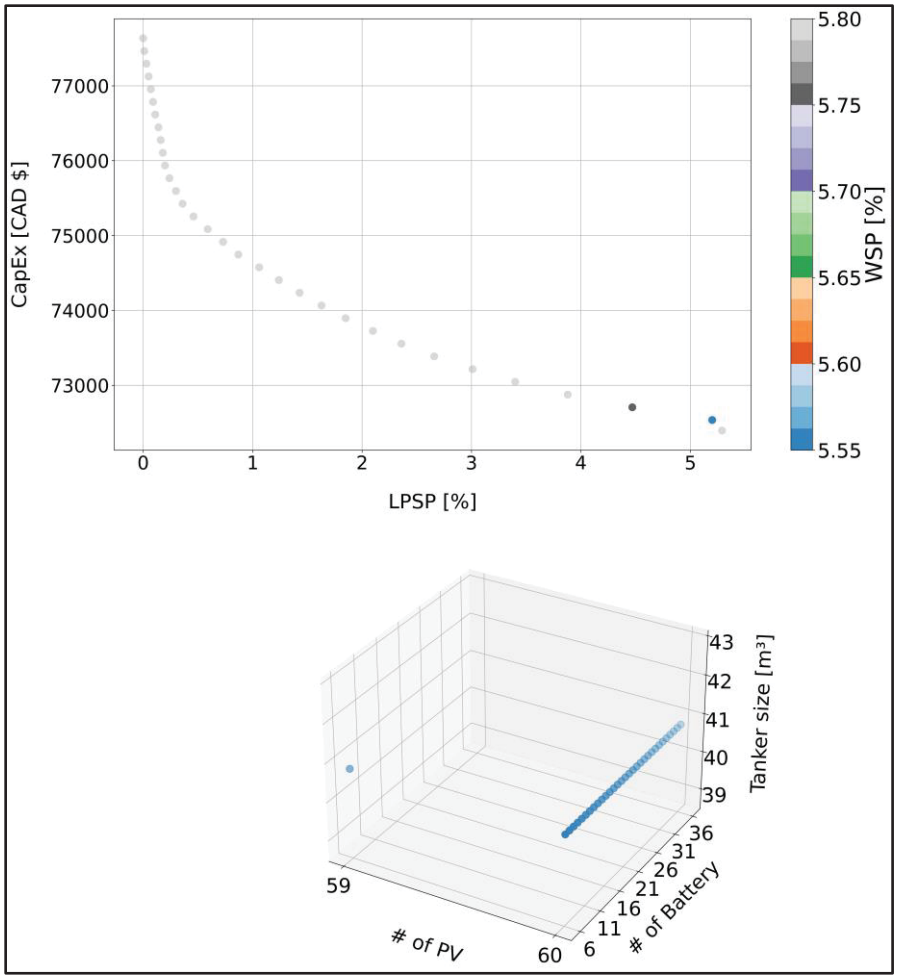

Figure 4.10 Optimized objectives (top) and
the corresponding system configuration (bottom)
for system with WT integrated

To demonstrate the performance of the designed system, we selected a system configuration of interest with 60 PV panels (6 kW capacity), four wind turbines (4 kW nominal power), 36 batteries (43.2 kWh storage capacity), and a water storage tank of 40.8 cubic meters, resulting in an LPSP of 0, WSP of 5.79%, and a CAPEX of C$ 77,634. The system performance is shown in Figure 4.11. Despite low solar insolation in cold seasons, the system remains reliable, and the batteries rarely reach their minimum SOC (only in fall). Furthermore, the daily irrigation water requirement, pumped water, reserved water, and water deficit throughout the year are shown in Figure 4.12. It is evident that there is abundant excess power in the hot

seasons, while the system can still run the pumps in fall and winter, leading to relatively higher reliability in terms of WSP compared to the system without WT integration.

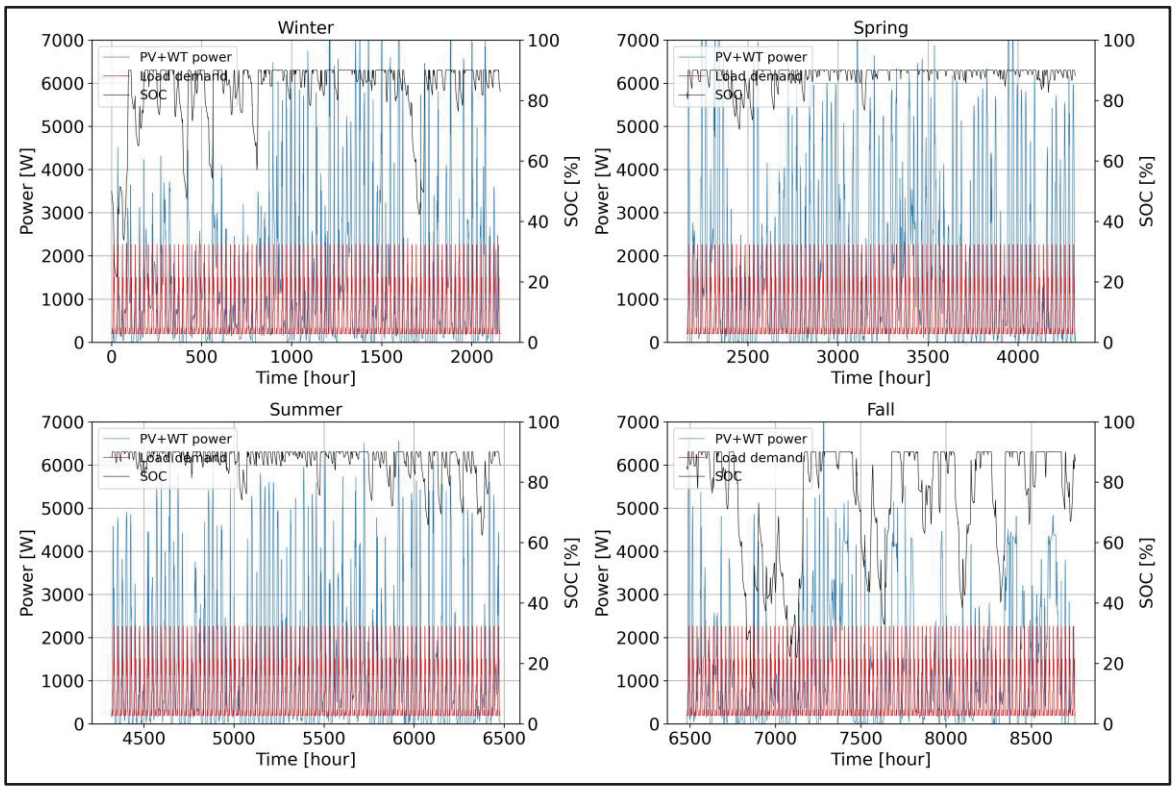

Figure 4.11 SOC, PV-generated power, and load demand over the course of a year for a specific system with WT integration

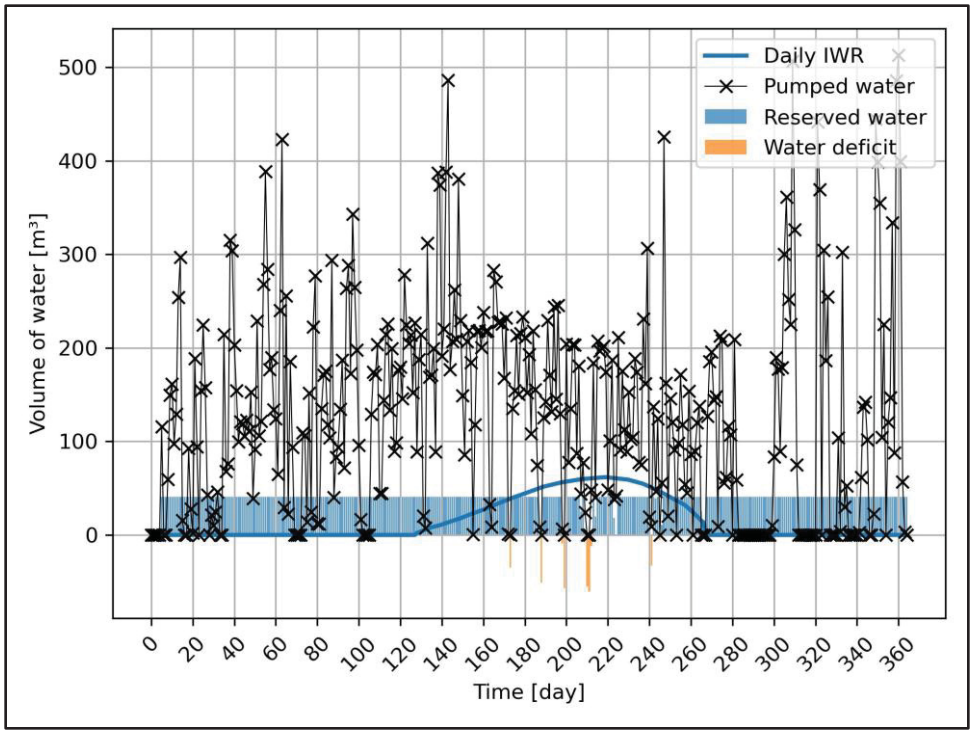

Figure 4.12 Dynamics of water volume for a specific system with wind turbine integration

To better understand the contribution of each energy production source, Figure 4.13 depicts the daily average energy production for a system with a 4 kW wind turbine and 6 kW PV capacity with 43.2 kWh battery storage and a 40.8 m³ water tanker. The blue bars show wind turbine production, and the yellow bars represent generation of solar PV panels. The red dashed line is the average daily energy consumption (13 kWh). As can be seen, in some hours total renewable generation is more than consumption that results in surplus energy, and at some other time periods, production is lower than demand. This shows the variability of these renewable energy sources. In summer, wind speeds are low for this location (see Figure 4.2), and solar PV production is increased and compensates for the reduced wind energy production. On the other side, in seasons with low irradiations, wind production is higher, which makes up for the low solar energy irradiation. It shows how wind and solar energy complement each other, and make a balanced and reliable system in comparison with a system that only relies on PV generation. Systems with one generation source can only be reliable when the source is stable for a whole year and the demand remains less than the generation. This is evident in the

study by Bhayo et al. (Bhayo et al., 2019), where the maximum hourly load was less than 300 W, and there were no consecutive days of very low irradiation in the case study of Malaysia. It is worth noting that the system corresponding to Figure 4.13 has an LPSP of 0 and a WSP of 5.79%, with a CAPEX of C$77,634. The mentioned complementary behavior of PV and WT minimizes the need to oversize the system with excessively large PV panels, wind turbines, or storage. In order to evaluate the economic feasibility of the project, the payback period is plotted for the optimized solutions, Figure 4.14. It can be seen that the system with the lowest LPSP has a payback period of 10.3 years, while systems with an LPSP of 5.3% have payback periods of 9.3 years. It should be mentioned that these payback period values are obtained based on scenarios where a diesel generator is used as an alternative to the renewable PV/WT system. However, when access to the grid is available, the payback period for renewable systems increases, making them unfeasible due to the considerably low electricity price in Quebec (Hydro Quebec, 2023), which is around 6.7 cents per kWh for the first 40 kWh of daily consumption.

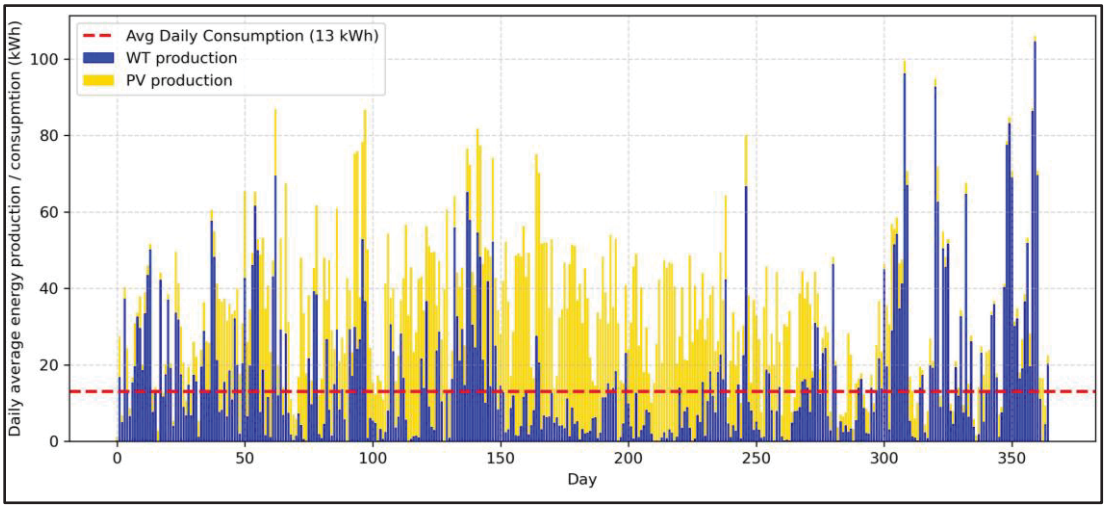

Figure 4.13 Daily total energy production from PV and WT for a specified system

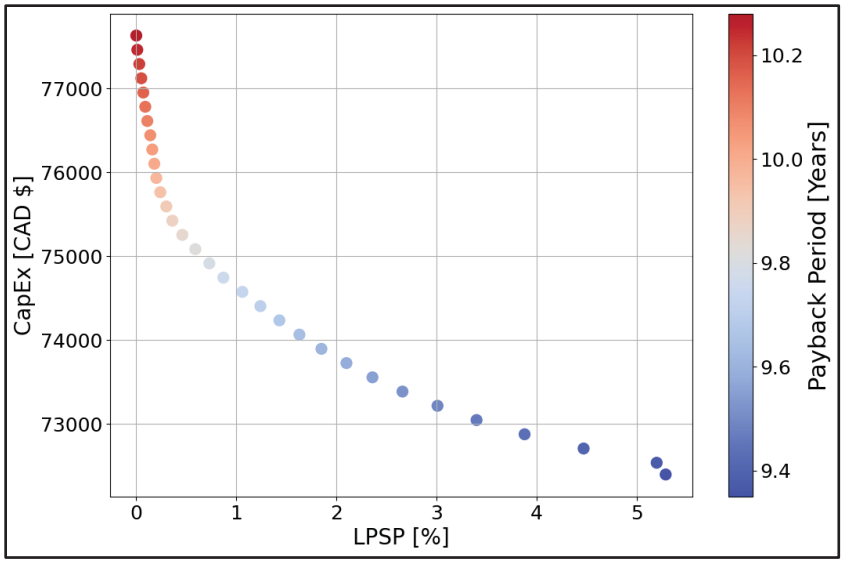

Figure 4.14 Payback period for optimized systems

4.3 Discussions

As discussed, an off-grid PV- Wind Turbine- battery and water storage system is designed. This system was responsible for meeting the residential load demand in addition to supplying irrigation water for a location with limited solar irradiation levels. The results show that the optimized systems are those with the maximum possible solar PV and WT capacities with respect to the constraints in number of PV panels and wind turbines. Additionally, the electricity production of PV and WT exhibits complementary behavior across different seasons, enhancing system reliability compared to systems where PV panels are the sole energy source. It was demonstrated that LPSP and WSP significantly influence system size and, consequently, its CAPEX. The integration of a wind turbine with a PV system is necessary to make the renewable system more stable for location with low irradiations. This is in contrast to the study of (Bhayo et al., 2019) and (Irandoostshahrestani & R. Rousse, 2023) where the solar irradiations had less intermittency, making them suitable for applications with low electricity consumption.

CONCLUSION

In this research, the utilization of renewable energy-based systems for dual purposes of providing electricity and using the excess power for water pumping is evaluated. Initially, solar water pumping systems are reviewed with a focus on SWPS in Iran, a country with abundant solar potential and it was shown that limited research is done in SWPS. The study showed the adaptability of SWPS in different locations of Iran, from its sunny southern parts to northern parts with relatively lower irradiations. In addition, it was concluded that there are different parameters like Iran`s exchange rate fluctuations, fuel subsidies, and interest rates that affect the extensive use of SWPS. It was also shown that there is an increase in research done in SWPS in Iran. This review paper provides information for researchers, farmers, and policymakers for the implementation of SWPS in the country.

In addition to this review, in another study, a PV- BESS for a case study of a small residential house in south of Iran with constant daily electricity consumption profile and a 1-ha agricultural farm with a specific irrigation water requirement was designed and the concepts of LPSP, WSP as technical criteria and CAPEX and LCOE as economic parameter were evaluated. In this study the goal was to show how tolerance of the residents in terms of power loss or water loss for the farm can affect system size and consequently its CAPEX. In sizing the system (capacity of PV panels, and battery storage system), it was shown that increasing PV panel capacity leads to higher electricity generation and less water shortages. Although this increase in energy production enhances capital cost of the project, it leads to lower LCOEs. It was shown that a small increase in tolerance of the residents for power loss can considerably lower system size and its cost and LCOE with limited change in water shortage probabilities. This means that dwellings should consider alternative solutions to avoid power and water shortage for systems with non-zero LPSP and WSP. Furthermore, when higher values of LPSP are considered in the design, water shortages can go lower as smaller battery banks mean more chances of water pumping to the farm. This is due to the fact that in the dispatch strategy, the system is mandated to fully charge the batteries before using the excess power for water pumping purposes. In the curve showing the relationship between CAPEX and number of PV

panels, a minimum was observed. Beyond this point, limited variation of LCOE and WSP happens at constant LPSP values. This is due to the fact that when PV panel capacity is very low, a very large battery storage system is required that are generally an expensive component of the system. This minimum PV capacity should be found for each project separately as the electricity consumption and solar irradiation profile can have a direct effect on it.

Furthermore, in another study, the electricity and water for a small community of 100 people on a remote island in Quebec were studied. A PV-WT-BESS system was designed where excess power was used to pump water into water storage systems. Similar to the previous study, in the energy dispatch strategy, the electricity generation of the community was prioritized and when it is met and the battery banks are fully charged, the excess power is used for the water pumping system. LPSP and WSP as reliability objectives and CAPEX as economic objectives were considered for the multi-objective purpose by using a genetic algorithm. Design of the system was conducted by finding the capacity of the wind turbine, PV panels, battery storage capacity, and water storage volume while considering an upper bound constraint for WT and PV nominal capacities, as well as water reservoir volumes due to the occupation of land area. In this study, the complementary behavior of WT and Solar PV system at different seasons were discussed and it was shown that the size and CAPEC of the system is considerably influenced with LPSP and WSP. The optimization resulted to different configuration of the system with payback period of 8 to 12 years and LCOE of 16.3 to 23.4 C$/kWh. The study was aimed at showing the feasibility of the implementation of a renewable energy-based system for simultaneous power and water supply for a community with low or no grid access.

For future works, the following suggestions could be considered. As reviewed and discussed, in this study (especially for the first case study of PV- BESS system) no tracking system was used as the goal of this study was to use a simple energy system with low CAPEX. However, when it is supposed to supply electricity for a larger population like the small community of the second case study in Quebec, the effect of increment of electricity production by using a sun tracking system could be evaluated. For instance, by using PVWATTS (NREL, 2022b), a fixed PV panel system with a nominal capacity of 6 kW south-facing and tilted at the latitude

of the location of Les Îles-de-la-Madeleine produces 6.70 MWh per year. However, if a 2-axis tracking system is implemented, this amount increases to 9.57 MWh, which equals an increment of 43%. This shows a considerable increase, but it is in the expense of a higher system CAPEX.

In addition, using PV/thermal system is becoming more popular as they increase the efficiency of the PV panels and whole system and provide a heat source to be used for different applications like hot water for domestic purposes. This study can be extended to evaluate the effect of using PV/thermal systems and for small-scale distributed generation systems and its feasibility in terms of technical and economic aspects can be evaluated. In the calculation of PV systems for a small-house in southern Iran and the PV-WT system for the case study of Quebec, it was revealed that even by using a water pumping system that uses the excess power, there are still considerable amounts of energy that are being curtailed. The study can be extended to find feasible solutions to use this excess power for other applications in a small community.

Finally, as mentioned in the conclusion of Chapter 3, the goal of this study is not to reach a fully renewable system but to show the possibility of increasing renewable energy penetration specially for applications of remote and rural areas. In fact, in the real world, conventional systems like diesel generators or diesel-fueled furnaces should be used beside the renewable systems for the times when there is insufficient renewable resource (low windspeeds or consecutive cloudy days), and the role of the renewable system is to lower dependency on fossil fuel-based systems.

APPENDIX I PROGRAM USED IN CHAPTER 3

```
import numpy as np

# Load data for the location
DHI = np.loadtxt('DHI.txt').T
DNI = np.loadtxt('DNI.txt').T
GHI = np.loadtxt('GHI.txt').T
rho = np.loadtxt('rho.txt').T # albedo
press = np.loadtxt('pressure.txt').T
T_amb = np.loadtxt('ambient.txt')
V_ref= np.loadtxt('wind.txt').T

# n is the number of the day in the year, e.g. 1st January=1
n = np.repeat(np.arange(1, 366), 24)

tet = np.zeros((91, 8760))
Id_bet = np.zeros((91, 8760))
Ib_bet = np.zeros((91, 8760))
Ir_bet = np.zeros((91, 8760))
I_betta = np.zeros((91, 8760))

Daily_ave_Jan = np.zeros(91)
Daily_ave_Feb = np.zeros(91)
Daily_ave_March = np.zeros(91)
Daily_ave_April = np.zeros(91)
Daily_ave_May = np.zeros(91)
Daily_ave_Jun = np.zeros(91)
Daily_ave_July = np.zeros(91)
Daily_ave_Aug = np.zeros(91)
Daily_ave_Sep = np.zeros(91)
Daily_ave_Oct = np.zeros(91)
Daily_ave_Nov = np.zeros(91)
Daily_ave_Dec = np.zeros(91)

Daily_ave_Winter = np.zeros(91)
Daily_ave_Spring = np.zeros(91)
Daily_ave_Summer = np.zeros(91)
Daily_ave_Fall = np.zeros(91)
Daily_ave_Annual = np.zeros(91)

# Solar declination angle
del_angle = 23.45 * np.sin(np.radians(360 * ((284 + n) / 365)))

phi = 47.4  # Latitude
LL = 61.77  # Longitude

LT = np.tile(np.arange(0, 24), 365) # Standard time
B = (n - 1) * 360 / 365
# Equation of time
EOT = 229.2 * (0.000075 + 0.001868 * np.cos(np.radians(B)) - 0.032077 * np.sin(np.radians(B)) -
               0.014615 * np.cos(np.radians(2 * B)) - 0.04089 * np.sin(np.radians(2 * B)))
```

```
51.
52. LSTM = 15 * (5) # Local standard time meridian
53. ST = LT + (EOT + 4 * (LSTM - LL)) / 60 # Solar time
54. w = 15 * (ST - 12) # Hour angle
55.
56. # solar zenith angle
57. tet_z = np.degrees(np.arccos(
58.     np.sin(np.radians(del_angle)) * np.sin(np.radians(phi)) +
59.     np.cos(np.radians(del_angle)) * np.cos(np.radians(phi)) * np.cos(np.radians(w))
60. ))
61.
62. gamma = 0 # azimuth angle
63.
64. for bett in range(91):
65. # tet is angle of incidence
66.     tet[bett, :] = np.degrees(np.arccos(
67.         ((np.sin(np.radians(phi)) * np.cos(np.radians(bett)) -
68.           np.cos(np.radians(phi)) * np.sin(np.radians(bett)) * np.cos(np.radians(gamma))) *
np.sin(np.radians(del_angle))) +
69.         ((np.cos(np.radians(phi)) * np.cos(np.radians(bett)) +
70.           np.sin(np.radians(phi)) * np.sin(np.radians(bett)) * np.cos(np.radians(gamma))) *
71.          np.cos(np.radians(del_angle)) * np.cos(np.radians(w))) +
72.         (np.cos(np.radians(del_angle)) * np.sin(np.radians(bett)) * np.sin(np.radians(gamma)) *
np.sin(np.radians(w)))
73.     ))
74.
75.     Id_bet[bett, :] = ((1 + np.cos(np.radians(bett))) / 2) * DHI # Diffuse
76.     Ib_bet[bett, :] = np.cos(np.radians(tet[bett, :])) * DNI # Normal
77.     Ir_bet[bett, :] = (Id_bet[bett, :] + Ib_bet[bett, :]) * rho * (1 - np.cos(np.radians(bett))) / 2    # Ground
reflected
78.
79.     Ib_bet[bett, :][tet[bett, :] > 90] = 0
80.     # Total radiation
81.     I_betta[bett, :] = Id_bet[bett, :] + Ib_bet[bett, :] + Ir_bet[bett, :]
82.
83.     Daily_ave_Jan[bett] = np.sum(I_betta[bett, :744]) / (1000 * 31) # average radiation for January
84.     Daily_ave_Feb[bett] = np.sum(I_betta[bett, 744:1416]) / (1000 * 28)
85.     Daily_ave_March[bett] = np.sum(I_betta[bett, 1416:2160]) / (1000 * 31)
86.     Daily_ave_April[bett] = np.sum(I_betta[bett, 2160:2880]) / (1000 * 30)
87.     Daily_ave_May[bett] = np.sum(I_betta[bett, 2880:3624]) / (1000 * 31)
88.     Daily_ave_Jun[bett] = np.sum(I_betta[bett, 3624:4344]) / (1000 * 30)
89.     Daily_ave_July[bett] = np.sum(I_betta[bett, 4344:5088]) / (1000 * 31)
90.     Daily_ave_Aug[bett] = np.sum(I_betta[bett, 5088:5832]) / (1000 * 31)
91.     Daily_ave_Sep[bett] = np.sum(I_betta[bett, 5832:6552]) / (1000 * 30)
92.     Daily_ave_Oct[bett] = np.sum(I_betta[bett, 6552:7296]) / (1000 * 31)
93.     Daily_ave_Nov[bett] = np.sum(I_betta[bett, 7296:8016]) / (1000 * 30)
94.     Daily_ave_Dec[bett] = np.sum(I_betta[bett, 8016:8760]) / (1000 * 31)
95.
96.     Daily_ave_Winter[bett] = np.sum(I_betta[bett, :2160]) / (1000 * 90) # average radiation (kWh/m2-day)
for Winter
97.     Daily_ave_Spring[bett] = np.sum(I_betta[bett, 2160:4344]) / (1000 * 91)
98.     Daily_ave_Summer[bett] = np.sum(I_betta[bett, 4344:6552]) / (1000 * 92)
99.     Daily_ave_Fall[bett] = np.sum(I_betta[bett, 6552:]) / (1000 * 92)
100.
```

```
    Daily_ave_Annual[bett] = np.sum(I_betta[bett, :]) / (1000 * 365) # average radiation (kWh/m2-day) for the year


max_Jan, loc_max_Jan = np.max(Daily_ave_Jan), np.argmax(Daily_ave_Jan)
max_Feb, loc_max_Feb = np.max(Daily_ave_Feb), np.argmax(Daily_ave_Feb)
max_March, loc_max_March = np.max(Daily_ave_March), np.argmax(Daily_ave_March)
max_April, loc_max_April = np.max(Daily_ave_April), np.argmax(Daily_ave_April)
max_May, loc_max_May = np.max(Daily_ave_May), np.argmax(Daily_ave_May)
max_Jun, loc_max_Jun = np.max(Daily_ave_Jun), np.argmax(Daily_ave_Jun)
max_July, loc_max_July = np.max(Daily_ave_July), np.argmax(Daily_ave_July)
max_Aug, loc_max_Aug = np.max(Daily_ave_Aug), np.argmax(Daily_ave_Aug)
max_Sep, loc_max_Sep = np.max(Daily_ave_Sep), np.argmax(Daily_ave_Sep)
max_Oct, loc_max_Oct = np.max(Daily_ave_Oct), np.argmax(Daily_ave_Oct)
max_Nov, loc_max_Nov = np.max(Daily_ave_Nov), np.argmax(Daily_ave_Nov)
max_Dec, loc_max_Dec = np.max(Daily_ave_Dec), np.argmax(Daily_ave_Dec)

with open('Global_Monthly_fix_Rad.txt', 'w') as f:
    np.savetxt(f, I_betta[loc_max_Jan, :744], fmt="%.2f")
    np.savetxt(f, I_betta[loc_max_Feb, 744:1416], fmt="%.2f")
    np.savetxt(f, I_betta[loc_max_March, 1416:2160], fmt="%.2f")
    np.savetxt(f, I_betta[loc_max_April, 2160:2880], fmt="%.2f")
    np.savetxt(f, I_betta[loc_max_May, 2880:3624], fmt="%.2f")
    np.savetxt(f, I_betta[loc_max_Jun, 3624:4344], fmt="%.2f")
    np.savetxt(f, I_betta[loc_max_July, 4344:5088], fmt="%.2f")
    np.savetxt(f, I_betta[loc_max_Aug, 5088:5832], fmt="%.2f")
    np.savetxt(f, I_betta[loc_max_Sep, 5832:6552], fmt="%.2f")
    np.savetxt(f, I_betta[loc_max_Oct, 6552:7296], fmt="%.2f")
    np.savetxt(f, I_betta[loc_max_Nov, 7296:8016], fmt="%.2f")
    np.savetxt(f, I_betta[loc_max_Dec, 8016:8760], fmt="%.2f")

    max_Winter, loc_max_Winter = np.max(Daily_ave_Winter), np.argmax(Daily_ave_Winter)
    max_Spring, loc_max_Spring = np.max(Daily_ave_Spring), np.argmax(Daily_ave_Spring)
    max_Summer, loc_max_Summer = np.max(Daily_ave_Summer), np.argmax(Daily_ave_Summer)
    max_Fall, loc_max_Fall = np.max(Daily_ave_Fall), np.argmax(Daily_ave_Fall)

with open('Global_Seas_fix_Rad.txt', 'w') as f:
    np.savetxt(f, I_betta[loc_max_Winter, :2160], fmt="%.2f")
    np.savetxt(f, I_betta[loc_max_Spring, 2160:4344], fmt="%.2f")
    np.savetxt(f, I_betta[loc_max_Summer, 4344:6552], fmt="%.2f")
    np.savetxt(f, I_betta[loc_max_Fall, 6552:], fmt="%.2f")


# max for annual average
max_Annual, loc_max_Annual = np.max(Daily_ave_Annual), np.argmax(Daily_ave_Annual)

with open('Global_Annual_fix_Rad.txt', 'w') as f:
    np.savetxt(f, I_betta[loc_max_Annual, :], fmt="%.2f")

# <<<<<<<<<<<<<< PV-WT-BATTERY  >>>>>>>>>>>>>>>>

SOC = np.zeros(8760)
TC = np.zeros(8760)
P_pv = np.zeros(8760)
```

```
P_total = np.zeros(8760)
pi = np.zeros(8760)
LPS = np.zeros(8760)
hourly_Pumped_water = np.zeros(8760)
Pumped_water_365 = np.zeros(365)
WS = np.zeros(365)
P1 = np.zeros(8760)
Q = np.zeros(8760)
VOR = np.zeros(365)
Vel = np.zeros(8760)
density = np.zeros(8760)
p_wind = np.zeros(8760)

G = np.loadtxt('Global_Annual_fix_Rad.txt')
# G = np.loadtxt('Global_Seas_fix_Rad.txt')
# G = np.loadtxt('Global_Monthly_fix_Rad.txt')

#  LOAD
PL = 1000 * np.loadtxt('load_hourly.txt').T # W
Head = 45

# PV specifications
I_mp = 5.59
volt_mp = 17.9
p_mp = I_mp * volt_mp
alpha_T = -0.0039
G_STC = 1000
TC_STC = 25
NOCT = 45

# Battery specifications
etta_bc = 1
etta_bd = 1
sig = 0

# inverter specifications
etta_inv = 0.92

# Simulation parameters
n_pv_min = 600
n_pv_max = 600

n_batt_min = 1000
n_batt_max = 1000

p_r=8900 #W
V_r=11
V_ci=2.5
V_co=20

n_wt_min=26
n_wt_max=26
Height=40  # hub height
Height_ref=2 # from NSRDB
```

```
density_ref=1.225 # kg/m3

for n_wt in range(n_wt_min, n_wt_max+1):
    for n_pv in range(n_pv_min, n_pv_max + 1, 20):
        for n_batt in range(n_batt_min, n_batt_max + 1, 20):
            SOC_all = n_batt * 2560  # each battery is 2560 Wh
            SOC[0] = 0.5 * SOC_all
            SOC_min = 0.1 * SOC_all
            SOC_max = 0.9 * SOC_all

            for t in range(1, 8760):
                # wind
                Vel [t] = V_ref [t] * ((Height / Height_ref) ** (1/7))
                density [t] =(100 * press [t]) / (287*(T_amb [t] + 273.15))

                if Vel [t] >= V_ci and Vel [t] <= V_r :
                    p_wind [t] = n_wt * (density [t] /density_ref) * p_r * (Vel [t]**3 -V_ci**3)/(V_r**3 -
V_ci**3)
                elif Vel [t] > V_r and Vel [t] <= V_co:
                    p_wind [t] = n_wt * (density [t] /density_ref) * p_r
                else:
                    p_wind [t]=0

                # solar
                TC[t] = T_amb[t] + ((NOCT - 20) / 800) * G[t]
                P_pv[t] = n_pv * I_mp * volt_mp * (G[t] / G_STC) * (1 + alpha_T * (TC[t] - TC_STC))
                P_total[t] = P_total[t - 1] + P_pv[t] + p_wind[t]

                if (P_pv[t]+p_wind[t]) >= (PL[t] / etta_inv):
                    if SOC[t - 1] <= SOC_max and SOC[t - 1] + (P_pv[t]+p_wind[t] - (PL[t] / etta_inv)) <=
SOC_max and SOC[t - 1] >= SOC_min:
                        # Charge the battery
                        SOC[t] = SOC[t - 1] * (1 - sig) + ((P_pv[t]+p_wind [t] - (PL[t] / etta_inv)) * etta_bc)
                        pi[t] = 0
                        hourly_Pumped_water[t] = 0
                        LPS[t] = 0
                    elif SOC[t - 1] <= SOC_max and SOC[t - 1] + (P_pv[t]+p_wind[t] - (PL[t] / etta_inv)) >=
SOC_max and SOC[t - 1] >= SOC_min:
                        SOC[t] = SOC_max
                        # Pump water
                        pi[t] = (P_pv[t]+p_wind[t] - (PL[t] / etta_inv)) - (SOC_max - SOC[t - 1])

                        # Lorenz_PS2_4000_C_SJ17_4
                        p00 = 3.276
                        p10 = -0.6048
                        p01 = 0.01748
                        p20 = -0.0007923
                        p11 = 0.0001245
                        p02 = -3.137e-06

                        if Head == 10:
                            if pi[t] < 150:
                                Q[t] = 0
                            elif pi[t] > 3500:
```

```
259.                 pi[t] = 3500
260.                 Q[t] = (p00 + p10 * Head + p01 * pi[t] +
261.                     p20 * Head**2 + p11 * Head * pi[t] + p02 * pi[t]**2)
262.             else:
263.                 Q[t] = (p00 + p10 * Head + p01 * pi[t] +
264.                     p20 * Head**2 + p11 * Head * pi[t] + p02 * pi[t]**2)
265.         elif Head == 15:
266.             if pi[t] < 320:
267.                 Q[t] = 0
268.             elif pi[t] > 3500:
269.                 pi[t] = 3500
270.                 Q[t] = (p00 + p10 * Head + p01 * pi[t] +
271.                     p20 * Head**2 + p11 * Head * pi[t] + p02 * pi[t]**2)
272.             else:
273.                 Q[t] = (p00 + p10 * Head + p01 * pi[t] +
274.                     p20 * Head**2 + p11 * Head * pi[t] + p02 * pi[t]**2)
275.         elif Head == 20:
276.             if pi[t] < 500:
277.                 Q[t] = 0
278.             elif pi[t] > 3500:
279.                 pi[t] = 3500
280.                 Q[t] = (p00 + p10 * Head + p01 * pi[t] +
281.                     p20 * Head**2 + p11 * Head * pi[t] + p02 * pi[t]**2)
282.             else:
283.                 Q[t] = (p00 + p10 * Head + p01 * pi[t] +
284.                     p20 * Head**2 + p11 * Head * pi[t] + p02 * pi[t]**2)
285.         elif Head == 25:
286.             if pi[t] < 700:
287.                 Q[t] = 0
288.             elif pi[t] > 3500:
289.                 pi[t] = 3500
290.                 Q[t] = (p00 + p10 * Head + p01 * pi[t] +
291.                     p20 * Head**2 + p11 * Head * pi[t] + p02 * pi[t]**2)
292.             else:
293.                 Q[t] = (p00 + p10 * Head + p01 * pi[t] +
294.                     p20 * Head**2 + p11 * Head * pi[t] + p02 * pi[t]**2)
295.         elif Head == 30:
296.             if pi[t] < 900:
297.                 Q[t] = 0
298.             elif pi[t] > 3400:
299.                 pi[t] = 3400
300.                 Q[t] = (p00 + p10 * Head + p01 * pi[t] +
301.                     p20 * Head**2 + p11 * Head * pi[t] + p02 * pi[t]**2)
302.             else:
303.                 Q[t] = (p00 + p10 * Head + p01 * pi[t] +
304.                     p20 * Head**2 + p11 * Head * pi[t] + p02 * pi[t]**2)
305.         elif Head == 35:
306.             if pi[t] < 1070:
307.                 Q[t] = 0
308.             elif pi[t] > 3350:
309.                 pi[t] = 3350
310.                 Q[t] = (p00 + p10 * Head + p01 * pi[t] +
311.                     p20 * Head**2 + p11 * Head * pi[t] + p02 * pi[t]**2)
312.             else:
```

```
                    Q[t] = (p00 + p10 * Head + p01 * pi[t] +
                            p20 * Head**2 + p11 * Head * pi[t] + p02 * pi[t]**2)
                elif Head == 40:
                    if pi[t] < 1210:
                        Q[t] = 0
                    elif pi[t] > 3350:
                        pi[t] = 3350
                        Q[t] = (p00 + p10 * Head + p01 * pi[t] +
                                p20 * Head**2 + p11 * Head * pi[t] + p02 * pi[t]**2)
                    else:
                        Q[t] = (p00 + p10 * Head + p01 * pi[t] +
                                p20 * Head**2 + p11 * Head * pi[t] + p02 * pi[t]**2)
                elif Head == 45:
                    if pi[t] < 1410:
                        Q[t] = 0
                    elif pi[t] > 3300:
                        pi[t] = 3300
                        Q[t] = (p00 + p10 * Head + p01 * pi[t] +
                                p20 * Head**2 + p11 * Head * pi[t] + p02 * pi[t]**2)
                    else:
                        Q[t] = (p00 + p10 * Head + p01 * pi[t] +
                                p20 * Head**2 + p11 * Head * pi[t] + p02 * pi[t]**2)
                else:
                    Q[t] = 0


                hourly_Pumped_water[t] = max(0, Q[t])
                LPS[t] = 0

            elif SOC[t-1] > SOC_max:
                print(f"At hour {t:.2f}, (P_PV + P_wind > PL) SOC is higher than SOC_max")
            else:
                print(f"At hour {t:.2f}, (P_PV + P_wind > PL) SOC is lower than SOC_min")
        else:
            if SOC[t-1] >= SOC_min and SOC[t-1] + (P_pv[t]+ p_wind[t] - (PL[t] / etta_inv)) >=
SOC_min and SOC[t-1] <= SOC_max:
                # discharge battery
                SOC[t] = SOC[t-1] * (1 - sig) - ((PL[t] / etta_inv) - P_pv[t]- p_wind[t]) / etta_bd
                pi[t] = 0
                hourly_Pumped_water[t] = 0
                LPS[t] = 0

            elif SOC[t-1] >= SOC_min and SOC[t-1] + (P_pv[t]+p_wind[t] - (PL[t] / etta_inv)) <=
SOC_min and SOC[t-1] <= SOC_max:
                SOC[t] = SOC_min
                pi[t] = 0
                hourly_Pumped_water[t] = 0
                LPS[t] = ((PL[t] / etta_inv) - P_pv[t]-p_wind[t]) - (SOC[t-1] - SOC_min)

            elif SOC[t-1] > SOC_max:
                print(f"At hour {t:.2f}, (P_PV + P_wind < PL) SOC is higher than SOC_max")

            else:
                print(f"At hour {t:.2f}, (P_PV + p_wind < PL) SOC is lower than SOC_min")
```

```
365.
366.          LPSP = (np.sum(LPS) / np.sum(PL)) * 100
367.
368.          # each person consumption 0.26 m3/day
369.          VOR_1 = 6.2 * 6
370.          VOR_2 = 6.2 * 15
371.          Volume_step = 6.2
372.          IWR_365 = [26] * 365
373.
374.          for VOR_max in np.arange(VOR_1, VOR_2 , Volume_step):  # Tanker volume in m³
375.
376.              for dd in range(1, 365):
377.                  Pumped_water_365[dd] = np.sum(hourly_Pumped_water[(24 * dd - 24):(24 * dd-1)])
378.                  VOR[dd] = VOR[dd - 1] + (Pumped_water_365[dd] - IWR_365[dd])
379.
380.                  if VOR[dd] < 0:
381.                      WS[dd] = VOR[dd]
382.
383.                      VOR[dd] = 0
384.                  elif VOR[dd] < VOR_max:
385.                      WS[dd] = 0
386.                  else:
387.                      WS[dd] = 0
388.                      VOR[dd] = VOR_max
389.
390.
391.              Tanker_number = VOR_max / Volume_step
392.              WSP = (abs(np.sum(WS)) / np.sum(IWR_365)) * 100
393.
394.              print()
395.
396.              # <<<<<<<<<<<<<<<<<<<<<<<<  Economic Analysis >>>>>>>>>>>>>>>>>>
397.
398.              r = 0.04 # Real discount rate for December  of 2024
399.
400.              # Wind turbine
401.              I0_WT=40000 * 1.3 # CAD $ 1.3 for structure
402.              I_WT= n_wt * I0_WT
403.
404.              # Battery bank
405.              I0_batt = 550  # CAD $
406.              I_batt = I0_batt * n_batt
407.
408.              # PV cost
409.              I0_PV = 150 * 1.3 # CAD $ 1.3 for structure
410.              I_PV = I0_PV * n_pv
411.
412.              I_MPPT = 0.20 * I_PV  # CAD $ ; 20% ; estimate
413.
414.              # Inverter
415.              I_inverter = 0.20 * (I_PV + I_WT); # 20% ; estimate
416.
417.              # Tanker
418.              I_tanker = Tanker_number * 2500 * 1.20  # 1.2 for structural costs
```

```
419.
420.        # Pumping cost
421.        I_pump = 10000   # PS2-4000-C-SJ17-4 Lorentz
422.
423.        # Total initial investment
424.        I_cost = I_WT + I_batt + I_MPPT + I_inverter + I_PV + I_tanker + I_pump
425.
426.        # Replacement costs
427.        R_batt = I_batt * ((1 / (1 + r)**10) + (1 / (1 + r)**20))  # replacements at 10 & 20 years
428.        R_MPPT = I_MPPT * ((1 / (1 + r)**10) + (1 / (1 + r)**20))  # replacements at 10 & 20 years
429.        R_inverter = I_inverter * ((1 / (1 + r)**10) + (1 / (1 + r)**20))  # replacements at 10 & 20 years
430.        R_pump= I_pump * ((1 / (1 + r)**10) + (1 / (1 + r)**20))
431.        R_WT = I_WT * (1 / (1 + r)**15)
432.
433.        # Total Replacement Cost
434.        R_cost = R_batt + R_MPPT + R_inverter + R_pump + R_WT
435.
436.        # Operation and maintenance (OM)
437.        lifetime = 30
438.        PWF = (1 - (1 + r)**-lifetime) / r  # Present Worth Factor
439.
440.        OM_WT = 600 * n_wt * PWF  # wind turbine
441.        OM_pv = 0.02 * I_PV * PWF  # 2% of PV cost per year
442.        OM_pump = 0.02 * I_pump * PWF  # 2% of pump cost per year
443.
444.        # Total O&M cost
445.        OM_cost = OM_WT + OM_pv + OM_pump
446.
447.        OpEx_t = OM_cost + R_cost
448.        Annualized_OpEx = OpEx_t / lifetime # $/year
449.
450.        # ////////////////////////////////////////
451.
452.        total_water_volume = np.sum(IWR_365)  # m³/year (Annual pumped water)
453.        flow_rate = 26  # m³/h
454.        max_power = 4.0  # kW
455.        head_max = 45  # m
456.
457.        efficiency_factor = Head / head_max
458.        power_operating = efficiency_factor * max_power
459.        pumping_hours = total_water_volume / flow_rate
460.        pumping_load = power_operating * pumping_hours
461.
462.        residential_load = (np.sum(PL))/1000  # kWh/year
463.        Total_energy_consumed = (residential_load * (1-(LPSP/100))) + pumping_load  # kWh/year
464.
465.        LCOE = (I_cost + OpEx_t)/ (lifetime * Total_energy_consumed) # $/kWh
466.
467.        # /////////// Diesel generator
468.
469.        Return_diesel= 10000
470.        fuel_price = 1.7 # $/L
471.        gen_efficiency = 4.2 # kWh/L
472.        fuel_cost = fuel_price / gen_efficiency # $/kWh
```

```
473.             Return_fuel = Total_energy_consumed * fuel_cost  # $/year
474.             Return_OM=200 # $/year O&M cost
475.
476.             Return= Return_diesel + Return_fuel + Return_OM
477.             Payback_Period = I_cost / (Return - Annualized_OpEx)
478.
479.             with open('result.txt', 'a') as ff:
480.                 ff.write(f"PV_number={n_pv:.0f}, Battery_number={n_batt:.0f}, LPSP_text={LPSP:.2f},
WSP_text={WSP:.2f}, "
481.                          f"Payback_Period={Payback_Period:.2f} yrs, Return={Return:.3f} $/year,
Initial_cost_text={I_cost:.1f} $, "
482.                          f"Head={Head:.0f} m, LCOE={100 * LCOE:.2f} $cents/kWh,
Tanker_size={VOR_max:.2f} m3, "
483.                          f"Annualized_OpEx=: {Annualized_OpEx:.2f} $/year, WT_number={n_wt:.0f}\n")
484.
485. import numpy as np
486. import pandas as pd
487. from deap import base, creator, tools
488.
489. def load_data(path):
490.     data = []
491.     with open(path, "r") as f:
492.         for line in f:
493.             entry = {}
494.             for item in line.strip().split(", "):
495.                 k, v = item.split("=")
496.                 try:
497.                     entry[k] = float(v.split()[0])
498.                 except:
499.                     entry[k] = v
500.             data.append(entry)
501.     return pd.DataFrame(data)
502.
503. def filter_data(df):
504.     return df[
505.         (df["LPSP_text"] < 10) &
506.         (df["WSP_text"] < 10) &
507.         (df["Initial_cost_text"] < 2500000)
508.     ]
509.
510. def setup_toolbox(vars, objs):
511.     creator.create("Fit", base.Fitness, weights=(-1.0, -1.0, -1.0))
512.     creator.create("Ind", list, fitness=creator.Fit)
513.     toolbox = base.Toolbox()
514.     toolbox.register("idx", np.random.randint, 0, len(vars))
515.     toolbox.register("individual", tools.initRepeat, creator.Ind, toolbox.idx, 1)
516.     toolbox.register("population", tools.initRepeat, list, toolbox.individual)
517.     toolbox.register("evaluate", lambda ind: tuple(objs[ind[0]]))
518.     toolbox.register("mate", tools.cxUniform, indpb=0.5)
519.
520.     def mutate_individual(ind):
521.         if np.random.rand() < 0.2:
522.             ind[0] = np.random.randint(0, len(vars))
523.         return ind,
```

```
524.
525.     toolbox.register("mutate", mutate_individual)
526.     toolbox.register("select", tools.selNSGA2)
527.     return toolbox
528.
529. def run(toolbox, objs, gens=1000, pop_size=1000):
530.     np.random.seed(100)
531.     pop = toolbox.population(n=pop_size)
532.     for ind in pop:
533.         ind.fitness.values = toolbox.evaluate(ind)
534.     for _ in range(gens):
535.         off = list(map(toolbox.clone, toolbox.select(pop, len(pop))))
536.         for i in range(0, len(off), 2):
537.             if i+1 < len(off) and np.random.rand() < 0.7:
538.                 toolbox.mate(off[i], off[i+1])
539.                 del off[i].fitness.values, off[i+1].fitness.values
540.         for ind in off:
541.             if np.random.rand() < 0.2:
542.                 toolbox.mutate(ind)
543.                 del ind.fitness.values
544.         for ind in off:
545.             if not ind.fitness.valid:
546.                 ind.fitness.values = toolbox.evaluate(ind)
547.         pop[:] = off
548.     front = tools.sortNondominated(pop, len(pop), True)[0]
549.     return [ind[0] for ind in front]
550.
551. def save(vars, objs, pay, idxs, out="pareto_solutions.txt"):
552.     df = pd.DataFrame({
553.         "PV_number": vars[idxs, 0].astype(int),
554.         "Battery_number": vars[idxs, 1].astype(int),
555.         "Tanker_size": vars[idxs, 2],
556.         "WT_number": vars[idxs, 3].astype(int),
557.         "LPSP_text": objs[idxs, 0],
558.         "WSP_text": objs[idxs, 1],
559.         "Initial_cost_text": objs[idxs, 2],
560.         "Payback_Period": pay[idxs]
561.     }).drop_duplicates().sort_values("Battery_number")
562.     with open(out, "w") as f:
563.         for _, r in df.iterrows():
564.             f.write(
565.                 f"PV_number={r['PV_number']}, Battery_number={r['Battery_number']}, "
566.                 f"Tanker_size={r['Tanker_size']:.1f}, WT_number={r['WT_number']}, "
567.                 f"LPSP_text={r['LPSP_text']}, WSP_text={r['WSP_text']}, "
568.                 f"Initial_cost_text={r['Initial_cost_text']:.1f}, Payback_Period={r['Payback_Period']}\n"
569.             )
570.
571. def main():
572.     df = filter_data(load_data("result.txt"))
573.     vars = df[["PV_number", "Battery_number", "Tanker_size", "WT_number"]].values
574.     objs = df[["LPSP_text", "WSP_text", "Initial_cost_text"]].values
575.     pay = df["Payback_Period"].values
576.     toolbox = setup_toolbox(vars, objs)
577.     idxs = run(toolbox, objs)
```

```
    save(vars, objs, pay, idxs)

if __name__ == "__main__":
    main()

```

APPENDIX II BASIC SOLAR EQUATIONS

In this section, basic solar geometric equations are presented, as derived from the reference book by Duffie and Beckman (Duffie & Beckman, 1982). The declination angle, in degrees, is calculated using the approximate equation by Cooper (Cooper, 1969):

$$\delta = 23.45 \times \sin\left(360 \times \frac{284+n}{365}\right) \quad \text{(A II.1)}$$

where n is the day number (e.g., n=1 for January 1st). The hour angle, in degrees, is defined as:

$$\omega = 15 \times (12\text{-}ST) \quad \text{(A II.2)}$$

where ST is the solar time, calculated using the following equation:

$$ST = LT + \frac{(EOT + 4 \times (LL - LSTM))}{60} \quad \text{(A II.3)}$$

where LT is the local time, LL is the longitude, LSTM is the local standard time meridian, and the equation of time (EOT) is determined by:

$$EOT = 229.2 \times (0.000075 + 0.001868 \times \cos(B) - 0.032077 \times \sin(B) - 0.014615 \times \cos(2B) - 0.04089 \times \sin(2B)) \quad \text{(A II.4)}$$

and Γ is given by:

$$\Gamma = 360 \times \frac{(n-81)}{365} \quad \text{(A II.5)}$$

The zenith angle and the angle of incidence are defined, respectively, as:

$$\theta_z = \arccos(\sin(\delta) \times \sin(\varphi) + \cos(\delta) \times \cos(\varphi) \times \cos(\omega)) \quad \text{(A II.6)}$$

$$\theta = \arccos(\theta_1 + \theta_2 + \theta_3) \quad \text{(A II.7)}$$

and θ_1, θ_2, and θ_3 are given by:

$$\theta_1 = (\sin(\varphi) \times \cos(\beta) - \cos(\varphi) \times \sin(\beta) \times \cos(\gamma)) \times \sin(\delta) \quad \text{(A II.8)}$$

$$\theta_2 = (\cos(\varphi) \times \cos(\beta) + \sin(\varphi) \times \sin(\beta) \times \cos(\gamma)) \times \cos(\delta) \times \cos(\omega) \quad \text{(A II.9)}$$

$$\theta_3 = \cos(\delta) \times \sin(\beta) \times \sin(\gamma) \times \sin(\omega) \quad \text{(A II.10)}$$

where φ, β and γ represent the latitude, tilt angle, and azimuth angle, respectively. The hourly global solar radiation (G) in W/m² on an inclined surface is calculated using the isotropic diffuse model by Liu and Jordan (Benjamin Y.H. Liu & Richard C. Jordan, 1963):

$$G_\beta = DNI \times \cos\theta + DHI \times \left(\frac{1+\cos(\beta)}{2}\right) + GHI \times \mu \times \left(\frac{1-\cos(\beta)}{2}\right) \quad \text{(A II.11)}$$

where μ is the albedo coefficient and the Global Horizontal Irradiance (GHI) are calculated using the Direct Normal Irradiance (DNI), and Diffuse Horizontal Irradiance (DHI) as follows:

$$GHI = DNI \times \cos(\theta_z) + DHI \quad \text{(A II.12)}$$

LIST OF REFERENCES

12V 200Ah Deep Cycle LiFePO4 Lithium Battery. (2025, January 20). Retrieved 15 March 2025, from https://www.dchousepower.com/products/

Abdolzadeh, M., & Ameri, M. (2009). Improving the effectiveness of a photovoltaic water pumping system by spraying water over the front of photovoltaic cells. *Renewable Energy*, *34*(1), 91–96. https://doi.org/10.1016/j.renene.2008.03.024

Abdolzadeh, M., Ameri, M., & Mehrabian, M. A. (2009). The effects of an operating head on the performance of photovoltaic water pumping systems: An experimental investigation. *Proceedings of the Institution of Mechanical Engineers, Part A: Journal of Power and Energy*, *223*(4), 341–347. https://doi.org/10.1243/09576509JPE693

Abdolzadeh, M., Ameri, M., & Mehrabian, M. A. (2011). Effects of Water Spray Over the Photovoltaic Modules on the Performance of a Photovoltaic Water Pumping System under Different Operating Conditions. *Energy Sources, Part A: Recovery, Utilization, and Environmental Effects*. https://doi.org/10.1080/15567036.2010.499416

Abo-Elnour, F., Zeidan, E. B., Sultan, A. A., El-Negiry, E., & Soliman, A. S. (2023). Enhancing the bifacial PV system by using dimples and multiple PCMs. *Journal of Energy Storage*, *70*. https://doi.org/10.1016/j.est.2023.108079

Alamdari, P., Nematollahi, O., & Alemrajabi, A. A. (2013). Solar energy potentials in Iran: A review. *Renewable and Sustainable Energy Reviews*, *21*, 778–788. https://doi.org/10.1016/J.RSER.2012.12.052

Al-Buraiki, A. S., & Al-Sharafi, A. (2022). Hydrogen production via using excess electric energy of an off-grid hybrid solar/wind system based on a novel performance indicator.

Energy Conversion and Management, *254*. https://doi.org/10.1016/j.enconman.2022.115270

Al-Ibrahim, A. M. (1996). *Optimal selection of direct-coupled photovoltaic pumping system in solar domestic hot water systems*. University of Wisconsin, Madison.

Aliyu, M., Hassan, G., Said, S. A., Siddiqui, M. U., Alawami, A. T., & Elamin, I. M. (2018). A review of solar-powered water pumping systems. *Renewable and Sustainable Energy Reviews*, *87*(August 2017), 61–76. https://doi.org/10.1016/j.rser.2018.02.010

Al-Omari, Z., Khlaifat, N., & Haddad, M. (2024). A feasibility study of combining solar/wind energy to power a water pumping system in Jordan's Desert/Al-Mudawwara village. *Environmental and Sustainability Indicators*. https://doi.org/10.1016/j.indic.2024.100555

Ammar, A., Hamraoui, K., Belguellaoui, M., & Kheldoun, A. (2022). *Performance Enhancement of Photovoltaic Water Pumping System Based on BLDC Motor under Partial Shading Condition*. 22. https://doi.org/10.3390/engproc2022014022

Argaw, Foster, R., & Ellis, A. (2003). Renewable Energy for Water Pumping Applications In Rural Villages. *New Mexico State, United States*, (July).

Ashraf, U., & Iqbal, M. T. (2020). Optimised Design and Analysis of Solar Water Pumping Systems for Pakistani Conditions. *Energy and Power Engineering*, *12*(10), 521–542. https://doi.org/10.4236/epe.2020.1210032

Atashpaz-Gargari, E., & Lucas, C. (2007). Imperialist competitive algorithm: An algorithm for optimization inspired by imperialistic competition. *2007 IEEE Congress on Evolutionary Computation*, 4661–4667. https://doi.org/10.1109/CEC.2007.4425083

Bakelli, Y., Hadj Arab, A., & Azoui, B. (2011). Optimal sizing of photovoltaic pumping system with water tank storage using LPSP concept. *Solar Energy*, *85*(2), 288–294. https://doi.org/10.1016/j.solener.2010.11.023

Bank of Canada. (2024). *Bank of Canada reduces policy rate by 50 basis points to 3¼%*. Retrieved from https://www.bankofcanada.ca/2024/12/fad-press-release-2024-12-11/

Barati, A. A., Pour, M. D., & Sardooei, M. A. (2023). Water crisis in Iran: A system dynamics approach on water, energy, food, land and climate (WEFLC) nexus. *Science of The Total Environment*, *882*, 163549. https://doi.org/https://doi.org/10.1016/j.scitotenv.2023.163549

Bazrafshan, O., Zamani, H., Ramezani Etedali, H., & Dehghanpir, S. (2019). Assessment of citrus water footprint components and impact of climatic and non-climatic factors on them. *Scientia Horticulturae*, *250*, 344–351. https://doi.org/10.1016/j.scienta.2019.02.069

Bazzi, H., Ebrahimi, H., & Aminnejad, B. (2021). A comprehensive statistical analysis of evaporation rates under climate change in Southern Iran using WEAP; Case study: Chahnimeh Reservoirs of Sistan Plain. *Ain Shams Engineering Journal*, *12*(2), 1339–1352. https://doi.org/10.1016/J.ASEJ.2020.08.030

Benghanem, M., Daffallah, K. O., & Almohammedi, A. (2018). Estimation of daily flow rate of photovoltaic water pumping systems using solar radiation data. *Results in Physics*, *8*, 949–954. https://doi.org/10.1016/j.rinp.2018.01.022

Benjamin Y.H. Liu, & Richard C. Jordan. (1963). *The long-term average performance of flat-plate solar-energy collectors: With design data for the U.S., its outlying possessions and Canada* (Vol. 7). https://doi.org/https://doi.org/10.1016/0038-092X(63)90006-9

BERGEY EXCEL 10 datasheet. (2012). Retrieved from https://bergey.com/wp-content/uploads/excel-10-spec-sheet_2013.pdf

BERNT LORENTZ GmbH & Co. KG. (2022). *Solar Submersible Pump System for 6″ wells: PS2-4000 C-SJ17-4*.

Besarati, S. M., Padilla, R. V., Goswami, D. Y., & Stefanakos, E. (2013). The potential of harnessing solar radiation in Iran: Generating solar maps and viability study of PV power plants. *Renewable Energy*, *53*, 193–199. https://doi.org/10.1016/j.renene.2012.11.012

Bhandari, R., & Stadler, I. (2009). Grid parity analysis of solar photovoltaic systems in Germany using experience curves. *Solar Energy*, *83*(9), 1634–1644. https://doi.org/10.1016/j.solener.2009.06.001

Bhayo, B. A., Al-Kayiem, H. H., & Gilani, S. I. (2019). Assessment of standalone solar PV-Battery system for electricity generation and utilization of excess power for water pumping. *Solar Energy*, *194*, 766–776. https://doi.org/10.1016/j.solener.2019.11.026

Bukar, A. L., Tan, C. W., & Lau, K. Y. (2019). Optimal sizing of an autonomous photovoltaic/wind/battery/diesel generator microgrid using grasshopper optimization algorithm. *Solar Energy*, *188*, 685–696. https://doi.org/10.1016/j.solener.2019.06.050

Cao, Y., Kamrani, E., Mirzaei, S., Khandakar, A., & Vaferi, B. (2022). Electrical efficiency of the photovoltaic/thermal collectors cooled by nanofluids: Machine learning simulation and optimization by evolutionary algorithm. *Energy Reports*, *8*, 24–36. https://doi.org/10.1016/j.egyr.2021.11.252

CC BY 4.0; Attribution 4.0 International. (2022, February 12). Retrieved 21 March 2025, from http://creativecommons.org/licenses/by/4.0/

Chahartaghi, M., Mehdi, &, & Jaloodar, H. (2019). Mathematical modeling of direct-coupled photovoltaic solar pump system for small-scale irrigation. *Energy Sources, Part A: Recovery, Utilization, and Environmental Effects*. https://doi.org/10.1080/15567036.2019.1685025

Chahartaghi, M., & Nikzad, A. (2021). Exergy, environmental, and performance evaluations of a solar water pump system. *Sustainable Energy Technologies and Assessments*, *43*. https://doi.org/10.1016/j.seta.2020.100933

Chandel, S. S., Nagaraju Naik, M., & Chandel, R. (2015). Review of solar photovoltaic water pumping system technology for irrigation and community drinking water supplies. *Renewable and Sustainable Energy Reviews*, *49*, 1084–1099. https://doi.org/10.1016/J.RSER.2015.04.083

Chandel, S. S., Naik, M. N., & Chandel, R. (2017). Review of performance studies of direct coupled photovoltaic water pumping systems and case study. *Renewable and Sustainable Energy Reviews*, *76*(February), 163–175. https://doi.org/10.1016/j.rser.2017.03.019

Chandler, W., Whitlock, C., & Stackhouse, P. (2022, March 3). Surface meteorology and solar energy. A renewable energy resource web site (release 6.0). Retrieved from NASA Surface meteorology and solar energy (SSE) website: eosweb.larc.nasa.gov/sse/

Chapin, D. M., Fuller, C. S., & Pearson, G. L. (1954). A New Silicon p-n Junction Photocell for Converting Solar Radiation into Electrical Power. *Journal of Applied Physics*, *25*(5), 676. https://doi.org/https://doi.org/10.1063/1.1721711

Cooper, P. I. (1969). The Absorption of Solar Radiation in Solar Stills. *Solar Energy*, *12*(3).

Cozzi, L., Wetzel, D., Tonolo, G., Diarra, N., & Roge, A. (2023, September 15). Access to electricity improves slightly in 2023, but still far from the pace needed to meet SDG7.

Retrieved 14 January 2025, from IEA (2023) website: https://www.iea.org/commentaries/access-to-electricity-improves-slightly-in-2023-but-still-far-from-the-pace-needed-to-meet-sdg7

CSIRO. (2022, May 23). CSIRO, Australia's national science agency and innovation catalyst. Retrieved 22 May 2022, from https://www.csiro.au/en/research/technology-space/it/adopt

Dalin, C., Wada, Y., Kastner, T., & Puma, M. J. (2017). Groundwater depletion embedded in international food trade. *Nature*, *543*(7647), 700–704. https://doi.org/10.1038/nature21403

Das, B. K., Alotaibi, M. A., Das, P., Islam, M. S., Das, S. K., & Hossain, M. A. (2021). Feasibility and techno-economic analysis of stand-alone and grid-connected PV/Wind/Diesel/Batt hybrid energy system: A case study. *Energy Strategy Reviews*, *37*. https://doi.org/10.1016/j.esr.2021.100673

Das, B. K., Hoque, N., Mandal, S., Pal, T. K., & Raihan, M. A. (2017). A techno-economic feasibility of a stand-alone hybrid power generation for remote area application in Bangladesh. *Energy*, *134*, 775–788. https://doi.org/10.1016/j.energy.2017.06.024

Deb, K., Pratap, A., Agarwal, S., & Meyarivan, T. (2002). A Fast and Elitist Multiobjective Genetic Algorithm: NSGA-II. In *IEEE TRANSACTIONS ON EVOLUTIONARY COMPUTATION* (Vol. 6).

Desai, U., Rathore, S., & Singh, A. (2022). Exploration of degradation pathways resulting in reduction in volume resistivity in photovoltaic backsheets under sand erosion and aging in desert conditions. *Solar Energy*, *236*, 860–869. https://doi.org/10.1016/j.solener.2022.03.045

Dewan, M. L., & Famouri, J. (1968). *The Cambridge history of Iran; Volume I, The land of Iran* (W. B. Fisher, Ed.). Cambridge: Cambridge University Press.

Diesel prices: global petrol prices. (2025, February 10). Retrieved 15 February 2025, from https://www.globalpetrolprices.com/diesel_prices/

Duffie, J. A., & Beckman, W. A. (1982). Solar engineering of thermal processes. In *Design Studies* (Vol. 3). https://doi.org/10.1016/0142-694x(82)90016-3

Ebaid, M. S. Y., Ghrair, A. M., & Al-Busoul, M. (2018). Experimental investigation of cooling photovoltaic (PV) panels using (TiO2) nanofluid in water -polyethylene glycol mixture and (Al2O3) nanofluid in water- cetyltrimethylammonium bromide mixture. *Energy Conversion and Management*, *155*(November 2017), 324–343. https://doi.org/10.1016/j.enconman.2017.10.074

Eckstein, J. H. (1990). *Detailed modelling of photovoltaic system components*. Madison. Retrieved from https://minds.wisconsin.edu/bitstream/handle/1793/45596/Eckstein1990.pdf?sequence=1&isAllowed=y

Ekinci, F., Yavuzdeğer, A., Nazlıgül, H., Esenboğa, B., Doğru Mert, B., & Demirdelen, T. (2022). Experimental investigation on solar PV panel dust cleaning with solution method. *Solar Energy*, *237*(April), 1–10. https://doi.org/10.1016/j.solener.2022.03.066

El-Maaroufi, A., Daoudi, M., & Ahl Laamara, R. (2024). Optimal design and techno-economic analysis of a solar-wind hybrid power system for laayoune city electrification with hydrogen and batteries as a storage device. *Physics and Chemistry of the Earth*, *136*. https://doi.org/10.1016/j.pce.2024.103719

Energy Information Canada. (2025, January 14). High-Frequency Electricity Data: Visualization Tool (Beta). Retrieved 10 March 2025, from Canadian Centre for Energy Information website: https://energy-information.canada.ca/en/resources/high-frequency-electricity-data

Fagbenle, R. O., Katende, J., Ajayi, O. O., & Okeniyi, J. O. (2011). Assessment of wind energy potential of two sites in North-East, Nigeria. *Renewable Energy*, *36*(4), 1277–1283. https://doi.org/10.1016/j.renene.2010.10.003

Fakruddin Babavali, SK., Latha Devi, N. S. M. P., Kaliappan, S., Garg, N., Nagalakshmi, V., & Rajagopalan, N. R. (2023). Thermal management of PV panel through the circulation of a nano-MgO/water-based nanofluid. *Materials Today: Proceedings*. https://doi.org/10.1016/j.matpr.2023.09.001

Fan, S., Wang, X., Cao, S., Wang, Y., Zhang, Y., & Liu, B. (2022). A novel model to determine the relationship between dust concentration and energy conversion efficiency of photovoltaic (PV) panels. *Energy*, *252*, 123927. https://doi.org/10.1016/j.energy.2022.123927

Fleck, B., & Huot, M. (2009). Comparative life-cycle assessment of a small wind turbine for residential off-grid use. *Renewable Energy*, *34*(12), 2688–2696. https://doi.org/10.1016/j.renene.2009.06.016

Fortin, F., Rainville, F. De, Gardner, M., Parizeau, M., & Gagné, C. (2017). DEAP: Evolutionary Algorithms Made Easy. *Journal of Open Source Software*, *2*(9).

Ghasemi-Mobtaker, H., Mostashari-Rad, F., Saber, Z., Chau, K. wing, & Nabavi-Pelesaraei, A. (2020). Application of photovoltaic system to modify energy use, environmental damages and cumulative exergy demand of two irrigation systems-A case study: Barley

production of Iran. *Renewable Energy*, *160*, 1316–1334. https://doi.org/10.1016/J.RENENE.2020.07.047

Ghoneim, A. A. (2006). Design optimization of photovoltaic powered water pumping systems. *Energy Conversion and Management*, *47*(11–12), 1449–1463. https://doi.org/10.1016/j.enconman.2005.08.015

Gomaa, M. R., Ahmed, M., & Rezk, H. (2022). Temperature distribution modeling of PV and cooling water PV/T collectors through thin and thick cooling cross-fined channel box. *Energy Reports*, *8*, 1144–1153. https://doi.org/10.1016/j.egyr.2021.11.061

Gorjian, S., Singh, R., Shukla, A., & Mazhar, A. R. (2020). Chapter 6 - On-farm applications of solar PV systems. In S. Gorjian & A. Shukla (Eds.), *Photovoltaic Solar Energy Conversion* (pp. 147–190). Academic Press. https://doi.org/https://doi.org/10.1016/B978-0-12-819610-6.00006-5

Gorjian, S., Zadeh, B. N., Eltrop, L., Shamshiri, R. R., & Amanlou, Y. (2019). Solar photovoltaic power generation in Iran: Development, policies, and barriers. *Renewable and Sustainable Energy Reviews*, *106*, 110–123. https://doi.org/10.1016/J.RSER.2019.02.025

Gouvernement du Québec. (2025, March 11). Faits saillants sur la consommation d'eau potable. Retrieved 10 March 2025, from https://www.quebec.ca/agriculture-environnement-et-ressources-naturelles/eau-potable/economiser/faits-saillants

Gualteros, S., & Rousse, D. R. (2021). Solar water pumping systems: A tool to assist in sizing and optimization. *Solar Energy*, *225*, 382–398. https://doi.org/10.1016/j.solener.2021.06.053

Guo, S., Zhang, F., Engel, B. A., Wang, Y., Guo, P., & Li, Y. (2022). A distributed robust optimization model based on water-food-energy nexus for irrigated agricultural sustainable development. *Journal of Hydrology*, *606*(October 2021), 127394. https://doi.org/10.1016/j.jhydrol.2021.127394

Habiballahi, M., Ameri, M., & Mansouri, S. H. (2015). Efficiency Improvement of Photovoltaic Water Pumping Systems by Means of Water Flow Beneath Photovoltaic Cells Surface. *Journal of Solar Energy Engineering, Transactions of the ASME*, *137*(4), 1–8. https://doi.org/10.1115/1.4029932

Hadj Arab, A., Chenlo, F., & Benghanem, M. (2004). Loss-of-load probability of photovoltaic water pumping systems. *Solar Energy*, *76*(6), 713–723. https://doi.org/10.1016/J.SOLENER.2004.01.006

Heydari, F., Maleki, A., Jabari Moghadam, A., & Haghighat, S. (2021). Emplacement of the Photovoltaic Water Pumping System in Remote Areas by a Multi-Criteria Decision-Making Method: A Case Study. *Frontiers in Energy Research*, *9*(December). https://doi.org/10.3389/fenrg.2021.770981

Hossain Mondal, M. A. (2010). Economic viability of solar home systems: Case study of Bangladesh. *Renewable Energy*, *35*(6), 1125–1129. https://doi.org/10.1016/j.renene.2009.10.038

https://www.restarsolar.com/mono-crystalline-panel/mono-crystalline-pan-rtm-100m.html. (2025). *Mono Crystalline Pan RTM-100M*.

Hydro Quebec. (2023). *Electricity rates chart- 2023- Hydro Quebec*. Retrieved from https://www.hydroquebec.com/data/documents-donnees/pdf/rates-chart-2023.pdf

Hydro Quebec. (2024, November 12). Consumption based on the home's specific features. Retrieved 10 March 2025, from Hydro Quebec website: https://www.hydroquebec.com/residential/customer-space/electricity-use/tools/electricity-use.html

Ibrahim, I. A., Khatib, T., & Mohamed, A. (2017). Optimal sizing of a standalone photovoltaic system for remote housing electrification using numerical algorithm and improved system models. *Energy*, *126*, 392–403. https://doi.org/10.1016/j.energy.2017.03.053

Imjai, T., Thinsurat, K., Ditthakit, P., Wipulanusat, W., Setkit, M., & Garcia, R. (2020). Performance study of an integrated solar water supply system for isolated agricultural areas in Thailand: A case-study of the royal initiative project. *Water (Switzerland)*, *12*(9). https://doi.org/10.3390/w12092438

International Renewable Energy Agency. (2022). *REthinking Energy 2017: Accelerating the global energy transformation*.

Irandoostshahrestani, M., & R. Rousse, D. (2023). Photovoltaic Electrification and Water Pumping Using the Concepts of Water Shortage Probability and Loss of Power Supply Probability: A Case Study. *Energies*, *16*(1). https://doi.org/10.3390/en16010001

Iran's Ministry of Energy- Tavanir Holding Company of Iran. (2022, April 23). Detailed Statistics of Iran Electricity Production Industry. Retrieved 31 July 2021, from https://amar.tavanir.org.ir/en/.

IRENA. (2021). *IRENA (2021), Renewable Power Generation Costs in 2020, International Renewable Energy Agency*. Abu Dhabi. Retrieved from https://www.irena.org/-/media/Files/IRENA/Agency/Publication/2021/Jun/IRENA_Power_Generation_Costs_2020.pdf

Islam, M. R., Saidur, R., & Rahim, N. A. (2011). Assessment of wind energy potentiality at Kudat and Labuan, Malaysia using Weibull distribution function. *Energy*, *36*(2), 985–992. https://doi.org/10.1016/j.energy.2010.12.011

Jahanfar, A., & Iqbal, M. T. (2022a). An Optimum Sizing for a Hybrid Storage System in Solar Water Pumping Using ICA. *2022 IEEE International IOT, Electronics and Mechatronics Conference, IEMTRONICS 2022*. Institute of Electrical and Electronics Engineers Inc. https://doi.org/10.1109/IEMTRONICS55184.2022.9795848

Jahanfar, A., & Iqbal, M. T. (2022b). Dynamic Modeling and Simulation of Solar Water Pumping With Hybrid Storage System. *2022 IEEE 13th Annual Information Technology, Electronics and Mobile Communication Conference, IEMCON 2022*, 562–566. Institute of Electrical and Electronics Engineers Inc. https://doi.org/10.1109/IEMCON56893.2022.9946480

Karami Rad, M., Omid, M., Alimardani, R., & Mousazadeh, H. (2015). A novel application of stand-alone photovoltaic system in agriculture: solar-powered Microner sprayer. *International Journal of Ambient Energy*, *38*(1), 69–76. https://doi.org/10.1080/01430750.2015.1035800

Karizaki, V. M. (2016). Ethnic and traditional Iranian rice-based foods. *Journal of Ethnic Foods*, *3*(2), 124–134. https://doi.org/10.1016/j.jef.2016.05.002

Kasaeian, A., Daviran, S., Azarian, R. D., & Rashidi, A. (2015). Performance evaluation and nanofluid using capability study of a solar parabolic trough collector. *Energy Conversion and Management*, *89*, 368–375. https://doi.org/10.1016/j.enconman.2014.09.056

Ketjoy, N., Chamsa-ard, W., & Mensin, P. (2021). Analysis of factors affecting efficiency of inverters: Case study grid-connected PV systems in lower northern region of Thailand. *Energy Reports*, *7*, 3857–3868. https://doi.org/10.1016/j.egyr.2021.06.075

Key World Energy Statistics. (2021). In *IEA Publications*. Retrieved from https://iea.blob.core.windows.net/assets/52f66a88-0b63-4ad2-94a5-29d36e864b82/KeyWorldEnergyStatistics2021.pdf

Khan, M. S., Tahir, A., Alam, I., Razzaq, S., Usman, M., Tareen, W. U. K., … Riaz, M. (2021). Assessment of solar photovoltaic water pumping of wasa tube wells for irrigation in quetta valley aquifer. *Energies*, *14*(20). https://doi.org/10.3390/en14206676

Komiyama, R., & Fujii, Y. (2015). Long-term scenario analysis of nuclear energy and variable renewables in Japan's power generation mix considering flexible power resources. *Energy Policy*, *83*, 169–184. https://doi.org/10.1016/j.enpol.2015.04.005

Komiyama, Ryoichi, & Fujii, Y. (2014). Assessment of massive integration of photovoltaic system considering rechargeable battery in Japan with high time-resolution optimal power generation mix model. *Energy Policy*, *66*, 73–89. https://doi.org/10.1016/j.enpol.2013.11.022

Kordzadeh, A. (2010). The effects of nominal power of array and system head on the operation of photovoltaic water pumping set with array surface covered by a film of water. *Renewable Energy*, *35*(5), 1098–1102. https://doi.org/10.1016/j.renene.2009.10.024

Kristoffer Welsien, Christopher Purcell, Reuben Kogi, C. B. (2018). *Solar Pumping-The basics*. Washington, DC.

Lewis, N. S., Crabtree, G., Nozik, A. J., Wasielewski, M. R., Alivisatos, P., Kung, H., … Nault, R. M. (2005). *Basic Research Needs for Solar Energy Utilization. Report of the Basic Energy Sciences Workshop on Solar Energy Utilization, April 18-21, 2005*. https://doi.org/10.2172/899136

Li, H., & Sun, Y. (2018). Operational performance study on a photovoltaic loop heat pipe/solar assisted heat pump water heating system. *Energy and Buildings*, *158*, 861–872. https://doi.org/10.1016/j.enbuild.2017.10.075

Li, Y., Gao, W., Ruan, Y., & Ushifusa, Y. (2018). The performance investigation of increasing share of photovoltaic generation in the public grid with pump hydro storage dispatch system, a case study in Japan. *Energy*, *164*, 811–821. https://doi.org/10.1016/j.energy.2018.09.029

Libra, M., Mrázek, D., Tyukhov, I., Severová, L., Poulek, V., Mach, J., … Sedláček, J. (2023). Reduced real lifetime of PV panels – Economic consequences. *Solar Energy*, *259*, 229–234. https://doi.org/10.1016/j.solener.2023.04.063

Liu, Y., Yao, L., Jiang, H., Lu, N., Qin, J., Liu, T., & Zhou, C. (2022). Spatial estimation of the optimum PV tilt angles in China by incorporating ground with satellite data. *Renewable Energy*, *189*, 1249–1258. https://doi.org/10.1016/j.renene.2022.03.072

Lunel, T., & Rousse, D. (2020). pvpumpingsystem: A Python package for modeling and sizing photovoltaic water pumping systems. *Journal of Open Source Software*, *5*(54), 2637. https://doi.org/10.21105/joss.02637

Maghrabie, H. M., Mohamed, A. S. A., Fahmy, A. M., & Abdel Samee, A. A. (2023). Performance enhancement of PV panels using phase change material (PCM): An experimental implementation. *Case Studies in Thermal Engineering*, *42*. https://doi.org/10.1016/j.csite.2023.102741

Maleki, A., Ngo, P. T. T., & Shahrestani, M. I. (2020). Energy and exergy analysis of a PV module cooled by an active cooling approach. *Journal of Thermal Analysis and Calorimetry*, *141*(6). https://doi.org/10.1007/s10973-020-09916-0

Mamun, M. A. A., Islam, M. M., Hasanuzzaman, M., & Selvaraj, J. (2022). Effect of tilt angle on the performance and electrical parameters of a PV module: Comparative indoor and outdoor experimental investigation. *Energy and Built Environment*, *3*(3), 278–290. https://doi.org/10.1016/j.enbenv.2021.02.001

Mark A. Shannon; Paul W. Bohn; Menachem Elimelech; John G. Georgiadis; Benito J. Mariñas; Anne M. Mayes. (2008). Science and technology for water purification in the coming decades. *Nature*, *452*, 301–310. https://doi.org/https://doi.org/10.1038/nature06599

Masoud Parsa, S., Yazdani, A., Aberoumand, H., Farhadi, Y., Ansari, A., Aberoumand, S., … Muhammad Ali, H. (2022). A critical analysis on the energy and exergy performance of photovoltaic/thermal (PV/T) system: The role of nanofluids stability and synthesizing method. *Sustainable Energy Technologies and Assessments*, *51*. https://doi.org/10.1016/j.seta.2021.101887

Mckenzie, R. H., & Shelley A. Woods. (2011). *Crop Water Use and Requirements*. Retrieved from www.agriculture.alberta.ca

Memme, S., & Fossa, M. (2022). Maximum energy yield of PV surfaces in France and Italy from climate based equations for optimum tilt at different azimuth angles. *Renewable Energy*, *200*, 845–866. https://doi.org/10.1016/j.renene.2022.10.019

Meunier, S., Heinrich, M., Quéval, L., Cherni, J. A., Vido, L., Darga, A., … Marchand, C. (2019). A validated model of a photovoltaic water pumping system for off-grid rural communities. *Applied Energy*, *241*, 580–591. https://doi.org/10.1016/j.apenergy.2019.03.035

Mohammad Zamanlou;Tariq Iqbal. (2019). Design and analysis of a solar water pumping system for drip irrigation of a fruit garden in Iran. *28th Annual Newfoundland Electrical and Computer Engineering Conference*, 2–6. St. John's.

Mohammadi, M. (2015). New computing method for techno-economic analysis of the photovoltaic water pumping system using fuzzy based NSGAII optimization approach. *Automatika*, *56*(2), 132–139. https://doi.org/10.7305/automatika.2015.07.656

Moshir Panahi, D., Kalantari, Z., Ghajarnia, N., Seifollahi-Aghmiuni, S., & Destouni, G. (2020). *Variability and change in the hydro-climate and water resources of iran over a recent 30-year period*. https://doi.org/10.1038/s41598-020-64089-y

Muhsen, D. H., Ghazali, A. B., & Khatib, T. (2016). Multiobjective differential evolution algorithm-based sizing of a standalone photovoltaic water pumping system. *Energy Conversion and Management*, *118*, 32–43. https://doi.org/10.1016/j.enconman.2016.03.074

Ndwali, K., Njiri, J. G., & Wanjiru, E. M. (2020). Multi-objective optimal sizing of grid connected photovoltaic batteryless system minimizing the total life cycle cost and the grid energy. *Renewable Energy*, *148*, 1256–1265. https://doi.org/10.1016/j.renene.2019.10.065

Niajalili, M., Mayeli, P., Naghashzadegan, M., & Poshtiri, A. H. (2017). Techno-economic feasibility of off-grid solar irrigation for a rice paddy in Guilan province in Iran: A case study. *Solar Energy*, *150*, 546–557. https://doi.org/10.1016/j.solener.2017.05.012

Nikzad, A., Chahartaghi, M., & Ahmadi, M. H. (2019). Technical, economic, and environmental modeling of solar water pump for irrigation of rice in Mazandaran province in Iran: A case study. *Journal of Cleaner Production*, *239*. https://doi.org/10.1016/j.jclepro.2019.118007

NREL. (2022a, May 4). NSRDB: The National Solar Radiation Database. Retrieved 31 July 2021, from https://maps.nrel.gov/nsrdb-viewer/

NREL. (2022b, July 22). National Renewable Energy Laboratory. PVWatts® Calculator. U.S. Department of Energy. Retrieved 28 March 2025, from Retrieved from https://pvwatts.nrel.gov/

Numbi, B. P., & Malinga, S. J. (2017). Optimal energy cost and economic analysis of a residential grid-interactive solar PV system- case of eThekwini municipality in South Africa. *Applied Energy*, *186*, 28–45. https://doi.org/10.1016/j.apenergy.2016.10.048

ONTARIO AGRA: Vertical Liquid Storage Tanks. (2025, January 20). Retrieved 15 March 2025, from https://www.ontarioagra.ca/products/liquid-storage-solutions/

Osmani, K., Ramadan, M., Lemenand, T., Castanier, B., & Haddad, A. (2021). Optimization of PV array tilt angle for minimum levelized cost of energy. *Computers and Electrical Engineering*, *96*(PA), 107474. https://doi.org/10.1016/j.compeleceng.2021.107474

P. Cooper. (1969). The Absorption of Solar Radiation in Solar Stills. *Solar Energy*, *12*(3).

Panidhara, K. M., & Ramamurthy, P. C. (2021). Development of low power laser in-situ thickness measurement for correlating the dust thickness to the PV performance. *Cleaner Engineering and Technology*, *5*, 100332. https://doi.org/10.1016/j.clet.2021.100332

Parvaresh Rizi, A., Ashrafzadeh, A., & Ramezani, A. (2019). A financial comparative study of solar and regular irrigation pumps: Case studies in eastern and southern Iran. *Renewable Energy*, *138*, 1096–1103. https://doi.org/10.1016/j.renene.2019.02.026

Pereira, L. S., & Alves, I. (2005). Encyclopedia of Soils in the Environment. *CROP WATER REQUIREMENTS*, 322–334.

Powell, J. W., Welsh, J. M., Pannell, D., & Kingwell, R. (2021). Factors influencing Australian sugarcane irrigators' adoption of solar photovoltaic systems for water pumping. *Cleaner Engineering and Technology*, *4*. https://doi.org/10.1016/j.clet.2021.100248

Rahimi, J., Ebrahimpour, M., & Khalili, A. (2013). Spatial changes of Extended De Martonne climatic zones affected by climate change in Iran. *Theoretical and Applied Climatology*, *112*(3–4), 409–418. https://doi.org/10.1007/s00704-012-0741-8

Rathore, P. K. S., Das, S. S., & Chauhan, D. S. (2018). Perspectives of solar photovoltaic water pumping for irrigation in India. *Energy Strategy Reviews*, *22*, 385–395. https://doi.org/10.1016/j.esr.2018.10.009

Ray, & Douglas. (2020). *Lazard's Levelized Cost of Energy Analysis—Version 13.0*.

Raza, F., Tamoor, M., Miran, S., Arif, W., Kiren, T., Amjad, W., … Lee, G. H. (2022). The Socio-Economic Impact of Using Photovoltaic (PV) Energy for High-Efficiency Irrigation Systems: A Case Study. *Energies*, *15*(3), 1–21. https://doi.org/10.3390/en15031198

Rezae, A., & Gholamian, S. A. (2013). Technical and Financial Analysis of Photovoltaic Water Pumping System for GORGAN, IRAN. *International Journal on Cybernetics & Informatics*, *2*(2), 21–31. https://doi.org/10.5121/ijci.2013.2203

Ridley, B., Boland, J., & Lauret, P. (2010). Modelling of diffuse solar fraction with multiple predictors. *Renewable Energy*, *35*(2), 478–483. https://doi.org/10.1016/j.renene.2009.07.018

Saatsaz, M., & Rezaei, A. (2023). The technology, management, and culture of water in ancient Iran from prehistoric times to the Islamic Golden Age. *Humanities and Social Sciences Communications*, *10*(1). https://doi.org/10.1057/s41599-023-01617-x

Salamah, T., Ramahi, A., Alamara, K., Juaidi, A., Abdallah, R., Abdelkareem, M. A., … Olabi, A. G. (2022). Effect of dust and methods of cleaning on the performance of solar PV module for different climate regions: Comprehensive review. *Science of the Total Environment*, *827*, 154050. https://doi.org/10.1016/j.scitotenv.2022.154050

Santra, P. (2021). Performance evaluation of solar PV pumping system for providing irrigation through micro-irrigation techniques using surface water resources in hot arid region of India. *Agricultural Water Management*, *245*(September 2020), 106554. https://doi.org/10.1016/j.agwat.2020.106554

SATBA Iran. (2022, June 6). Renewable Energy and Energy Efficiency Organization (SATBA), Iran. Retrieved 31 July 2021, from http://www.satba.gov.ir/en/home

Shah Irshad, A., Kargar, N., Elkholy, M. H., Ahmad Ludin, G., Elias, S., Hilali, A., … Pinter, G. (2024). Techno-economic evaluation and comparison of the optimal PV/Wind and grid hybrid system with horizontal and vertical axis wind turbines. *Energy Conversion and Management: X*, *23*. https://doi.org/10.1016/j.ecmx.2024.100638

Shahverdi, K., Bellos, E., Loni, R., Najafi, G., & Said, Z. (2021). Solar-driven water pump with organic Rankine cycle for pressurized irrigation systems: A case study. *Thermal Science and Engineering Progress*, *25*, 100960. https://doi.org/10.1016/J.TSEP.2021.100960

Shalaby, S. M., Elfakharany, M. K., Moharram, B. M., & Abosheiasha, H. F. (2022). Experimental study on the performance of PV with water cooling. *Energy Reports*, *8*, 957–961. https://doi.org/10.1016/j.egyr.2021.11.155

Shayeteh, F., Reihaneh, ·, & Moghaddam, K. (2020). Optimization of Kalagh Ashian's Photovoltaic Water Pump System Using a New Proposed Multi-objective Firefly Algorithm. *Journal of Control, Automation and Electrical Systems*, *31*, 648–664. https://doi.org/10.1007/s40313-020-00570-3

Shirinabadi, M., Samadi Saray, H., & Maanifar, M. (2018). *The feasibility of using solar energy in order to supply the power of water pumping station Tabriz- Iran and consideration of losses and environmental benefits using the right software*.

Solar module prices continue to fall. (2023, August 23). Retrieved 22 November 2023, from PV-Magazine website website: https://www.pv-magazine.com/2023/08/23/solar-module-prices-continue-to-fall/

Solar module prices dive to record low. (2023, October 27). Retrieved 22 November 2023, from PV-Magazine website website: https://www.pv-magazine.com/2023/10/27/solar-module-prices-dive-to-record-low/

Sontake, V. C., & Kalamkar, V. R. (2016). Solar photovoltaic water pumping system - A comprehensive review. *Renewable and Sustainable Energy Reviews*, *59*, 1038–1067. https://doi.org/10.1016/J.RSER.2016.01.021

Tabaei, H., & Ameri, M. (2012). The effect of booster reflectors on the photovoltaic water pumping system performance. *Journal of Solar Energy Engineering, Transactions of the ASME*, *134*(1), 1–4. https://doi.org/10.1115/1.4005339

Tabaei, H., & Ameri, M. (2015). Improving the effectiveness of a photovoltaic water pumping system by using booster reflector and cooling array surface by a film of water. *Iranian Journal of Science and Technology - Transactions of Mechanical Engineering*, *39*(M1), 51–60.

The MathWorks Inc. (2022). *MATLAB Curve Fitter tool*. Retrieved from https://www.mathworks.com/

Tiwari, A. K., Kalamkar, V. R., Pande, R. R., Sharma, S. K., Sontake, V. C., & Jha, A. (2020). Effect of head and PV array configurations on solar water pumping system. *Materials Today: Proceedings*, *46*, 5475–5481. https://doi.org/10.1016/j.matpr.2020.09.200

United Nations. (2022). United Nations Sustainable Development Goals (SDGss). *Https://Sdgs.Un.Org/Goals*. Retrieved from https://sdgs.un.org/goals

Valve-Regulated Lead-Acid (VRLA) Gelled Electrolyte (gel) and Absorbed Glass Mat (AGM) Batteries. (2004).

van der Walt, S., Colbert, S., & Varoquaux, G. (2011). The NumPy Array: A Structure for Efficient Numerical Computation. *Computing in Science & Engineering*, *13*(2), 22–30.

Venkatesh, T., Manikandan, S., Selvam, C., & Harish, S. (2022). Performance enhancement of hybrid solar PV/T system with graphene based nanofluids. *International Communications in Heat and Mass Transfer*, *130*, 105794. https://doi.org/10.1016/j.icheatmasstransfer.2021.105794

Vishnupriyan, J., Partheeban, P., Dhanasekaran, A., & Shiva, M. (2022). Analysis of tilt angle variation in solar photovoltaic water pumping system. *Materials Today: Proceedings*, *58*, 416–421. https://doi.org/10.1016/j.matpr.2022.02.353

Yu, Y., Liu, J., Wang, Y., Xiang, C., & Zhou, J. (2017). The feasibility of solar water pumping system for Cassava irrigation in Guangxi Autonomous Region, China. *Energy Procedia*, *142*, 447–454. Elsevier Ltd. https://doi.org/10.1016/j.egypro.2017.12.070

Zabihi, M. S., Asl Soleimani, E., & Farhangi, S. (1998). Photovoltaic manufacturing, system design and application trend in Iran. *Renewable Energy*, *15*(1–4), 496–501. https://doi.org/10.1016/S0960-1481(98)00212-2

Zaheeruddin, Mishra, S., & Haque, A. (2016). Performance evaluation of modified perturb & observe maximum power point tracker for solar PV system. *International Journal of System Assurance Engineering and Management*, *7*, 229–238. https://doi.org/10.1007/s13198-015-0369-z

Zarei, T., Abdolzadeh, M., & Yaghoubi, M. (2022). Comparing the impact of climate on dust accumulation and power generation of PV modules: A comprehensive review. *Energy for Sustainable Development*, *66*, 238–270. https://doi.org/10.1016/j.esd.2021.12.005

Zhou, Z., Tkachenko, S., Bahl, P., Tavener, D., de Silva, C., Timchenko, V., … Green, M. (2022). Passive PV module cooling under free convection through vortex generators. *Renewable Energy*, *190*, 319–329. https://doi.org/10.1016/j.renene.2022.03.133